



**The role of the adhesion protein tensin-3 (TNS3) in controlling basement membrane
remodelling during breast cancer progression in mammalian models**

Haya Alomaim

**This Thesis is Submitted in Partial Fulfilment of the Requirements for the Degree of
Doctor of Philosophy**

The University of Sheffield

Faculty of Science

School of Biosciences

24/01/2025

Abstract:

Breast cancer is one of the most common cancers in women, often beginning as ductal carcinoma *in situ* (DCIS), where mammary epithelial cells proliferate within ducts due to the presence of the basement membrane (BM). In 30% of patients, cancer cells progress to invasive ductal carcinoma (IDC) and metastasis. The mechanisms underlying this progression remain poorly understood. Tensin 3 (TNS3), a member of the TNS family that includes TNS1, TNS2, and TNS4, interacts with β 1 integrin to promote cell-ECM adhesion during this transition.

We found that TNS3 is upregulated in DCIS and IDC tumours compared to normal mammary glands in a mouse model of breast cancer. Interestingly, TNS3 downregulation in MCF10DCIS and MCF10CA1 cells suppressed invasive protrusions and reduced spheroid growth. Additionally, MCF10DCIS and MCF10CA1 cell growth on Matrigel was impaired under glutamine deprivation.

Mechanistically, downregulating β 1 integrin and TNS3 significantly reduced laminin-332 expression in 3D cultured MCF10DCIS cells and impaired filopodia formation. Moreover, silencing TNS3 lowered α 3 and α 6 integrin levels. Blocking α 3 and α 6 integrin function further decreased laminin-332 expression and filopodia formation, suggesting that TNS3 modulates BM dynamics through α 3 and α 6 integrins. Consistently, TNS3 knockdown reduced laminin-332, α 3 integrin expression, and filopodia formation in MCF10CA1 cells.

Reports suggest that TNS3 acts as a tumour promoter in cancer cells but as a tumour suppressor in non-transformed epithelial cells. Our results indicate that silencing TNS3 promotes proliferation and invasion of MCF10A cells while increasing α 3 integrin, laminin-332, and filopodia formation. Overexpression of TNS3 in a *Drosophila* cancer model strongly impaired tumour growth and metastasis.

Overall, these findings highlight TNS3's critical role in regulating the basement membrane and filopodia formation, acting as both a tumour promoter in cancer cells and a tumour suppressor in normal mammary epithelial cells.

Declaration:

I, Haya Mubarak Alomaim declare that this thesis has not been submitted before at University of Sheffield.

Haya Alomaim

22 December 2024

Acknowledgement:

I'd like to express a sincere thanks to my supervisor Dr Elena Rainero for her guidance throughout my PhD. I'd also like to thank technician Bian Yanes for her support, guidance, training me on my experiments, and providing general support along the way.

Special thanks to Dr Jason King and Dr Anne-Gaelle Borycki for their general advice and suggestions throughout my PhD.

Special thanks to my sponsor King Saud bin Abdulaziz University for Health Science for providing the necessary funds and encouragement to carry out this project.

Finally, I want to express my heartfelt gratitude to my family for their unconditional love, understanding, and continued support, which kept me going through the difficult times of this journey.

Table of contents:

Abstract.....	2
Declaration.....	3
Acknowledgement	4
Table of content.....	5
List of figures.....	8
List of tables.....	10
Abbreviations.....	11
Chapter 1: Introduction.....	13
1.1 Breast cancer epidemiology and progression.....	13
1.2 Risk factors.....	13
1.2.1 The impact of modifying cancer risk factors.....	14
1.3 Breast cancer progression.....	15
1.3.1 Myoepithelial cells (MECs).....	18
1.3.2 Adipocytes.....	18
1.3.3 Fibroblasts.....	19
1.4 Molecular Subtypes of Breast Cancer.....	19
1.5 The MCF10 series of cell lines as a breast cancer progression model.....	20
1.6 The extracellular matrix (ECM) in cancer.....	21
1.7 Components of the extracellular matrix.....	22
1.7.1 Collagens.....	22
1.7.2 Fibronectin.....	24
1.8 Basement membrane (BM).....	25
1.8.1 Laminins.....	27
1.8.2 Laminins in breast cancer.....	28
1.9 ECM receptors.....	29
1.10 Focal adhesion proteins.....	30
1.11 Tensins.....	31
1.12 Role of tensins in cancer.....	33
1.13 Cell migration in cancer.....	34
1.14 Research hypothesis and aims.....	38
Chapter 2: Materials and methods.....	39
2.1 Materials.....	39

2.2 Methods.....	42
2.2.1 Cell culture.....	42
2.2.2 Western blot.....	42
2.2.3 siRNA-mediate knockdown.....	43
2.2.3.1 Transfection in 6-well plates.....	43
2.2.4 2D immunofluorescence microscopy.....	44
2.2.5 Cell proliferation assay.....	45
2.2.6 Fluorescence Immunohistochemistry staining.....	45
2.2.7 3D Culture.....	46
2.2.8 3D-Immunofluorescence microscopy	47
2.2.9 3D-spheroid invasion assay.....	49
2.2.10 Drosophila cancer model.....	50
2.2.11 Statistical analysis.....	50
Chapter 3: TNS3 is upregulated during breast cancer progression and promotes cancer cell invasion.....	51
3.1 Introduction.....	51
3.2 Results.....	53
3.2.1 TNS3 expression is up-regulated in breast cancer.....	53
3.2.2 TNS3 expression is upregulated in DCIS and adenocarcinoma in a breast cancer mouse model.....	54
3.2.3 TNS3 is upregulated in metastatic breast cancer cells compared to non-transformed mammary epithelial cells.....	55
3.2.4 TNS4 localises in the cytoplasm.....	56
3.2.5 3D culture promotes DCIS cell invasion.....	57
3.2.6 Characterisation of MCF10DCIS cell spheroid invasion.....	59
3.2.7 TNS3 is required for DCIS cell invasion in 3D spheroids.....	60
3.2.8 TNS3 is required for MCF10ACA1 cell invasion.....	61
3.2.9 TNS3 downregulation reduced MCF10DCIS and MCF10CA1 cell growth on Matrigel under glutamine deprivation.....	63
3.3 Discussion.....	64
Chapter 4. TNS3 regulates BM organisation and filopodia formation.....	67
4.1 Introduction.....	68
4.2 Results.....	69
4.2.1 TNS3 and β 1 integrin downregulation prevents BM deposition.....	69

4.2.2 TNS3 downregulation reduced laminin-332 expression.....	71
4.2.3 TNS3 and β 1 integrin down regulation did not affect laminin-332 secretion/deposition in 2D.....	71
4.2.4 Filopodia formation precedes laminin deposition.....	73
4.2.5 TNS3 and β 1-integrin downregulation reduced filopodia formation.....	75
4.2.6 TNS3 knockdown did not affect β 1-integrin distribution in MCF10DCIS cells.....	75
4.2.7 TNS3 knock-down reduced α 3 and α 6 integrin levels in MCF10DCIS cells.....	76
4.2.8 α 3 integrin inhibition prevented laminin-332 deposition and filopodia formation in MCF10DCIS cells.....	78
4.2.9 α 6 integrin inhibition prevented laminin-332 deposition and filopodia formation in MCF10DCIS cells.....	80
4.2.10 Downregulation of TNS3 in MCF10CA1 cells reduced laminin-332 levels.....	82
4.2.11 Downregulation of TNS3 reduced filopodia formation in MCF10CA1 cells.....	84
4.2.12 TNS3 downregulation reduced α 3 integrin levels in MCF10ACA1 cells.....	84
4.3 Discussion.....	85
Chapter 5. TNS3 restricts transformation in normal epithelial cells.....	89
5.1 Introduction.....	89
5.2 Results.....	91
5.2.1 TNS3 knockdown increased invasiveness and cell proliferation in MCF10A cells.....	91
5.2.2 TNS3 knockdown increased laminin-332 deposition in MCF10A cells.....	93
5.2.3 TNS3 silencing increased the number and length of filopodia in MCF10A cells.....	95
5.2.4 TNS3 knock-down increased α 3 integrin levels in 3D systems.....	95
5.2.5 TNS overexpression in the Apc/Ras background reduced tumour formation.....	96
5.2.6 TNS overexpression in the Apc/Ras/Sna background reduced tumour formation and metastasis.....	97
5.3 Discussion.....	99
Chapter 6. General discussion.....	101
6.1 Discussion.....	101
6.2 Conclusion and future direction.....	105
References.....	106

List of figures:

Chapter 1:

Figure 1.1 Breast anatomy.....	15
Figure 1.2 Breast cancer progression.....	17
Figure 1.3 Collagen-1 synthesis and assembly.....	24
Figure 1.4 Schematic illustration of fibronectin.....	25
Figure 1.5 Structure of the basement membrane (BM).....	26
Figure 1.6 Laminin structure.....	28
Figure 1.7 Integrin signalling pathways.....	30
Figure 1.8 Focal adhesion formation.....	31
Figure 1.9 Tensin structure.....	33
Figure 1.10 Invasion/metastasis cascade.....	35
Figure 1.11 Mechanisms controlling filopodia formation.....	37

Chapter 2:

Figure 2.1 Diagram representing the 3D culture protocol.....	47
Figure 2.2: Diagram representing the 3D spheroid invasion protocol.....	50

Chapter 3:

Figure 3.1 TNS3 expression is up-regulated in breast cancer.....	53
Figure 3.2 TNS3 expression is upregulated in DCIS and adenocarcinoma in a breast cancer mouse model.....	54
Figure 3.3 TNS3 is upregulated in metastatic breast cancer cells compared to MCF10A.....	56
Figure 3.4 TNS4 localises in the cytoplasm.....	57
Figure 3.5 3D culture promotes invasion in DCIS cells.....	58
Figure 3.6 Characterisation of DCIS cell spheroid invasion.....	59
Figure 3.7 TNS3 is required for DCIS cell invasion in 3D spheroids.....	61

Figure 3.8 TNS3 is required for CA1 cell in invasion.....62

Figure 3.9 TNS3 downregulation reduced DCIS and CA1 cell growth on Matrigel under glutamine deprivation.....64

Chapter 4:

Figure 4.1 TNS3 and β 1-integrin downregulation prevented BM deposition.....70

Figure 4.2 TNS3 knockdown reduced laminin-332 expression.....71

Figure 4.3 TNS3 and β 1 integrin down regulation did not affect laminin-332 secretion/deposition in 2D.....72

Figure 4.4 Filopodia formation preceded laminin-332 deposition.....74

Figure 4.5 TNS3 β 1-integrin knockdown reduced filopodia formation.....75

Figure 4.6 TNS3 knockdown did not affect β 1-integrin distribution.....76

Figure 4.7 TNS3 knock-down reduced α 3 and α 6 integrin levels in 3D systems.....78

Figure 4.8 α 3 integrin blocking antibody prevented laminin-332 deposition and filopodia formation.....80

Figure 4.9 α 6 integrin blocking antibody prevented laminin-332 deposition and filopodia formation in DCIS.....82

Figure 4.10 Downregulation of TNS3 in MCF10CA1 cells reduced Laminin 332 levels.....83

Figure 4.11 Downregulation of si-TNS3 in MCF10CA1 reduced filopodia formation.....84

Figure 4.12: TNS3 knockdown slightly reduced α 3 integrin levels in MCF10CA1 cells.....85

Chapter 5:

Figure 5.1 Suppressing TNS3 promotes MCF10A cell invasion.....92

Figure 5.2 TNS3 knockdown increased the growth of MCF10A cells.....93

Figure 5.3 TNS3 downregulation increased laminin-332 expression in MCF10A cells.....94

Figure 5.4 TNS3 silencing increased the number and length of filopodia in MCF10A cells....95

Figure 5.5 TNS3 knock-down increased the ITGA3 levels in 3D systems.....96

Figure 5.6 TNS overexpression in the Apc/Ras background reduced tumour formation.....97

Figure 5.7 TNS overexpression in the Apc/Ras/Sna background reduced tumour formation and metastasis.....98

List of tables:

Chapter 1:

Table 1.1 Laminin isoforms.....27

Table 1.2 TNS expression levels were compared in various cancer diseases to normal tissues.....34

Chapter 2:

Table 2.1 Reagent list.....39

Table 2.2 Antibody list.....40

Table 2.3 Blocking antibody list.....40

Table 2.4. Solution composition41

Table 2.5. The antibodies used for western blotting.....43

Table 2.6. Antibodies used for 2D Immunofluorescence microscopy.....44

Table 2.7. Antibodies used for 3D immunofluorescence microscopy.....48

Abbreviations:

Basement membrane (BM)

Extracellular matrix (ECM)

Ductal carcinoma *in situ* (DCIS)

Invasive ductal carcinoma (IDC)

laminin 332 (LN332)

Tumour microenvironment (TME)

Myoepithelial cells (MECs)

Cancer-associated fibroblasts (CAF)

Matrix metalloproteinase (MMP)

Cancer-associated adipocytes (CAAs)

α-Smooth muscle actin (*α*SMA)

Platelet-derived growth factor receptor- α (PDGFR α)

Epidermal growth factor receptor (HER2)

Oestrogen receptor (ER)

Progesterone receptor (PR)

Central nervous system (CNV)

Triple Negative Breast Cancer (TNBC)

Ketogenic diet (KD)

β -hydroxybutyrate (β -OHB)

Haemoglobin A1C (HbA1c)

LDL cholesterol

HDL cholesterol

Hyperbaric oxygen therapy (HBO2T)

Hepatocellular Antigen Synthesiser (HRAS)

Atypical ductal hyperplasia (ADH)

Fibril associated collagen with interrupted triple helices (FACITs)

Endoplasmic reticulum (ER)

Focal adhesion kinase (FAK)

Tensin-1 (TNS1),

Tensin-2 (TNS2)

Tensin-3 (TNS3)

Tensin-4 (TNS4)

C-terminal tensin-like (CTEN)

Src homology 2 (SH2)

Phosphotyrosine (pTyr)

Protein tyrosine phosphatase (PTP)

Phosphotyrosine-binding (PTB)

Actin binding domain (ABD)

Focal adhesion binding site (FAB)

Ena/VASP (enabled/vasodilator-stimulated phosphoprotein)

Chapter 1: Introduction

1.1 Breast cancer epidemiology and progression:

Breast cancer is the most often diagnosed cancer among women. Every year, around 2.3 million new patients are diagnosed with breast cancer, and it represents the 5th reason for death due to cancer (Łukasiewicz et al., 2021). A study performed a Systematic Review and Meta-Analysis to assess the diagnosed breast cancer distribution (Benitez Fuentes et al., 2024). Data from 2.4 million breast cancer women from 81 countries were used. The percentage of patients with metastatic disease has decreased during the last two decades, beginning in the early 2000s and continuing through 2015 in high-income countries. Aged women had the highest rate of metastatic disease. Following preventive strategies and engaging in programs for screening are critical steps toward potentially reducing the incidence of breast cancer and allowing for early intervention. The prevalence and mortality rates of breast cancer have shown an upward trend during the past 30 years. The rate of breast cancer has increased by more than 2-fold in 60 out of 102 countries (such as Afghanistan, Philippines, Brazil, and Argentina) between 1990 and 2016. On the other hand, the number of fatalities caused by breast cancer rose twofold in 43 out of 102 countries (such as Yemen, Paraguay, Libya, and Saudi Arabia). Present estimates suggest that by 2030, the global yearly incidence of newly identified cases will reach 2.7 million, with a corresponding mortality rate of 0.87 million. The estimated rise in breast cancer occurrence in low- and medium-income countries can be attributed to the adoption of Western lifestyles (such as delayed pregnancies, decreased nursing, premature menstruation, lack of exercise, and unhealthy diet), improved cancer registration, and enhanced cancer detection.

1.2 Risk factors:

Risk factors associated with the progression of breast cancer in women include breast cancer history, family history of any other form of cancer, dense breasts, no pregnancy, and obesity (Łukasiewicz et al., 2021). Recent evidence suggests that genetic factors account for 10–15% of the risk of developing cancer, with lifestyle being the primary contributor. For instance, we cannot modify genetic factors. We can manage our lifestyle to lower the risk of health issues like cancer. This adaptation includes eating a balanced healthy diet, participating in daily physical activities, avoiding smoking, and managing stress levels.

1.2.1 The impact of modifying cancer risk factors:

Adjusting lifestyle factors such as diet and exercise can lower the risk of cancer and other diseases while also improving the outcomes of many more, such as heart diseases. They play an important role in improving metabolic and immune health, which both play important roles in cancer progression. Several studies have suggested that ketogenic diets contribute to enhancing the treatment of cancer and diabetes and increase the survival rate. A ketogenic diet (KD) is a high-fat dietary regimen. In clinical trials conducted since 1920, a low to no carbohydrate diet with a consistent protein content has been established. The mechanism of action of the ketogenic diet is that by reducing carbohydrate intake, the body will deplete its supply of sugar. Subsequently, the liver will transition to using fat for oxidation. Following that, the final product will consist of ketone bodies. Key components of ketone bodies are acetoacetate, β -hydroxybutyrate (β -OHB), and acetone. The KD has been shown to enhance the prognosis of the following diseases: cancer, diabetes, cardiovascular disease, and epilepsy (Dowis & Banga, 2021). A scientific investigation demonstrated that individuals diagnosed with type 2 diabetes who adhere to a KD for 15 months exhibit a significant decrease in haemoglobin A1C (HbA1c) levels from 7.5% to 5.9%. HbA1c evaluates the mean blood glucose levels over the last three months. This indicates that they have successfully achieved the recommended normal value for HbA1c, which is below 6% (Westman et al., 2008). Another study used KD for 56 weeks on 66 obese people, with nearly half of them having high cholesterol and the other half being normal. The results show a significant improvement in blood lipid profile. It shows a significant reduction in triglycerides, total cholesterol, glucose, and LDL cholesterol while increasing HDL cholesterol (Dashti et al., 2006). Another study administered KD to mice with brain metastatic cancer, and the tumour was monitored *in vivo* using bioluminescent imaging. The results show that the KD fed group had smaller tumours than the control group. Also, KD increased the survival rate by 56.7%. On the other hand, when KD and Hyperbaric oxygen therapy (HBO2T) - the oxygen nourishes the tumour, thereby halting the cancer-causing effects of hypoxia - were combined, the outcome improved significantly, with a decrease in tumour growth and a 77.9% increase in survival rate (Poff et al., 2013). In a different study on mice with lung cancer, the combinations of KD and radiation showed a significant reduction in tumour growth when compared to the control (B. G. Allen et al., 2013). Another healthy diet that research has demonstrated is a plant-based diet which can inhibit the growth of cancer. Plant-based diets rich in vegetables and fruits that contain high antioxidant and anti-inflammatory properties have been shown to improve survival rates in

cancer patients, including CRC (Hardt et al., 2022). A study conducted by the NHS found that consuming a high amount of vegetables and fruits reduced all-cause mortality by up to 16% (Shah & Iyengar, 2022).

This suggests that diet is critical in preventing or reducing the risk of cancer growth. As a result, attempting to incorporate a healthy lifestyle would contribute to a reduction in global cancer incidence.

1.3 Breast cancer progression:

Mammary epithelial cells in the normal mammary gland are a single layer of polarized cells that grow around the empty lumen of the duct where milk can flow, and the entire duct is surrounded by a specialized thin layer of extracellular matrix (ECM) called the basement membrane (BM) (Figure 1.1).

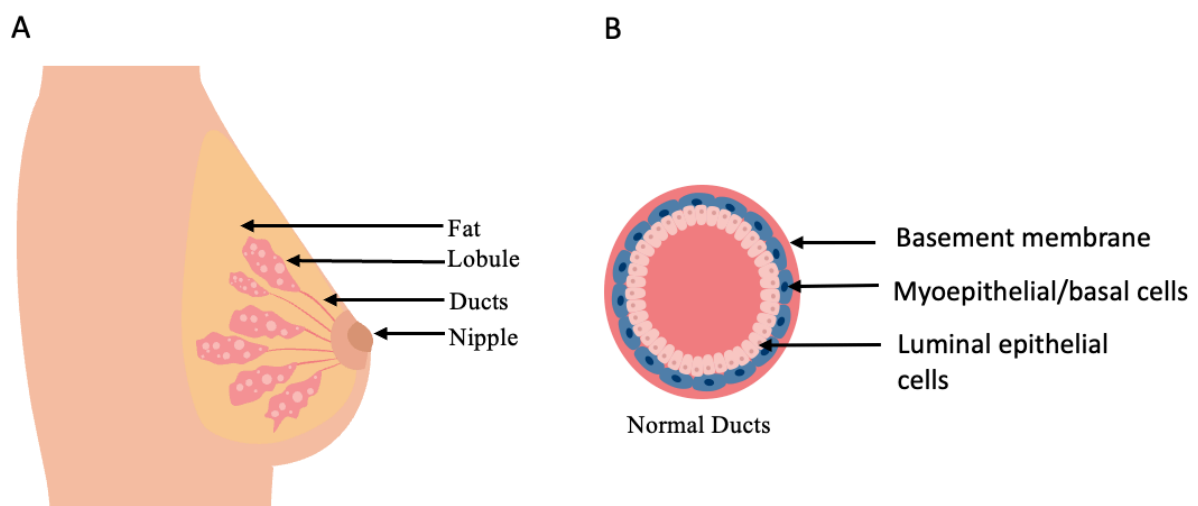


Figure 1.1: Breast anatomy. (A) Schematic illustration of breast anatomy. (B) The breast duct and lobules are breast tissues that surround a hollow space known as the lumen, which is surrounded by epithelial and myoepithelial cells. Following this, a basement membrane layer separates the myoepithelial cells from the surrounding stroma.

Breast cancer progression can be classified into three stages. When breast cancer is in its early stages uncontrolled division of mammary epithelial cells occurs, resulting in the formation of a mass of epithelial tumor cells inside the duct lumen. This results in the development of Ductal carcinoma *in situ* (DCIS). It is considered non-invasive because the BM is still intact and surrounds the tumour. DCIS accounts for around 20% of all breast cancer diagnoses (Gupta et al., 2021). Cancer cells can develop the ability to degrade the BM, allowing them to invade the

surrounding tissues. This stage is known as Invasive Ductal Carcinoma (IDC) (Mannu et al., 2020). The third stage is characterised by the ability of breast cancer cells to enter the blood or lymphatic vessels, allowing them to spread throughout the body, resulting in the formation of secondary tumors at distant sites. This is referred to as metastatic breast cancer (**Figure 1.2**). This stage of cancer is extremely difficult to control and is the leading cause of breast cancer mortality in patients. The underlying mechanisms behind the progression of DCIS to IDC are still not well understood.

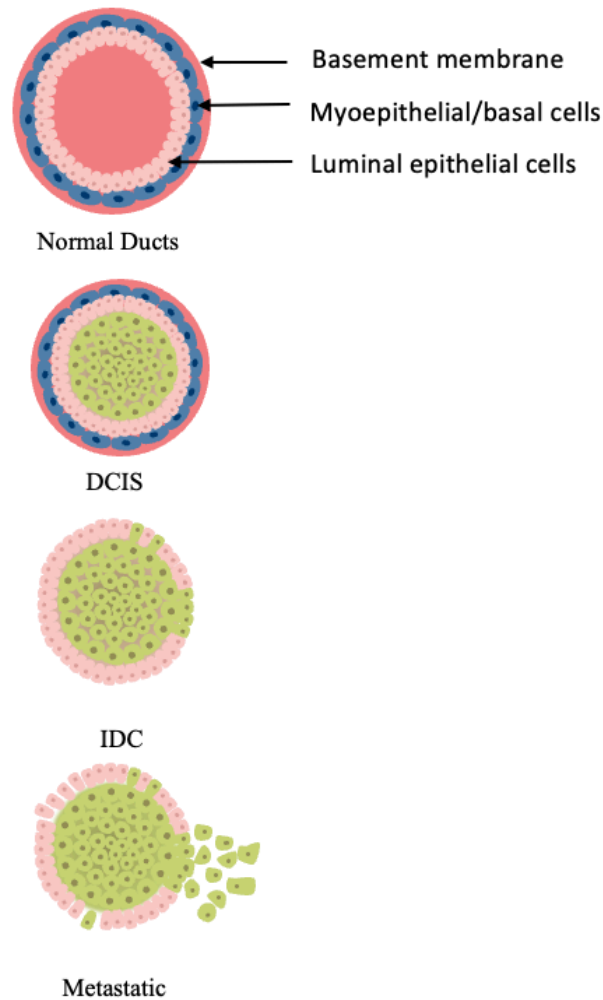


Figure 1.2: Breast cancer progression: Breast cancer progression is characterised by excessive division of mammary epithelial cells, which results in the formation of ductal carcinoma in situ (DCIS). Cancer cells breakdown the basement membrane and infiltrate surrounding tissues. This stage is referred to as Invasive Ductal Carcinoma (IDC). Breast cancer cells can enter the blood or lymphatic vessels and spread throughout the body, forming secondary tumours at distant sites. This is known as metastasis.

Several factors, including prognostic markers like tumour size, age, the thickness of the DCIS lesion, and the tumour microenvironment (TME) can influence the transition from DCIS to IDC (Silverstein & Lagios, 2015). The TME is complex and heterogeneous. Its composition varies according to the type of cancer; however, it exhibits similar characteristics, including Myoepithelial cells (MECs), extracellular matrix (ECM), adipocytes, immune cells, and cancer-associated fibroblasts (CAF) (Anderson & Simon, 2020).

1.3.1 Myoepithelial cells (MECs):

Breast MECs naturally suppress tumours, and express anti-tumour protein markers such as p63 and p73 (Hernández Borrero & El-Deiry, 2021). Breast cancer has been associated with the loss of these markers. p63 and p73 has been shown to suppress the tumour by controlling cell growth. They achieved this by modulating cell proliferation, apoptosis, and migration—all essential processes for the progression of the tumour (Hayward et al., 2022). This is how they maintain the whole mammary epithelium integrity and ensure the cells' functional stability.

MECs derived from DCIS tumours exhibits distinct characteristics, notably low expression of p63 and high expression of $\alpha\beta6$ integrin, among other markers (Anderson & Simon, 2020). A research study found that increased levels of $\alpha\beta6$ promote cancer progression by upregulating different matrix metalloproteinase (MMP) expression and activity (M. D. Allen et al., 2014). Another study reported that in epithelial cells the high levels of $\alpha\beta6$ upregulate the TGF β signalling pathway. The TGF signalling pathway involves the binding of LPA2, which activates intracellular Gq α , thereby initiating the RhoA and Rho kinase cascade (Xu et al., 2009). This could explain how $\alpha\beta6$ promotes invasion by activating the TGF β signalling pathway, which leads to the upregulation of matrix metalloproteinase levels.

1.3.2 Adipocytes:

Obesity has been linked to an increased risk of breast cancer (Dehesh et al., 2023). Researchers discovered that the denser the breast, the more adipocytes it contains (Soguel et al., 2017). Cancer-associated adipocytes (CAAs) have been shown to promote tumour growth in xenograft models as well as cancer cell proliferation and invasion in culture (Zhao et al., 2020). This effect was enhanced following the secretion of adipokines such as leptin (Atoum et al., 2020). Additionally, increased leptin levels can lead to chronic inflammation by increasing the secretion of proinflammatory cytokines like tumour necrosis factor α (TNF α) and interleukin 6 (IL-6) (Iikuni et al., 2008). According to another study, upregulation of TNF α promotes breast cancer progression through increased cell proliferation (Mercogliano et al., 2020). Another study found that CAAs increased the expression of YAP/TAZ, in the other hand suppressing YAP/TAZ by using pharmacological inhibitor in turn reduced tumour growth. Therefore, it suggests that CAAs promote tumour growth via the YAP/TAZ signalling pathway (Song et al., 2024). While immune cells play a vital part in DCIS progression, relying on them to estimate the progression or relapses of the cancer presents a challenge. This is due to a variety of factors, including heterogeneity, which varies from person to person; technical

challenges, which make it difficult to accurately measure immune cells; and limited techniques. Taken together, we need further research to understand how the immune system regulates the progression of DCIS to IDC.

1.3.3 Fibroblasts:

It has been widely reported that cancer-associated fibroblasts (CAFs) play an important role in the initiation and progression of breast cancer (Zheng & Hao, 2023). There is no specific marker for CAFs, but they are distinguished by high expression of several markers, including *α-Smooth muscle actin* (α SMA) and platelet-derived growth factor receptor- α (PDGFR α) (Nurmik et al., 2020). It has been reported that CAFs exhibit different gene expression profiles when compared to normal fibroblasts isolated from malignant breast tissue (Singer et al., 2008). In one study, fibroblasts raised the level of COX-2 in DCIS, which led to higher levels of VEGF and MMP14, which help the cancer invasion, It is unclear what type of fibroblast was used or whether it became CAF when cocultured with cancer cells. (Min Hu et al., 2009). Reports indicate that CAFs secrete several factors, including HGF (Tyan et al., 2012). Studies have demonstrated that HGF stimulates the proliferation of the mammary duct. Furthermore, growing MDA-MB-468 breast cancer cells with CAF increased the production of HGF, which led to more colony formation and tumour growth *in vivo* (Scherz-Shouval et al., 2014). Overall, studies have shown that CAFs promote breast cancer progression by increasing the secretion of various factors. We need more research to comprehend how this effect triggers the downstream pathways that progress DCIS to IDC.

1.4 Molecular Subtypes of Breast Cancer

Breast cancer is classified using immunohistochemistry, which determines the expression of several markers such as human epidermal growth factor receptor (HER2), oestrogen receptor (ER), proliferation marker Ki-76, and progesterone receptor (PR). Breast cancer can be divided into different subtypes based on the expression of these receptors: luminal A, luminal B, HER2-positive, and triple-negative (Łukasiewicz et al., 2021; Matro, 2015).

The luminal A subtype is characterised by the expression of ER and/or PR and absence of HER2. Furthermore, it expresses Ki-67 at a low level in approximately 20% of tumours (Łukasiewicz et al., 2021). It is considered the most common form, as it accounts for around 70% of all breast cancer cases. Second tumours occur most frequently at the bone level, while they are less common in the central nervous system (CNV). Similarly, in the case of the

recurrent, the survival rate is high (Matro, 2015). The 5-year survival rate percentage is 95.1% and the percentage of the relapse is 27.2% (Eroles et al., 2012).

Luminal B exhibits aggressive behaviour and accounts for nearly 40% of breast cancer patients. It is distinguished by a high level of Ki-67 and low expression of the ER, as well as low expression of the PR. The 5-year survival rate percentage is 95.1% and the percentage of the relapse is 29.4% (Li et al., 2016).

HER2- non-luminal breast cancer is more aggressive and presents a worse prognosis than luminal breast cancer when it recurs. It is distinguished by the high expression of Ki67 and HER2 and the lack of ER and PR. It accounts for 10-15% of all breast cancer cases (Łukasiewicz et al., 2021). The 5-year survival rate percentage is 92.2% and the percentage of the relapse is 25.9% (Orsaria et al., 2021).

Triple Negative Breast Cancer (TNBC) is extremely aggressive and accounts for 10-15% of all breast cancer cases. Its distinguishing feature is the lack of expression of ER, PR, HER2. The 5-year survival rate percentage is 77% and the percentage of the relapse is 40% (Dass et al., 2021). Click or tap here to enter text. Click or tap here to enter text.

1.5 The MCF10 series of cell lines as a breast cancer progression model:

In cancer research various methods and techniques are used to elucidate the molecular mechanisms driving tumour progression. These include *in vivo* models, *in vitro* cell culture models and clinical studies (Brock et al., 2019). The MCF10 series of cell lines has been extensively used in breast cancer research. The MCF10A cell line was established in the 1990s by Soule and colleagues from human breast epithelial tissue and are thus non-transformed epithelial cells. (Soule HD, 1990). MCF10A cell line is simple to work with because it has a stable normal genome in culture, allowing the generation of consistent and reproducible results. The great feature of this series of cell lines is that it allows researchers to study different stages of breast cancer using the same cell line derivatives, which includes MCF10AT1, MCF10DCIS and MCF10CA1 (Santner et al., 2001; So et al., 2014). MCF10AT1 cells were generated by introducing active Hepatocellular Antigen Synthesiser (HRAS) into MCF10A, resulting in the formation of a pre-malignant cell line. When introduced into immunodeficient mice, it initiates the formation of lesions resembling

atypical ductal hyperplasia (ADH) and DCIS, and 25% of them progress to IDC, suggesting a carcinogenic characteristic (Dawson et al., 1996; So et al., 2014). MCF10AT1's xenograft lesion was extracted from mice, cells were grown, and cloned to generate MCF10DCIS.com, a cell line that was later inserted into immunodeficient mice's mammary fat pads and started to form tumour lesions that resembled DCIS (Fred R. et al., 2000; So et al., 2014). MCF10CA1a is a highly invasive cell line that spread rapidly. It was generated through several passages of MCF10AT1 in immunodeficient mice. When MCF10CA1a is inserted into immunodeficient mice, larger metastatic tumours form in their lungs (Santner et al., 2001; So et al., 2014).

1.6 The extracellular matrix (ECM) in cancer:

The ECM is a vital component of a cell's environment that is remarkably dynamic and adaptable, influencing key elements of cell biology. The ECM affects practically all cellular behaviours, either directly or indirectly, and is critical for developmental events (P. Lu et al., 2012). ECM stores signalling molecules and growth factors in addition to the core matrix components, which include around 300 proteins, proteoglycans, glycoproteins, and polysaccharides (Naba et al., 2012). Each ECM component has different physical and biochemical properties (P. Lu et al., 2012). One of the core aspects in traditional embryology is that niches or local microenvironments play a significant role in regulating cell behaviours. This notion is becoming widely acknowledged in cancer biology too (Lin & Scott, 2012). Extensive research has been done to find out how genetic changes originate and encourage cancer growth. These findings increased our knowledge of how tumours form and accelerated the discoveries of new genetic therapies in cancer (Bhowmick et al., 2004). However, new research has revealed the relevance of non-cellular niche components, particularly the ECM in cancer growth. Different regulatory mechanisms have been proposed to guarantee that ECM dynamics, as measured by its formation and degradation, are tightly controlled during organ growth and functioning (Bauer et al., 2007). Disruption of these regulatory mechanisms causes changes in the ECM organisation, resulting in abnormal cell activity in the niche and, ultimately, failure of organ stability and function. In ailments like tissue fibrosis and cancer, aberrant ECM dynamics are one of the most obvious clinical results (Cox & Ertler, 2011). Several abnormalities in the ECM have been linked to breast cancer and have been shown to hasten the disease's progression (Oskarsson, 2013). Pregnancy causes significant changes in the structure of the mammary gland. This is especially noticeable during post-lactational mammary gland involution. The mammary gland is made up of milk-transporting lactiferous ducts that increase and branch widely

throughout pregnancy as a result of oestrogen, growth hormone, cortisol, and prolactin. The involution process begins at the end of the lactation process. Mammary gland involution is the procedure by which mammary glands revert back to a non-lactating state following weaning, which is characterised by epithelial cell death and tissue repair. It has been claimed that involuting mammary gland contains cancer-promoting components. Indeed, tumorigenic matrix fragments in ECM extracted from involuting mammary glands stimulated breast cancer cell proliferation *in vitro* and promoted metastasis in animal models (Lyons et al., 2011; Oskarsson, 2013). Interestingly, the composition of the involuting mammary gland ECM and cancer-associated ECM share some similarities (Oskarsson, 2013). ECM has a critical role in the progression and metastasis of breast cancer; consequently, understanding its role will aid in the development of novel treatments that target cell-ECM interaction. Laminins, entactin, type IV collagen, and proteoglycans make up the majority of the BM. Many ECM proteins, including type I, II, and III fibrillar collagens, vitronectin, fibronectin, elastin, are key component of the interstitial matrix and can be produced by stromal cells, adipocytes, and immune cells. COL I, III, IV, VI, fibronectin, laminin 332, periostin, and vitronectin enhance tumour proliferation and metastasis, while DMBT1 and SPARC suppress breast cancer formation and tumor growth (Zhu et al., 2014).

1.7. Components of the extracellular matrix:

1.7.1. Collagens:

Collagen is one of the most common proteins found in the body. It is commonly found incorporated into the ECM structure of connective tissues such as skin. Collagen is best known for its role as a structural protein within the ECM, providing structural strength support, but it also participates in other cell processes such as adhesion and migration (Kular et al., 2014). There have been 28 different types of collagen identified. Collagen type 1 accounts for nearly 90% of total collagen in the human body. Thus, type 1 is the major component of connective tissues and organs (B. Sun, 2021). Collagen type 1 is made up of three polypeptide chains that intertwine to form a trihelix structure. The collagen motifs are made up of three repeated amino acid sequences, Gly-X-Y. Gly stands for glycine, and X or Y may contain any type of amino acid other than Gly. X and Y are typically proline and hydroxyproline (Keller et al., 2022). Collagen can be classified as fibril forming collagen such as type1 collagen, fibril associated collagen with interrupted triple helices (FACITs) such as type IX, network forming collagen such as type IV, VI, VIII and X, transmembrane collagens such as type XIII, anchoring fibrils such as type VIII and beaded filament forming collagen such as type VI (Onursal et al., 2021).

Collagen synthesis starts with one α -polypeptide (two $\alpha 1$ and one $\alpha 2$) chain made up of glycine, proline, and hydroxyproline. Three of these chains combine to create a triple-helical structure known as procollagen. The procollagen structure is reinforced with propeptides at the end to prevent collagen assembly within the cell. Procollagen, is then released into the extracellular matrix. Once procollagen is secreted in the ECM, Metalloproteinase enzyme procollagen peptidase cleaves the propeptides at the N and C termini of the procollagen to form mature collagen. Following that, mature collagen begins to self-assemble into collagen fibres, which then aggregate to form larger collagen fibres (**Figure 1.3**)(Gomes & Salgueiro, 2022).

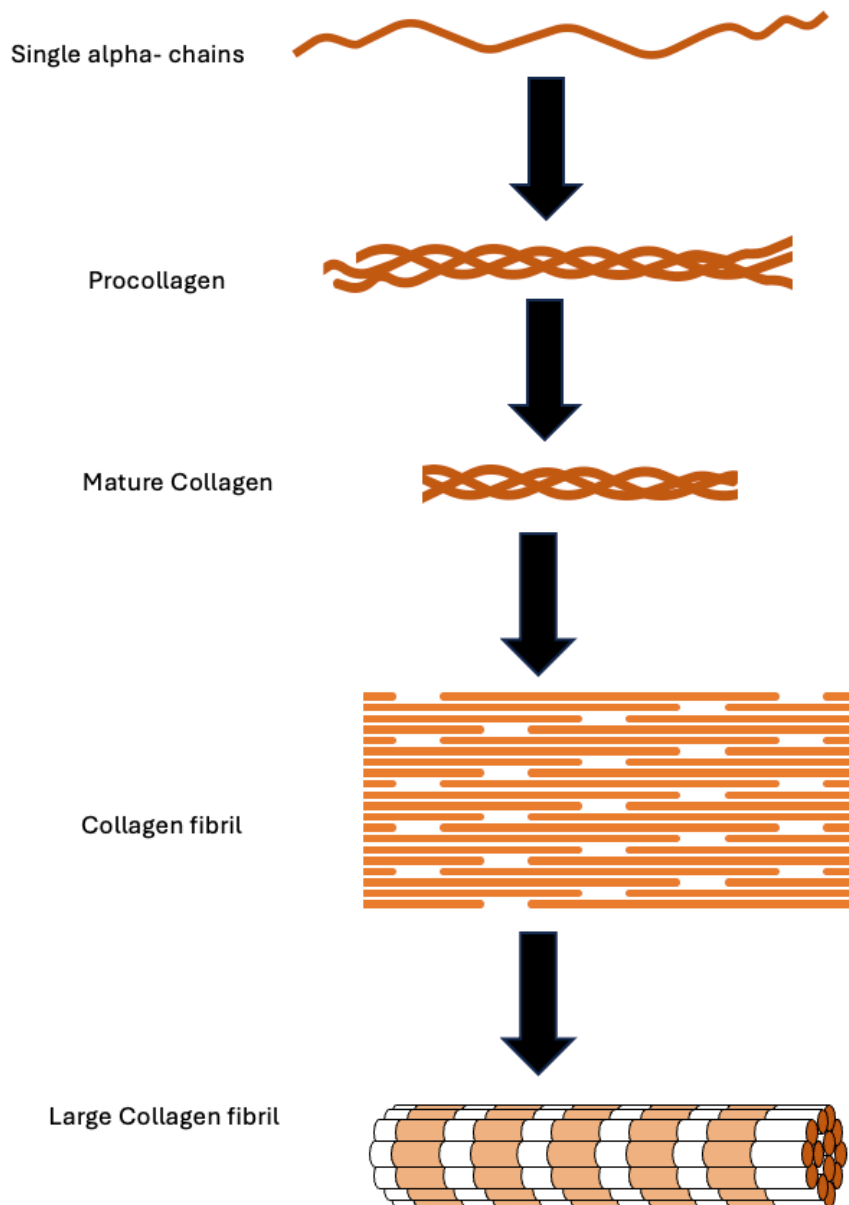


Figure 1.3: Collagen-1 synthesis and assembly. Collagen synthesis begins with a single alpha-polypeptide chain consisting of glycine, proline, and hydroxyproline. Three of these chains wrap around each other to form a triple-helical structure known as procollagen. Later, it is secreted into the extracellular matrix, where it is cleaved into mature collagen. Subsequently, it initiates the formation of collagen fibres, which then aggregate to form larger collagen fibres.

1.7.2.Fibronectin:

Fibronectin is considered the second most common ECM protein. It is divided into two types. Insoluble fibronectin is found in the ECM, whereas soluble fibronectin is found in the plasma. Hepatocytes synthesise plasma fibronectin and secrete it into the bloodstream (Tamkun & Hynes, 1983). Fibronectin consists of two monomers that are linked together by a disulphide bond at the C-terminus. Each monomer is composed of repetitions of three types of modules:

Laminin and collagen IV have a unique feature because they self-assemble. Basement membranes are assembled in two primary stages. The first component to be deposited around the cell surface is laminin, which forms the basic BM layer (Meghan A Morrissey et al., 2013; Peuhu et al., 2022). Type IV collagen is subsequently incorporated and covalently crosslinked through disulphide and sulfimine bonds to enhance the mechanical strength of the BM. Laminin and collagen establish separate networks, while nidogen and perlecan interlink these networks to create a cohesive ECM (**Figure 1.5**) (Jayadev & Sherwood, 2017).

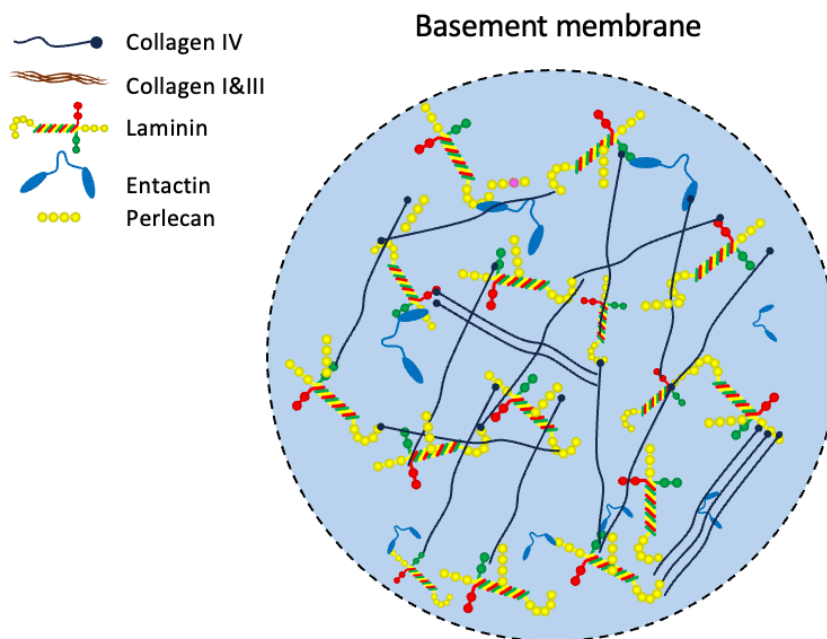


Figure 1.5: Structure of the basement membrane (BM). The BM is composed of different proteins such as laminin, collagen IV, entactin (nidogen), and perlecan. These proteins work together to form a network that separates epithelial cells from the stroma and supports cells.

Given that BM degradation is essential in various processes, including tissue remodelling, immune response, and wound healing, any disruption to this system constitutes a significant issue (Jayadev & Sherwood, 2017; Pozzi et al., 2017). MMPs, specifically MMP-2 and MMP-9, are implicated in the degradation of type IV collagen and laminin, and they promote cellular migration across the BM during physiological processes (Jayadev & Sherwood, 2017). However, when degradation is uncontrolled, it leads to various diseases or pathological conditions (Meghan A Morrissey et al., 2013). For example, increased BM breakdown in cancer facilitates the invasion of adjacent tissues and the dissemination of cancer cells to other regions of the body.

Matrigel and Geltrex are BM preparations derived from murine tumours. They are widely used in *in vitro* experiment because they are native BM components and provide a setting to examine cell invasion behaviours in 3D systems (Jean A Engbring & Hynda K Kleinman, 2003).

1.8.1. Laminins:

Laminin is a heterotrimeric protein, composed of an α , β and γ chain. There are 5 α , 4 β , and 3 γ genes. Disulfide linkages link them together, resembling crossed-shaped structures (**Figure 1.6**) (Givant-Horwitz et al., 2005). Laminin exists in a variety of isoforms. Each one is named based on its unique composition (**Table 1.1**). For instance, Laminin 111 consists of $\alpha 1$, $\beta 1$, and $\gamma 1$. Laminins play numerous important roles, including cell adhesion, migration, and signalling (Halder et al., 2022; Hamill et al., 2009; Rousselle & Scoazec, 2020).

Table 1.1: Laminin isoforms. Laminins are named based on their three-chain structure, with the first number referring to the α chain, the second number to the β chain and the third number to the γ chain.

Type	α	β	γ
Laminin-111	$\alpha 1$	$\beta 1$	$\gamma 1$
Laminin-211	$\alpha 2$	$\beta 1$	$\gamma 1$
Laminin-121	$\alpha 1$	$\beta 2$	$\gamma 1$
Laminin-221	$\alpha 2$	$\beta 2$	$\gamma 1$
Laminin-332	$\alpha 3$	$\beta 3$	$\gamma 2$
Laminin-311	$\alpha 3$	$\beta 1$	$\gamma 1$
Laminin-321	$\alpha 3$	$\beta 2$	$\gamma 1$
Laminin-411	$\alpha 4$	$\beta 1$	$\gamma 1$
Laminin-421	$\alpha 4$	$\beta 2$	$\gamma 1$
Laminin-511	$\alpha 5$	$\beta 1$	$\gamma 1$
Laminin-521	$\alpha 5$	$\beta 2$	$\gamma 1$
Laminin-213	$\alpha 2$	$\beta 1$	$\gamma 3$

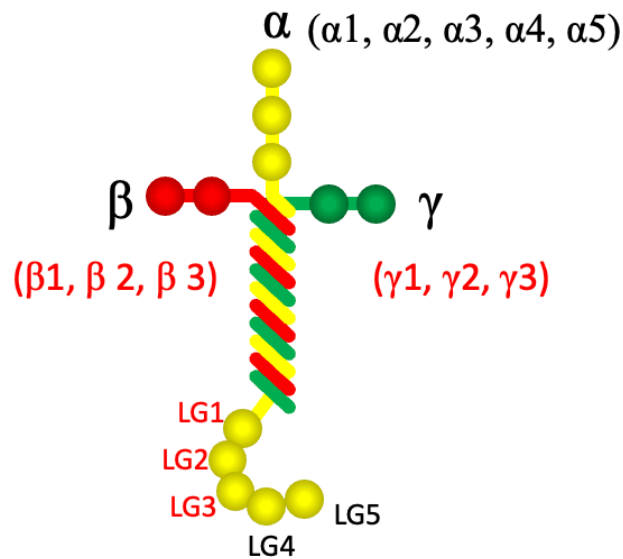


Figure 1.6: Laminin structure. Three chains of polypeptide, alpha, beta, and gamma, make up the cross-shaped structure known as laminin.

1.8.2. Laminins in breast cancer:

Cancer's development and spread require changing the balance of ECM signalling (Oskarsson, 2013). Matrix biology poses two major challenges: understanding how it functions in a state of health and how disruptions in ECM dynamics may contribute to the development and spread of cancer (Walker et al., 2018). Furthermore, extensive reports suggest that a high level of laminin contributes to cancer growth and metastasis (Gonzales et al., 1999; Zhou et al., 2020).

Several epithelial tumour types express high levels of laminin 332, which flock at the tumour's interface with the surrounding matrix. The expression of laminin 332 in various cancer types, including breast and cervical cancer, positively correlates with tumour invasiveness and poor patient prognosis (Givant-Horwitz et al., 2005; Ramovs et al., 2017; Tsuruta et al., 2008). Laminin 332 in breast cancer was reported in several studies to promotes tumour invasiveness and the migration of breast cancer cells (Kim et al., 2012; Troughton et al., 2022; Yin et al., 2022). Reports suggest that laminin 332 could enhance breast cancer cell motility via integrins (Carpenter et al., 2009). Research has shown that the laminin binding receptors $\alpha3\beta1$ and $\alpha6\beta1$ are significantly up regulated and contribute to the progression of breast cancer (Faraldo et al., 2024; Gonzales et al., 1999; Troughton et al., 2022; Zhou et al., 2020). Research suggests that the activation of the FAK/ERK signalling cascade by laminin binding to $\alpha3\beta1$ initiates breast cancer cell proliferation (Miskin et al., 2021; Mitchell et al., 2010; Ramovs et al., 2019)

Research has linked different laminin isoforms, such as laminin-111 and laminin-511, to the progression of tumours in various cancer types, including breast and liver cancer (Banerjee et al., 2022). Researchers have discovered that laminin-111 promotes cancer through a variety of physiological processes, including cell adhesion and migration, as well as by facilitating tumour growth and metastasis (Kikkawa et al., 2013). According to recent research, one peptide derived from the laminin-111 sequence and synthesized manually using Solid Phase Peptide Synthesis (SPPS) corresponding to the cleaved fragment YIGSR (β 1 chain) peptide acts as a tumour suppressor, whereas the IKVAV (α 1 chain), and KAFDITYVRLKF (γ 1 chain) peptides act as tumour promoters. This leads to the conclusion that Laminin-111 has multiple active sites that either suppress or promote tumour growth (Mendonça et al., 2024). Another study found that laminin-511 promotes the migration and invasion of metastatic breast cancer cells in the bone. This effect occurs in response to an increase in MMP-9 levels and stimulation of the ERK and AKT signalling pathways (Denoyer et al., 2014).

1.9. ECM receptors

Matrix receptors typically connect ECM to cells, mediating the connection and initiating cellular signalling pathways (Chua et al., 2016; Hynes, 2009; Walker et al., 2018). The most studied ECM receptors are the members of the integrin family. In addition, other families of ECM receptors also play a role in cell-ECM adhesion and each of these receptors has specific functions and signalling properties that enable tissue formation and cell signalling. These include: CD44, discoidin domain receptor, Hyaluronan-mediated motility receptor also called Rhamm, and dystroglycans (Zhu et al., 2014).

Integrins receptors are the most abundant ECM receptors in all eukaryotes (Chua et al., 2016). They play roles in modulating cellular function such as cell adhesion, migration, growth, and proliferation (Hynes, 2009; Walker et al., 2018). Integrins consist of heterodimers composed of an α and a β subunit (Pang et al., 2023; L. Sun et al., 2023). There are 18 α and 8 β subunits, forming 24 different heterodimeric integrin receptors (L. Sun et al., 2023). Integrins can be stimulated using two primary signalling mechanisms, Inside-Out Signalling and Outside-In Signalling. Inside-Out Signalling is triggered by adaptor proteins like talin binding to the tail of a β integrin. This activates integrins, resulting in conformational changes from a bended to an extended shape. This eventually recruits proteins like Kindlins, resulting in the activation of signalling pathways promoting cell adhesion, migration, ECM assembly, and remodelling (Pang et al., 2023; L. Sun et al., 2023). Outside-In Signalling is triggered by an ECM protein

binding to an integrin, resulting in the recruitment of several focal adhesion proteins like FAK and Src and leading to the activation of different signalling pathways, including Rac, mitogen activated protein kinase (MAPK) and phosphatidylinositol 3 kinase (PI3K)/AKT. This leads to the regulation of gene expression, survival, and other processes (**Figure 1.7**) (Pang et al., 2023; L. Sun et al., 2023).

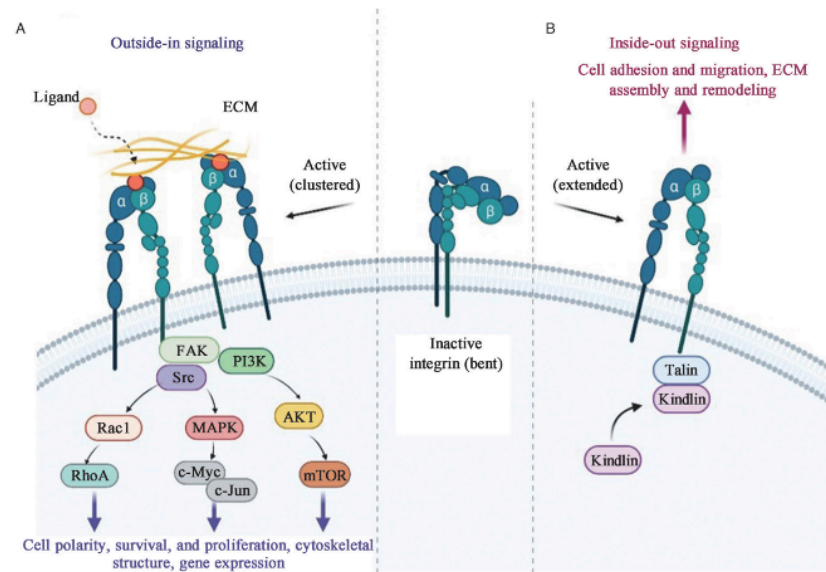


Figure 1.7: Integrin signalling pathways. (A) An ECM protein binds to an integrin to initiate outside-in signalling, which attracts several focal adhesion proteins and stimulates various signalling pathways. (B) The binding of talin to the b integrin tail initiate the inside-out signalling. This promotes in integrin activation, which attracts proteins like kindlins, resulting in the activation of signalling pathways that promote cell adhesion, migration, ECM assembly, and remodelling. Figure taken from Gao Q, et al, 2023.

1.10. Focal adhesion proteins

Focal adhesions comprise a large, complex group of proteins that play a critical role in initiating cell-ECM interactions (Murphy & Brinkworth, 2021). This is critical for cellular processes such as migration, proliferation, and survival. Integrins, tensin, talin, vinculin, kindlin, paxillin, focal adhesion kinase (FAK), Src family kinases, actin, and myosin II are some of the proteins that are enriched in focal adhesion (Legerstee & Houtsmuller, 2021). FA formation is a tightly controlled process. ECM binding activates integrins, triggering a conformational change that leads to the unfolding of bended integrins. Consequently, the formation of cell adhesion starts with the recruitment of focal adhesion proteins, specifically talin. This triggers the autophosphorylation of FAK-talin, which in turn attracts other focal adhesion proteins. First, Src is phosphorylated. This makes FAK-related proteins like tensin,

vinculin, kindlin, and paxillin phosphorylated as well (Legerstee & Houtsmuller, 2021; Murphy & Brinkworth, 2021). After this, it appears that myosin II initiates the assembly process for FA maturation. Actin fibres pull FA maturation and enrich it with the protein TNS, leading to the formation of fibrillar adhesion (**Figure 1.8**) (Beedle et al., 2023)

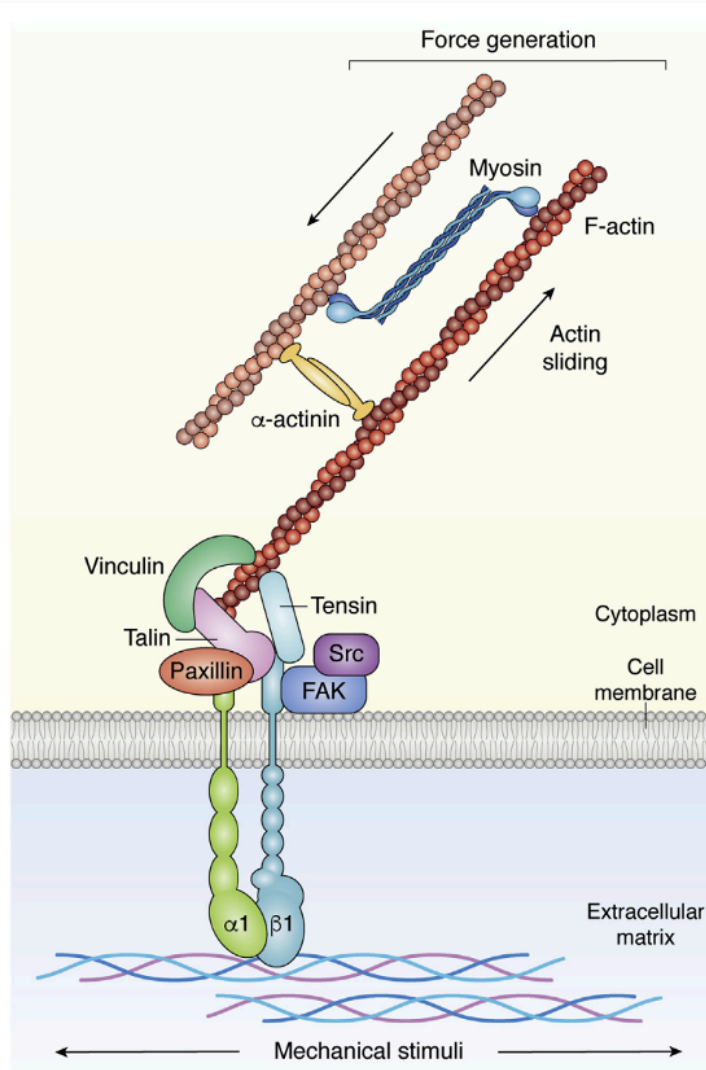


Figure 1.8: Focal adhesion formation. When the ECM comes into contact with integrin, it activates integrin, which then begins to recruit focal adhesion proteins such as Focal adhesion kinase (FAK), Src, paxillin, talin, vinculin and tensin to form focal adhesion. . This connects the ECM to the actin cytoskeleton. α -actin, F-actin, and myosin generate traction force to facilitate vital cellular processes. Figure is taken from Andrea Zancla et al.,2023.

1.11.Tensins:

Tensins are focal-adhesion binding proteins that were first reported in 1991 (Liao & Lo, 2021). Mammals contain four different isoforms. The firstly identified tensin protein was named as tensin-1 (TNS1), and three more proteins belonging to this family, namely tensin-

2 (TNS2), tensin-3 (TNS3) and tensin-4 (TNS4), were identified as similar to TNS1. TNS2 is also called C1-Ten (TENC1) and tensin 4 is also referred to as C-terminal tensin-like (CTEN) (**Figure 1.9**) (Liao & Lo, 2021). Tensins are known to play a significant role in regulating cell adhesion and fibrillar adhesion formation which arise after the focal adhesion maturation (Liao & Lo, 2021). Tensins are large proteins as their size ranges between 170 kDa and 220kDa excluding TNS4, which has a size of ~80 kDa (Lo, 2017). Tensins contain several domains. The Src homology 2 (SH2) domain is a motif known to recognize and associates specifically with phosphotyrosine (pTyr), that makes tensin a part of signal transduction pathways. It serves to connect these pathways with cytoskeletal networks. A protein tyrosine phosphatase (PTP), phosphotyrosine-binding (PTB) domain is found at the carboxyl termini. The PTB binds to the cytoplasmic tails of β -integrins, as well as other pTyr containing proteins (Cui et al., 2004). The actin binding domain (ABD) mediates the interaction with actin filaments, while the focal adhesion binding site (FAB) is required for tensin recruitment to focal adhesions (Fig 3) (Liao & Lo, 2021). When phosphorylated the SH2 domain of TNS becomes an effective binding sites for ligands which include Src, FAK, p130Cas among others, making it a site of signaling activity (H. Huang et al., 2008). There are three tyrosines in the TNS3 SH2 domain: Y1173, Y1206, and Y1256. Phosphorylation of the tyrosines in the SH2 domain is mediated by Src. Additionally, reports suggest that the residence tyrosines in SH2 domain play a significant role in the biological activity of TNS3. Qian et al. (2009) observed a high expression of Src in primary breast cancers compared to normal breast tissue. Furthermore, mutating the SH2 tyrosines in H1299 lung cancer cells resulted in a reduction in cell migration compared to WT (Qian et al., 2009). In another study, it has been demonstrated that TNS3 is important for proper growth of new born mice. One third of the mice lacking TNS3 exhibited growth retardation and died within 3 weeks after birth. The cause of death is not completely understood but it might be due to a combination of defects in the intestine, lung, and bone (Chiang et al., 2005). The common theme of these defects is related to incomplete development in these tissues. However, these observations indicate that TNS3 is essential for normal development and functions of the small intestine, lung, and bone (Chiang et al., 2005). Studies have demonstrated the role of Tensin 1 in maintaining renal function and skeletal muscle (H. Chen et al., 2002; Lo, 2017). Mice with TNS1 KO developed cysts and eventually died of renal failure. Researchers have also shown that Tensin 1 deficiency impairs skeletal muscle angiogenesis and regeneration (H. Chen et al., 2002; Lo, 2017). TNS2 knockout in FVBGN mice causes nephrotic syndrome, which leads to renal failure; the mice died eight weeks later. However, this

behaviour has been shown to be strain-dependent, as in C57BL6 or SV129 strains, TNS2 knockout mice developed normally (Uchio-Yamada et al., 2016). Finally, TNS4 knockout mice showed no defects (Lo, 2017).

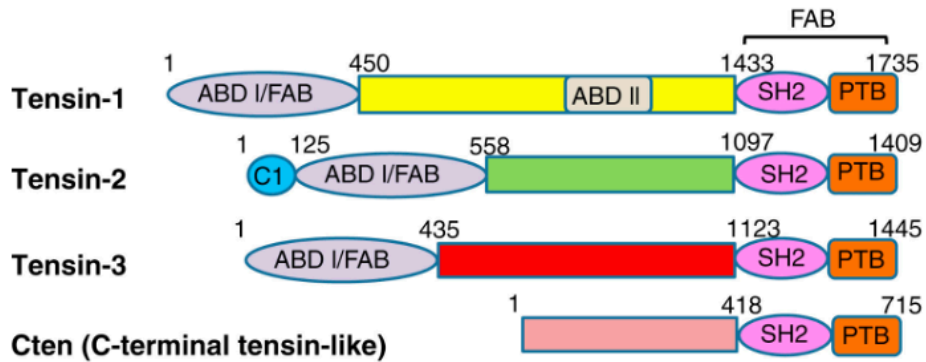


Figure 1.9: Tensin structure. This diagram represents the various forms of tensins and their functional domains. Figure is taken from Su Hao Lo, 2017.

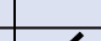
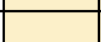
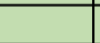
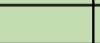
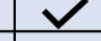
1.12. Role of tensins in cancer

Several studies have been performed to examine the role of the different tensins in cancer. TNS1 levels are low in twelve cancer types such as breast, colorectal, kidney, lung and ovarian cancer while high in three cancer types, including gastric cancer, esophageal cancer and lymphoma (Table.1.2). TNS2 has been shown to be down-regulated in different cancer types such as breast, colorectal, kidney, and lung cancer, whereas TNS3 has been shown to be elevated in some cancers, such as breast cancer, and decreased in others like kidney and lung cancer (Table.1.2) (Liao & Lo, 2021). TNS4 has been found to be up-regulated in cancers such as gastric, lung, and colorectal, while it has also been found to be down-regulated in cancers such as kidney cancer and melanoma (**Table 1.2**) (Liao & Lo, 2021; Lo, 2017; Mouneimne & Brugge, 2007). TNS1 and TNS2 have been shown to promote cell migration. The Boyden chamber migration assay was used on HEK293 cells to assess cell motility upon overexpression of TNS1 and TNS2. Cells expressing GFP-TNS1 or GFP-TNS2 migrated significantly faster than GFP control cells, The author did not provide any evidence of the molecular mechanism behind how overexpression of TNS1 or TNS 2 promotes migration (H. Chen et al., 2002). In another study, endothelial cells were isolated from both TNS1-null and WT mouse embryos. Cells lacking TNS1 migrated and proliferated at a significantly slower rate than their WT. In addition, this occurs in a TNS1 DLC1 RhoA signaling-dependent manner (Shih et al.,

2015). Additionally, TNS2 over-expression in HepG2 and BEL7402 cells, which endogenously have low TNS2 levels, significantly inhibited the formation of colony (Yam et al., 2006). TNS4 has shown to be downregulated in the majority of prostate cancer cell lines (Lo, 2017; Mouneimne & Brugge, 2007), as well as overexpressed in a breast cancer cell line (Albasri et al., 2011a).

Several publications highlighted that TNS3 levels are high in breast cancer cell lines (Chiang et al., 2005; Qian et al., 2009; Shinchu et al., 2015). Additionally, it was found that knocking down TNS3, but not TNS4, dramatically reduced cell migration, soft agar growth *in vitro* and tumor formation *in vivo* (Qian et al., 2009). It has also previously been shown that the deregulation of TNS3 promote cell migration, invasion and tumorigenesis in different cell lines from breast cancer, as well as melanoma and advanced lung cancer (Qian et al., 2009). Therefore, its role remains controversial.

Table 1.2: TNS expression levels were compared in various cancer diseases to normal tissues.

	TNS1		TNS2		TNS3		TNS4	
								
Breast Cancer		✓		✓	✓		✓	✓
Colorectal Cancer		✓		✓			✓	
Bladder Cancer		✓		✓				
Kidney Cancer		✓		✓		✓		✓
Leukemia		✓		✓	✓	✓		
Lung Cancer		✓		✓		✓	✓	
Melanoma		✓						✓
Gastric Cancer		✓						
Ovarian Cancer		✓		✓				
Prostate Cancer		✓				✓		
Sarcoma		✓						
Bladder Cancer		✓		✓				

1.13. Cell migration in cancer:

The hallmarks of cancer have been defined as key features associated with oncogenic transformation. These include the ability to sustain proliferation pathways, which allow cancer cells to continue to grow avoiding normal regulators; evading growth suppressors, due to the

loss of tumour suppressor genes such as p53; angiogenesis, in which cancer cells stimulate the formation of new blood vessels to support their growth; genome mutation and instability and invasion and metastasis activation (Hanahan & Weinberg, 2000). To be able to metastasise, cells must go through the invasion-metastasis cascade (**Figure 1.10**). Localised tumours enter the bloodstream, spread out, and form tumours at various locations. The first stage of invasion is localised invasion. During this stage, the cells migrate in various ways.

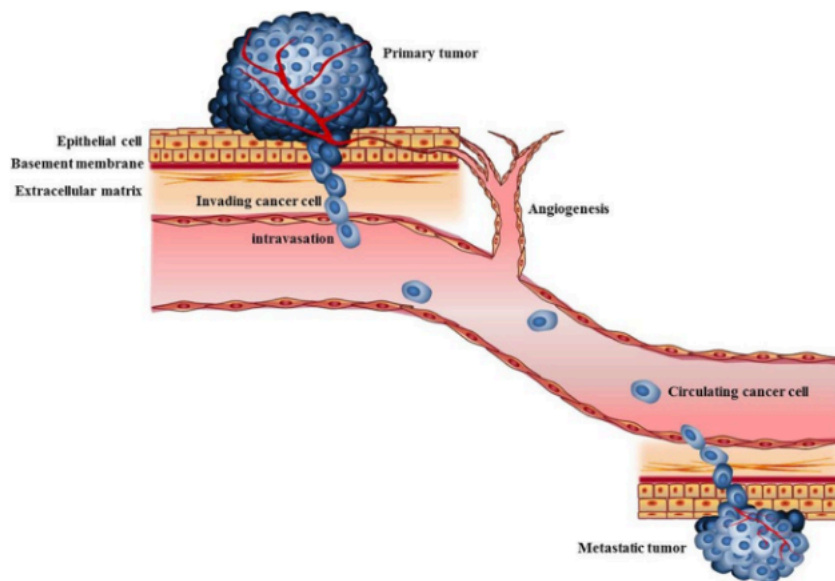


Figure 1.10: Invasion/metastasis cascade. After the formation of the primary tumour, cancer cells can acquire the ability to breach the BM and invade into the surrounding tissues. Subsequently, cancer cells can enter the bloodstream via the intravasation process and reach different tissues. Following extravasation, circulating cancer cells can established secondary tumours. Figure is taken from Shih-Chi Su et al., 2016.

Cell migration is an essential physiological process, such as during wound healing. During cancer metastasis, cells migrate to various parts of the body via individual cell migration including mesenchymal, amoeboid and collective cell migration (Friedl & Alexander, 2011). The microenvironment and cell types influence this process (Anderson & Simon, 2020). Cells that adopt mesenchymal migration begin to develop spindle-elongated morphology, and later, via integrin, they initiate cell-matrix interaction, this mode of migration is dependent on MMP-mediated ECM degradation. (Anderson & Simon, 2020). This type of migration is usually seen in sarcomas. Leukaemia mainly utilise amoeboid or rounded migration, which starts by forming spherical (round) shapes, this mode of migration is independent of MMP and is primarily driven by blebbing (Anderson & Simon, 2020). Collective migration refers to a group of cells migrating together as a cluster, solid strands; this type of migration is dependent on

cell-cell adhesion. The leader cells at the front of the cluster guide the follower cells. Another type of collective migration is bud protrusion, in which cells constantly change their positions without the need for leader cells (Anderson & Simon, 2020). Breast cancer commonly exhibits this type of migration (Anderson & Simon, 2020). Recent reports indicate that breast cancer cells invade nearby tissue and migrate collectively (Chang et al., 2024).

The migration cycle is described as a continuous chain of events that influence one another. Forming a protrusion is the first step in the cycle, followed by adhesion to the extracellular matrix using integrins. Following this, the cells contract with the help of myosin protein interactions with actin filaments to facilitate motility, which is essential during cell migration. The final step is the separation of the cells from the ECM to prevent movement resistance (Caswell & Zech, 2018). Actin cytoskeleton remodelling occurs when cellular protrusions form, allowing cancer cells to invade and migrate to different sites (Sarantelli et al., 2023). Lamellipodia, pseudopodia, and filopodia are three types of protrusions (Sarantelli et al., 2023). Lamellipodia, defined as sheet-like protrusions, are caused by actin filament branching and polymerisation, which creates tension and drives cell motion (Carmona et al., 2016; Machesky, 2008). Lamellipodia are formed at the front edges of migrating cells. Actin polymerisation is a highly controlled process; many proteins regulate it, particularly in the lamellipodia branch network, which is formed by actin polymerisation induced by Arp 2/3 complex proteins (Chávez-Paredes et al., 2019). Arp 2/3 complex proteins play an important role in the dynamics of lamellipodia formation, especially in metastatic cells that form lamellipodia at high rates, facilitating invasion and migration (Machesky, 2008). Pseudopodia are dense, sheet-like structures that cancer cells use to sense and interact with environmental stimuli in three dimensions. It allows cancer cells to migrate through the ECM (Choi et al., 2018). Reports link the formation of pseudopodia to the activation of Rho/ROCK signalling pathways (Jia et al., 2005). Filopodia are slim, finger-like structures. They protrude and extend actin filaments outside the cells to facilitate cell migration and invasion (Peuhu et al., 2022). Different proteins control different steps in the formation of filopodia (**figure 1.11**). One of these proteins, IRSp53, plays a crucial role in the formation of filopodia by sensing and causing membrane curvature, a necessary step for protrusion formation. To add to the list of proteins, myosin-X helps to bring integrin and actin crosslinking proteins to the edges of filopodia. These include Ena/VASP (enabled/vasodilator-stimulated phosphoprotein), which helps filopodia elongation, which makes filopodia longer. These proteins collaborate to ensure the correct assembly and formation of filopodia. This, in turn, aids in the migration and communication

of cells. Researchers have extensively investigated filopodia *in vivo* and *in vitro* in cancer migration and invasion (Jacquemet et al., 2017). Research suggests that the progression of cancer leads to the upregulation of filopodia proteins like Fascin and MYO10, which in turn promotes cell invasion (Jacquemet et al., 2017; Miihkinen et al., 2021).

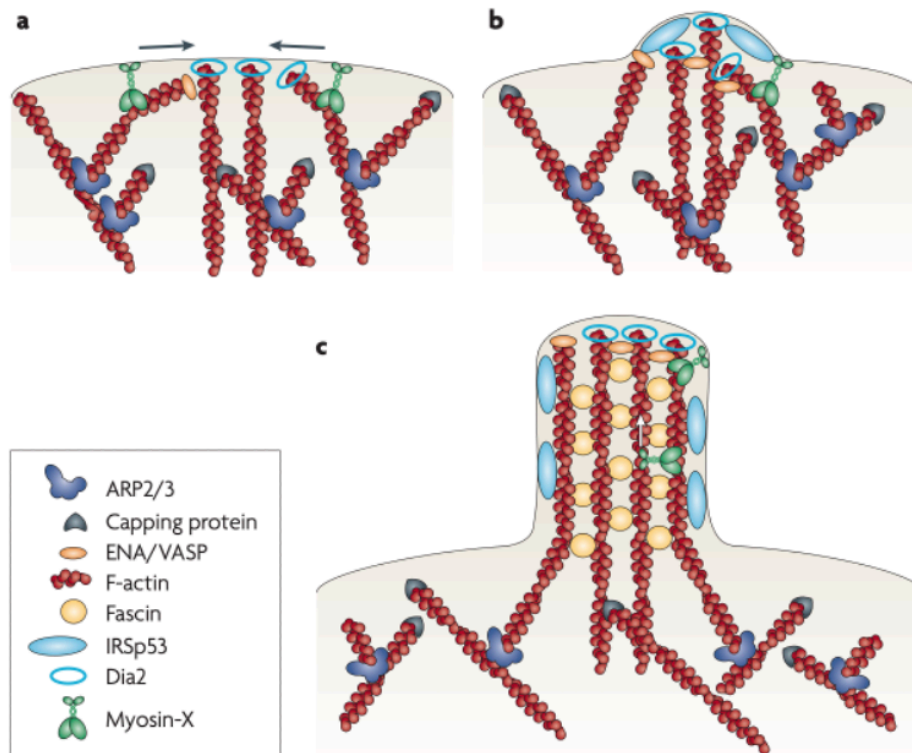


Figure 1.11: Mechanisms controlling filopodia formation. These proteins are critical in the maintenance of filopodia formation; each of them serves a specific function in coordinating a proper filopodia formation. The ARP2/3 complex is involved in managing the initial actin polymerization push. A capping protein is a type of protein that covers the barbed end of an actin filament. ENA/VASP promotes actin filament elongation. F-actin is the base of the actin filaments. Fascin: it helps the actin filament twist into parallel bundles. IRSp53 promotes filopodia formation. Dia2 promotes actin filament elongation (unbranched) alongside the ENA/VASP. Myosin-X is a motor protein that helps transport proteins to the tip of the filopodia. Figure is taken from Pieta K, Mattila & Pekka Lappalainen., 2008.

1.14. Research hypothesis and aims:

This research examined the role of the integrin-binding protein TNS3 in cancer progression. The ECM has been shown to promote the progression of DCIS to IDC. Longitudinal studies revealed that around 20-50% of the DCIS progressed to IDC (Cowell et al., 2013). Moreover, TNS3 has been reported in several studies to be upregulated, promote tumorigenesis and metastasis in breast cancer (Qian et al., 2009; Shintchi et al., 2015). In addition, preliminary data generated in Dr Rainero lab support the role TNS3 in controlling extracellular matrix dynamics. Therefore, my hypothesis is that TNS3 controls the transition of DCIS to IDC by controlling ECM dynamics.

This project is composed of 3 integrated aims:

Aim 1: characterization of the expression of TNS3 during breast cancer progression and its role in controlling cancer cell invasion.

Aim 2: investigation of the role of TNS3 in controlling DCIS to IDC progression and elucidation of the molecular mechanisms through which TNS3 modulates cancer cell invasion. This focuses on the role of TNS3 in modulating BM component secretion and/or organization

Aim 3: Elucidation of the role of TNS3 in controlling tumour formation and metastasis *in vivo* using a Drosophila cancer model established in Dr Campbell lab (School of Biosciences, The University of Sheffield)

Chapter 2: Materials and methods

2.1 Materials:

Table 2.1. Reagent list:

Reagent	Company
8 well chamber-slides	ThermoFisher Scientific
8 well high glass bottom	Ibidi
10cm petri dishes	Greiner bio-one
6-well tissue culture plates	Greiner bio-one
12-well tissue culture plates	Greiner bio-one
96-well, black, optically clear flat-bottom	Perkin Elmer Greiner bio-one
3.5cm glass-bottom dishes	SPL Life Science
0.45µm syringe filter	Gilson
Horse serum (HS)	Gibco
Distilled water	Gibco
Phosphate buffer saline (PBS)	Gibco
5X siRNA buffer	Horizon Discovery
Trypan Blue stain 0.4%	Gibco by life technologies
RNase-free water	Horizon Discovery
Antibiotic-antimycotic	Gibco
Insulin solution human	Sigma
Epidermal growth factor (EGF)	Sigma
Hydrocortisone	Sigma
Dulbecco's Modified Eagle Medium / nutrient Mixture F12 (DMEM-F12)	Gibco
0.5% Trypsin-EDTA solution 10X	Gibco
Opti-MEM (1X), reduced serum medium	Gibco
Dharmafect I	Dharmacon/Horizon Discovery
Dimethyl sulfoxide (DMSO)	Fisher Scientific
Collagen I high concentration (HC) rat tail	Corning
Matrigel basement membrane (BM) matrix	Corning
Soluble collagen I	Bio Engineering
Methylcellulose	Sigma
Glycine	Sigma
Triton X-100	Sigma
Tween-20	Sigma
Alexa Fluor TM 555 Phalloidin	Invitrogen
DMEM/F12, no glutamine	Gibco
Alexa Fluor TM 488 Phalloidin	Invitrogen
Red cell tracker	Fisher
VECTASHIELD Antifade Mounting Medium with DAPI	VECTOR laboratories
Bovine serum albumin (BSA)	Sigma

4-15% Mini-PROTEAN precast polyacrylamide gels	Bio-Rad
NuPAGE™ LDS Sample buffer (NuPAGE)	Thermo Fisher
Qia-Shredder columns	QIAGEN
Dithiothreitol (DTT)	Melford
FL-PVDF membrane	IMMOBILON-FL
DRAQ5™	Rocher
Geltrex	QIAGEN
Cell Scraper, sterile, 28cm	Greiner Bio-One Ltd
Trident universal protein blocking reagent	GeneTex
Paraformaldehyde (PFA)	Science Fisher
15ml Falcon	Biodistribution
50mL falcons	Star Lab
1.5mL Eppendorfs	Star Lab
Color Protein Standard Broad Range	BioLabs
Live Cell Fluorogenic DNA Labelling Probe	SPOROCHROM

Table 2.2 Antibody list:

IR Dye 800 anti-mouse antibody	LI-COR
TNS3	Santa Cruz Biotechnology (sc-376467)
TNS4	Invitrogen (684524)
Anti-Laminin-5 antibody	Sigma-Aldrich (MAB19562)
GAPDH mouse monoclonal	Abcam (sc-47724)

Table 2.3 Blocking antibody list:

Mouse anti-human (IgG1) integrin $\alpha 3$ blocking antibody	Merck (MAB1952Z)
Mouse (IgG1) Ctrl blocking Antibody	Biologend (401401)
Rat anti-human/mouse (IgG2a) CD49f blocking antibody	Biologend (313637)
Rat (IgG2a) Ctrl blocking antibody	Biologend (400543)

Table 2.4. Solution composition

Solutions	Ingredients
SDS lysis buffer	1% SDS (v/v), 50mM Tris-Hcl pH7
Loading buffer	1mM DTT, 1X NuPAGE
TBST	10mM Tris-HCl pH 7.4, 150mM NaCl, 0.1% (v/v) Tween-20
Towbin buffer 10X	1.92M Glycine, 0.25M Tris
Transfer buffer	20% methanol, 10% Towbin buffer 10X in deionised water
1X PBS-Glycine	PBS, 0.75g Glycine
1X IF wash	PBS, 0.2% Triton X-100, 0.04% (v/v) Tween-20
citric acid-based antigen unmasking	1:100 dilution

2.2 Methods:

2.2.1. Cell culture

MCF10A-DCIS cells were grown in DMEM/F12 supplemented with 5% horse serum (HS), 20 ng/ml EGF, and 1% Penicilline and streptomycin (PS). MCF10A and MCF10CA1 cells were grown in DMEM/F12 was supplemented with 5% HS, 20 ng/ml EGF, 0.5mg/ml hydrocortisone, 10µg/ml insulin, and 1% PS. All of the cells were kept at 37° C and 5% carbon dioxide, and they were passaged away every three to four days.

To split the cells, the culture medium was removed, the cells were washed twice in 1% PBS, and then they were incubated in 0.25% trypsin-EDTA for five minutes at 37° C and 5% carbon dioxide. Following the detachment of the cells, they were resuspended in complete growth media and seeded in tissue culture dishes at the desired density.

To prepare cells for cryofreezing for long-term preservation, trypsinised cells were resuspended in complete media and centrifuged at a speed of 1000 revolutions per minute (rpm) for three minutes at room temperature (RT). Shortly after this, the pelleted cells were resuspended in 1 ml of a freezing solution which contained 10% DMSO, 25% complete media, and 65% HS. The vials were kept at a temperature of -80° Celsius for a few days before being moved to liquid nitrogen for longer-term storage.

Cells are checked regularly to make sure they are free of contamination. This is accomplished by collecting 1 ml of cultured cell supernatant in free antibiotics to run the mycoplasma test. Furthermore, cells are checked on a regular basis for morphology, which is done under a microscope to avoid contamination and maintain consistent morphology.

2.2.2. Western blot

8 x 10⁵ cells/well were seeded onto 6 well plastic plates for one day. The cells were then washed with ice-cold 1% PBS and lysed in SDS lysis buffer. The cell lysates were loaded into Qia-shredder columns (Qiagen) and centrifuged using a mini centrifuge at the highest speed for 5 minutes. Eppendorf tubes were used to collect the filtered cell lysates, loading buffer was added and the samples were heated at 75 °C for 5 minutes. The lysates were placed in the refrigerator at -20°C for later use in western blot analysis. 20-25 µl of each sample and 2 µl of Color Protein Standard Broad Range ladder were subsequently loaded into Bio-Rad 4-15% Mini-PROTEAN Gels. Electrophoresis was performed for 1hour and 30 minutes at a constant voltage of 100 volts. The proteins were then transferred to IMMOBILON-FL -PVDF membranes. In order to

boost transfer efficiency by activating the chemical groups in the membrane, the membranes were pre-wetted with pure methanol. The transfer procedure was conducted in towbin transfer buffer for 75 minutes at 100 volts. The membranes were incubated in a blocking solution containing 5% (w/v) BSA in TBS-T for 1 hour at room temperature and with primary antibodies (table 3) in a solution of 5% (w/v) BSA in TBS-T overnight at 4° C. The membranes were washed three times in TBS-T for a total of ten minutes each time, with gentle rocking. This was followed by the incubation with the secondary antibody (**table 2.5**), in TBS-T with 0.01% (w/v) SDS, for 1 hour at room temperature. Three additional rinses were performed in TBS-T, and three in distilled water. The membranes were imaged by the 800nm channel with a resolution of 200µm in a LiCor Odyssey Sa software system. ImageStudioLite was utilised to quantify band intensity. The intensity of the protein of interest was normalised to that of the GAPDH.

Table 2.5. The antibodies used for western blotting:

Primary antibody	Dilution
Mouse ant-TNS3	1:1000
Mouse anti-LN5	1:1000
Mouse anti-GAPDH	1:1000
Secondary antibody	Dilution
IR Dye 800 anti-mouse IgG	1:30000

2.2.3.siRNA-mediated knockdown:

2.2.3.1 Transfection in 6-well plates

3x10⁵ cells were plated for 24 hours, to reach 30% confluence. 10µl of 5µM siRNA and 190µl of Opti-MEM for each well were added in one microtube. 2µl of Dharmafect I (DF1) and 198µl of Opti-MEM per well were mixed in a separate microtube and incubated for 5 minutes. Then, the Dharmafect I solution was added to the siRNA mixture and incubated for 20 minutes while rocking gently to ensure the formation of siRNA:Dharmafect I complex. The media was

aspirated from the cells, which were then washed twice with 1% PBS. Subsequently, the transfection mix was added on top of the cells. Finally, 1600 µl of media without P/S was added to each well.

2.2.4 2D immunofluorescence microscopy microscopy:

A 0.25 mg/ml Geltrex solution was made by diluting it with ice-cold PBS on ice. Following that, 3.5cm² glass-bottomed dishes were coated with 100µl per dish. Then, the Matrigel was polymerised by incubating at 37°C for 1-2 hours. After 2 washes with PBS, 2 x10⁵ cells were seeded on the Geltrex coated dishes overnight. The cells were fixed with 4% (w/v) paraformaldehyde (PFA) in 1x PBS for 15 minutes. Subsequently, cells were permeabilised with 0.25% (v/v) Triton X-100 in 1x PBS for 5 minutes at room temperature. Cells were rinsed three times with 1x PBS and blocked in 1% (w/v) BSA for one hour at room temperature. Cells were incubated with primary antibodies (**table 2.6**) in a 1% (w/v) BSA solution for one hour at room temperature. After, cells were rinsed 3 times with 1x PBS and, if required, incubated with secondary antibodies (table 4) in 1% (w/v) BSA at a 1:1000 dilution for 45 minutes at room temperature. The cells were then washed twice with 1%PBS and then incubated with Phalloidin Alexa Fluor 555 for 10 minutes. After two washes with PBS and one wash with sterilised water, Vectashield containing DAPI was used for nucleus staining and sample preservation. The dishes were then sealed with parafilm and stored at 4°C for a maximum of two weeks.

The samples were acquired using a Nikon A1 confocal microscope. To visualise TNS3, LN332 or TNS4 expression, three channels were used: DAPI ($\lambda_{ex}=403.5\text{nm}$), FITC ($\lambda_{ex}=480.0\text{nm}$), and Alexa Fluor 568 ($\lambda_{ex}=562.0\text{nm}$). Phalloidin staining was used to identify the actin cytoskeleton, which was then tracked in the ROI manager of Image J to define the cells' outlines. The intensity of TNS or LN332 in each cell was measured in the FITC channel. Each experiment involved acquiring a minimum of ten images.

Table 2.6. Antibodies used for 2D Immunofluorescence microscopy microscopy:

Primary antibodies	Dilution
mouse anti-TNS3 antibody	1:100

mouse anti-TNS4 antibody	1:100
Mouse anti-LN5	1:100
Secondary antibody	Dilution
Alexa Fluor 488 Goat Anti-mouse IgG	1:1000

2.2.5 Cell proliferation assay:

96-well plates were coated with a 3 mg/ml Matrigel solution (15µl/well) and let polymerise for three hours. Then, 0.6µl of 30nM siRNA was mixed with 9.4µl of DMEM media containing 5% HS but no antibiotics for each well and added to the wells, giving a total of 10µl. Separately, 0.24µl of DF1 was diluted in 9.76 µl of DMEM media with 5% HS and no antibiotics per well and added to each well. The plate was incubated in the hood for 30 minutes to allow the DF1 and siRNAs to form complexes. 2×10^3 cells in 80 µl of antibiotic-free media were added to each well. This yielded a final siRNA concentration of 30 nM. The cells were kept in the incubator overnight. The following day, the media was removed, following washes with 100µl of 1x PBS and 200µl of fresh complete or free glutamine media was introduced to each well then left to grow for up to 7 days. Cells were fixed on days two and six. To fix the cells, the media was aspirated, and 40µl of 4% PFA was added, followed by a 15-minute incubation and two washes with 100µl of 1x PBS and stained with 5µM DRAQ5 for 1 hour at room temperature while gently rocking. Following this, the cells were washed twice with 1% PBS. The second wash was left in for 30 minutes with gentle rocking to reduce the intense background fluorescence, then the plates were imaged using the Licor Odyssey system Sa with specific settings. The plates were imaged by a 700nm channel with a resolution of 200µm in LiCor Odyssey Sa software system. Each well's signal intensity was calculated as the total intensity exploded by the total background. Image Studio Lit software was used to measure the signal intensity of each well.

2.2.6 Fluorescence Immunohistochemistry staining:

Tissue slides were obtained from SEARCHBreast (<https://searchbreast.org/>), from a polyoma middle T-driven mouse model (MMTV-PyMT) at pre-tumor initiation (normal mammary gland) at 42 to 44 days old, ductal adenocarcinoma stage (DCIS) at 73 days old, and invasive ductal carcinoma at 91 days old.

The slides underwent deparaffinization by dipping the slides in xylene for 3 minutes each for two times. After that, the samples were rehydrated in alcohol, by immersing them twice in 100% ethanol (EtOH) for 5 minutes, twice in 95% EtOH for 5 minutes and twice in 70% EtOH for 5 minutes. Finally, the samples are re-hydrated by placing them in dH₂O for 5 minutes. A citric acid-based antigen unmasking solution was utilized to enhance the entry of the antibody within the tissue. Subsequently, the slides were blocked using trident universal protein blocking reagent (animal serum free) for 30 minutes at room temperature. Slides were incubated with anti-TNS3 primary antibody (1:100 dilution) in 1% PBS for 1 hour at room temperature, washed with 1% PBS while stirring for 5 minutes, then rinsed once more with 1% PBS. Afterward, the slides were incubated with the secondary antibody (Alexa Fluor 488 anti-mouse IgG, 1:500) for 30 minutes at room temperature. They were then washed with 1% PBS while stirring for 5 minutes. Then, remove any residual PBS. Subsequently, 1-2 drops of Vectashield were added on top of the tissues. Finally, a glass coverslip was placed over the tissue. The images were taken by an Olympus microscope, 20X objective. The mean intensity of TNS3 staining was quantified using ImageJ.

2.2.7 3D Culture:

5 µl of pure Matrigel is added to each well of an eight-well glass chamber slide and incubated in the cell culture incubator for a minimum of 15 minutes and a maximum of 30 minutes (**figure 2.1**). During Matrigel polymerisation, cells were detached with trypsin and resuspended in DMEM/F12 media containing 2% Matrigel to reach a final concentration of 12500 cells/mL. In each well of the chamber slide, 400 µl of the cell suspension was added to the solidified Matrigel. This produces a final concentration of 5000 cells per well in a medium containing 2% Matrigel. Cells were grown for up to 6 days in a humidified incubator with 5% CO₂ at a temperature of 37 °C. After 3 days, the media was replaced with a fresh one containing 2% Matrigel. Where indicated, cells were treated with integrin blocking antibodies either at the time of seeding (day 0) or the following day (day 1).

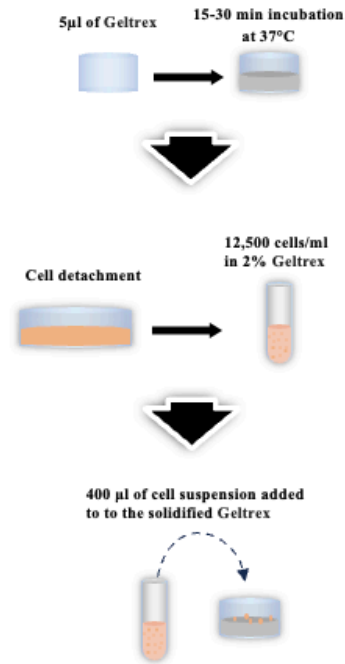


Figure 2.1: Diagram representing the 3D culture protocol. 5 µl of pure Geltrex is added to a well of a glass-bottom 8-well chamber and incubated at 37° C for a minimum of 15 minutes and a maximum of 30 minutes. Cells were detached with trypsin and resuspended in media containing 2% Geltrex to reach a final concentration of 12,500 cells/ml. 400 µl of the cell suspension was added to the solidified Geltrex. Cells were grown for the desired time.

2.2.8 3D-Immunofluorescence microscopy microscopy:

Cells were fixed by gently removing the media followed by applying 400µl of 2% PFA for 20 minutes at room temperature. Later, cells were permeabilized by overlying it with 250µl of 0.5% Triton X-100 in PBS for 10 minutes at room temperature. The cells were washed three times with 1x PBS-Glycine for 10 minutes each at room temperature.

The cells underwent incubation with 200 µl of a blocking buffer solution (IF wash and 1% BSA) for 1 hour at room temperature. Subsequently, the cells were stained by applying 100 µl of primary antibody per well (diluted 1:100 in blocking buffer) overnight at 4°C. The next day, the chamber slides were allowed to warm up to room temperature. Following that, the cells were washed three times with IF wash, with each wash lasting for 20 minutes at room temperature. After the washes, 100 µl of secondary antibody per well, prepared in blocking buffer at a 1:500 dilution, was added and left for 1 hour at room temperature. Once again, the cells were washed with IF wash for 20 minutes at room temperature. Subsequently, the cells were rinsed twice with 1% PBS, with each rinse lasting for 10 minutes. Finally, the cells were incubated with 100 µl of Phalloidin Alexa Fluor 555 (1:200 in 1% PBS) per well, for 30

minutes at room temperature. Lastly, the cells were rinsed with 1% PBS and then three drops of Vectashield containing DAPI were applied, followed by sealing the chamber slide with parafilm. Cells were imaged using a Nikon A1 confocal microscope, 60x objective.

For cell live imaging experiments, cells were seeded as described above and on the second day the cells stained with Live Cell Fluorogenic DNA Labelling Probe (1:1000) for 1 hour prior to imaging. Cells were imaged using a Nikon time lapse microscope, 20x/0.75 Ph2 objective. Images were acquired every 10 minutes for 48 hours. Acini circularity ($4\pi \times [\text{Area}] / [\text{Perimeter}]^2$) was measured with Image J. A perfect circle has a circularity value equal to one, which decreases in the presence of protrusions.

Table 2.7. Antibodies used for 3D immunofluorescence microscopy

Primary antibodies/ Blocking antibodies	Dilution / Final concentration
Mouse anti-human (IgG1) integrin α 3 (P1B5) blocking antibody	5 μ g/ml
Mouse (IgG1) Ctrl blocking Antibody	5 μ g/ml
Rat anti-human/mouse (IgG2a) integrin α 6 (GoH3) blocking antibody	10 μ g/ml
Rat (IgG2a) Ctrl blocking antibody	10 μ g/ml
Mouse Anti-Laminin-5 antibody	1:100
Mouse Anti-integrin α 3 antibody	1:100
Mouse Anti-integrin α 6 antibody	1:100
Mouse Anti- β 1 antibody, conjugated with Alexa Fluor 488	1:100
Secondary antibody	Dilution
Alexa Fluor 488 Anti-mouse IgG	1:1000

2.2.9 3D-spheroid invasion assay

MCF10A-DCIS cell spheroids were generated by the hanging-drop technique, as described in Bayarmagnai et al. 2019a. Initially, cells were washed with PBS and stained with 2 μ M Cell Tracker Red in serum-free media at 37°C for 45 minutes. 1x10⁵ cells were resuspended in 2 ml of spheroid medium, containing 4.8 mg/ml of methylcellulose and 20 μ g/ml of soluble collagen I in full growth medium (**figure 2.2**). After this, 20 μ l of cell suspension was carefully positioned onto the inner surface of a 10cm² tissue culture dish lid, resulting in 10³ cells in each droplet. A moist environment was created by adding 5 ml of 1x PBS to the culture dish and incubated at 37° C and 5% CO₂ for 48 hours. This was done in order to prevent the hanging drops from drying out while the spheroids were being formed.

After spheroids were formed, they were carefully washed with 500 μ l of complete growth medium. After that, the spheroid suspension was moved into a 1.5 ml microcentrifuge tube. After gravity had caused all of the spheroids to settle to the bottom, growth medium was carefully removed and spheroids were washed twice with 500 μ l growth media. Spheroids were embedded in a mixture consisting of 4mg/ml Matrigel and 3mg/ml collagen I. One to two spheroids were mixed together in a uniform manner then added into a 60 μ l of the Matrigel/collagen I mixture. 45 μ l of the gel mixture and spheroids were deposited in the middle of each well of a glass-bottomed 24-well plate. The plate was inverted slowly and then incubated upside down at 37 °C for 20 minutes in order to prevent the embedded spheroids from sinking to the bottom of the wells. After that, the plate was turned over so that the right side was facing up, and left in the incubator for 20 minutes at 37 °C.

The final step was to carefully add one ml of fresh growth medium all around the well in order to prevent the gel droplets from becoming detached. Spheroids were placed in an incubator at 37°C with 5% carbon dioxide, and live images were taken at Day 0, Day 1, Day 2, and Day 3 with a Nikon A1 confocal microscope, 10x objective. The invasion, core, and total area were quantified with Image J.

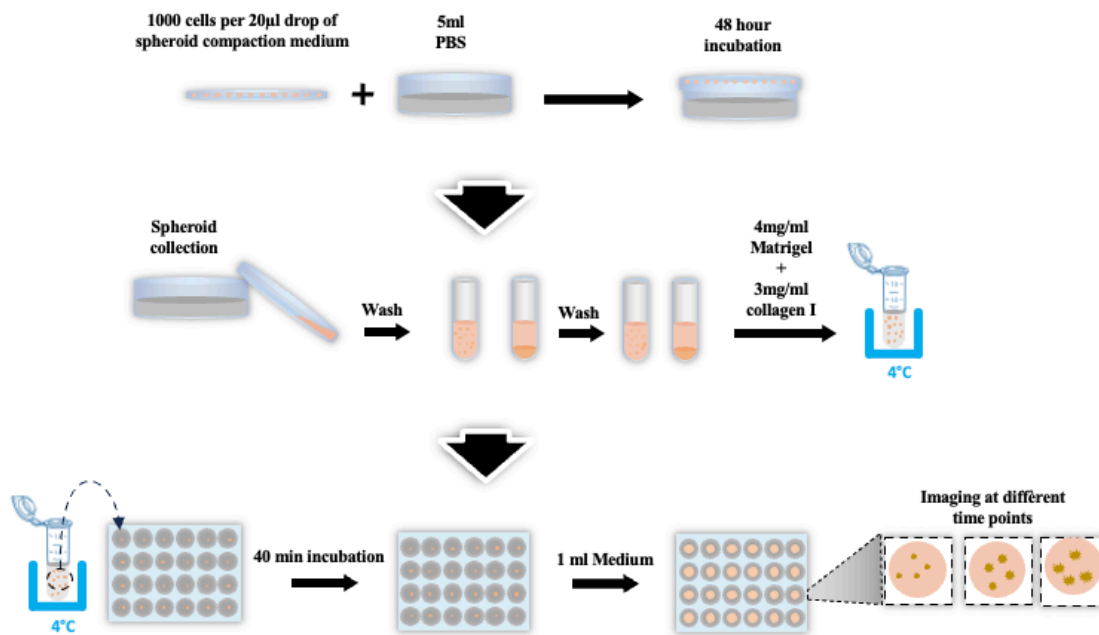


Figure 2.2: Diagram representing the 3D spheroid invasion protocol. 1×10^5 MCF10A-DCIS cells were resuspended in 2 ml of spheroid compaction medium. 20 μ l of cell suspension was carefully positioned onto the inner surface of a 10cm² tissue culture dish lid. 5 ml of 1x PBS were added to the culture dish and incubated at 37° C for 48 hours. Cells were washed twice with 500 μ l of complete growth medium. The spheroid suspension was moved into a 1.5 ml microcentrifuge tube. Spheroids were embedded in a mixture consisting of 4mg/ml Matrigel and 3mg/ml collagen I. 45 μ l of the gel and spheroid mixture were deposited in the middle of each well of a glass-bottomed 24-well plate and incubated at 37 °C for 40 minutes, before adding 1 ml of fresh medium. Live images were taken at Day 0, Day 1, Day 2, and Day 3.

2.2.10 Drosophila cancer model:

These experiments were performed by Dr Jamie Adams in the Campbell lab at the University of Sheffield, as described in Campbell et al., 2019.

2.2.11 RNA-Seq Data Analysis:

The analysis was carried out using <https://TNMplot.com>. The methodology for data collection is detailed in their published paper (Bartha & Györfy, 2021). Using the available data, I chose the TNS3 gene and human breast invasive carcinoma tissue to compare TNS3 expression in normal and tumour tissues.

2.2.12 Statistical analysis:

Statistical analyses were performed using Graphpad Prism (Version 9.4.1) software. An unpaired t-test (Mann-Whitney test) was used to compare the two datasets, one-way ANOVA

with multiple comparisons (Kruskal-Wallis test) was for multiple datasets with a single independent variable, while two-way ANOVA with multiple comparisons (Tukey test) was used to compare multiple datasets with two independent variables.

Chapter 3: TNS3 is upregulated during breast cancer progression and promotes cancer cell invasion

3.1 Introduction

The MCF10 series cell line is a powerful tool for studying the molecular pathways behind breast cancer progression and it has been extensively employed as a breast cancer *in vitro* model (Bessette et al., 2015; Goh et al., 2022; So et al., 2014). It consists MCF10A, MCF10DCIS, and MCF10CA1. Click or tap here to enter text. Click or tap here to enter text. The extracellular matrix (ECM) consists of a variety of proteins that offer structural and chemical support to cells. Cell receptors like integrins facilitate communication between the ECM and cells, initiating signalling pathways that control cell migration, growth, and balance. Interaction with ECM components activate integrin receptors. This reaction leads to integrin clustering, initiating focal adhesion formation by recruiting proteins such as TNS, paxillin and focal adhesion kinase (FAK) (Legerstee & Houtsmuller, 2021; Rainero et al., 2015; Shinchu et al., 2015). Nascent focal adhesions later become mature focal adhesions and then longer fibrillar adhesions. Fibrillar adhesions are particularly enriched in tensin proteins (Atherton et al., 2022). The TNS family members are found at both focal and fibrillar adhesion sites. In particular, Tns1 localises to focal and fibrillar adhesion, TNS2 predominantly in focal adhesion, and TNS3 is enriched in fibrillar adhesion (Clark et al., 2010). A variety of studies have been conducted to investigate the role of TNS on cancer. TNS expression levels vary in cancer. TNS1 and TNS2 are downregulated in breast cancer, but TNS3 is upregulated. TNS4 expression reported to be upregulated or downregulated (Liao & Lo, 2021; X. Lu et al., 2021). The expression level of TNS3 can be regulated by intracellular signalling. For instance, when EGFR is activated, it triggers the activation of ERK/MAPK pathway that enhances the expression of TNS4 (also known as c-ten) while diminishing TNS3. Consequently, TNS3 is replaced by TNS4, leading to a decrease in the formation of stress fibres and the creation of focal adhesion (Cui et al., 2004). TNS3 has been shown to either promote or suppress cancer cell migration and invasion, depending on the cell type and environmental conditions. For

instance, knocking down TNS3 in breast cancer cells MDA-MB-231 and MDA-MB-468 reduced cell invasion and migration, while it increased migration in WM793 melanoma, 05MG glioblastoma, and MCF10A non-transformed cells (Liao & Lo, 2021). Alterations in ECM composition and cell/ECM interaction can lead to abnormal cell division, potentially causing diseases, such as cancer metastasis, arthritis, and cardiovascular diseases (Chua et al., 2016; Hynes, 2009; Rainero, 2018; Walker et al., 2018). Some cancers, such as breast and pancreatic, are extremely fibrotic, featuring high ECM deposition and nutrient deprivation. Data from our lab showed that breast cancer cells can use the ECM as a nutrient source. We reported before that plating breast cancer cells MCF10DCIS on Matrigel under glutamine starvation resulted in higher proliferation compared to plastic (Nazemi et al., 2024). Another study reported that silencing TNS3 in tonsil-derived mesenchymal stem cells reduced the cell proliferation (Park et al., 2020). However, the role of TNS3 in controlling proliferation in breast cancer progression has not been elucidated yet. Therefore, further study to demonstrate the effect of silencing TNS3 in breast cancer cells plated on ECM is needed.

The 3D culture approach was adopted to investigate the connection between DCIS and the ECM, which may facilitate the progression of DCIS to IDC (Brock et al., 2019; So et al., 2014). 3D culture methods have been used to better recapitulate the tumour's *in vivo* environment, allowing for a better understanding of cell-cell and cell-matrix interactions in a physiological setting. It has been reported that elevated accumulation of ECM proteins such as fibronectin, coupled with increased expression of integrin receptors, like the fibronectin receptor $\beta 6$, could promote the switch from non-invasive to invasive cells. A study has reported increased expression of $\alpha \beta 6$ led to increased levels of MMP9 in HT29 and WiDr cells (colorectal adenocarcinoma cell lines). Metalloproteases are proteins that play an important role in remodelling the ECM. They have the ability to break down the basement membrane, facilitating invasion and migration (Yang et al., 2008). Despite this, the detailed molecular mechanisms controlling DCIS to IDC transition are poorly defined and deserve further exploration.

Here I demonstrated that TNS3 levels were higher in human invasive breast cancer tissues than normal mammary tissues, while TNS1, TNS2, and TNS4 were downregulated in tumours. I validated this observation further by measuring TNS3 expression in the MMTV-PyMT breast cancer mouse model, confirming an upregulation of TNS3 in DCIS and IDC compared to the normal mammary gland. In addition, western blotting and immunofluorescence microscopy

microscopy experiments show that TNS3 expression was upregulated in a stage-dependent manner in the MCF10 series of cell line. Moreover, 3D invasion experiments indicated that TNS3 was required for in both MCF10DCIS and MCF10CA1 cells. Finally, proliferation experiments demonstrated that, while TNS3 knockdown did not affect cell proliferation in complete media, it significantly reduced the ECM-dependent cell growth observed under glutamine starvation.

Altogether, these data indicates that TNS3 is upregulated during breast cancer progression and promotes cells invasion and ECM-dependent proliferation.

3.2 Results

3.2.1 TNS3 expression is up-regulated in breast cancer

Previous reports have indicated that TNS3 expression is elevated in various cancer types, including gastric cancer and breast cancer (Liao & Lo, 2021). The expression of the different TNS isoforms was assessed in normal vs invasive breast carcinoma tissues by RNA-seq using datasets available in TNMplot.com (Bartha & Györffy, 2021). The results in **figure 3.1** show that the expression of TNS3 was significantly increased in human tumours compared to normal tissues, while TNS1, TNS2 and TNS4 were significantly reduced in tumours compared to normal mammary tissues.

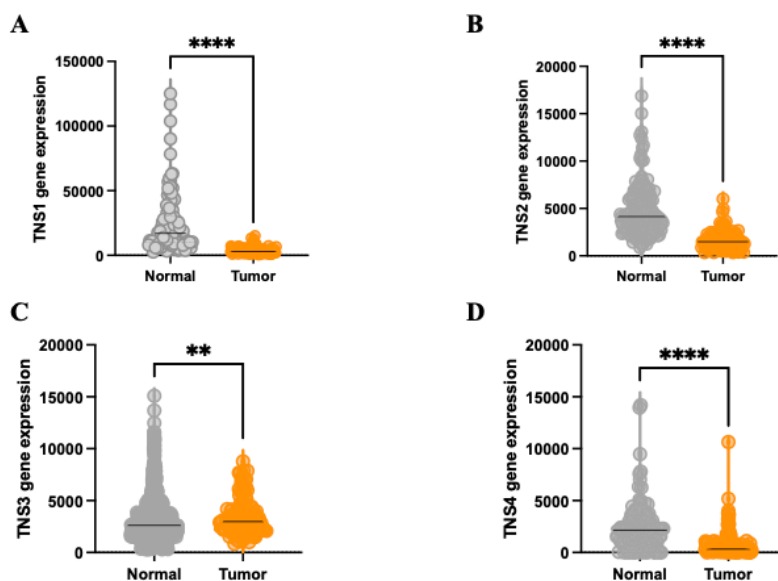


Figure 3.1: TNS3 expression is up-regulated in breast cancer. The expression of TNS1 (A), TNS2 (B), TNS3 (C) and TNS4 (D) was analysed in invasive breast cancer (tumor) compared to normal mammary tissues by RNAseq. Data were obtained from TNMplot.com. Mann-Whitney test, T-test.

3.2.2 TNS3 expression is upregulated in DCIS and adenocarcinoma in a breast cancer mouse model.

In order to corroborate the high expression of TNS3 in breast cancer tissues in comparison to normal tissues at the protein level, we evaluated the expression of TNS3 during the progression of breast cancer, from healthy mammary gland to DCIS, and IDC in a mouse model of breast cancer. Tissue samples were collected from a polyoma middle T-driven mouse model (MMTV-PyMT) (Attalla et al., 2021) at 42 to 44 days old (pre-tumour initiation, normal mammary gland), at 73 days old (ductal adenocarcinoma, DCIS stage) and at 91 days old (invasive ductal adenocarcinoma). The validation of TNS3 antibody was done by Fiona J Wright, by using positive control (placenta) and negative control (brain) tissue. TNS3, staining in the normal mammary gland was faint and appeared to be diffuse in the mammary epithelial cells. TNS3 levels were higher DCIS tumours, and appeared brighter at the periphery of the tumours compared to the centre. In the IDC sample, high TNS3 staining was detected all over the tumour. The very bright green dots observed in some images are believed to be a result of non-specific signal and were excluded from the analysis of the fluorescence intensity. When compared to the normal group, DCIS and IDC samples had a significantly higher mean intensity of TNS3 (**figure 3.2**), supporting the idea that there is a correlation between breast cancer progression and an increase in TNS3 expression.

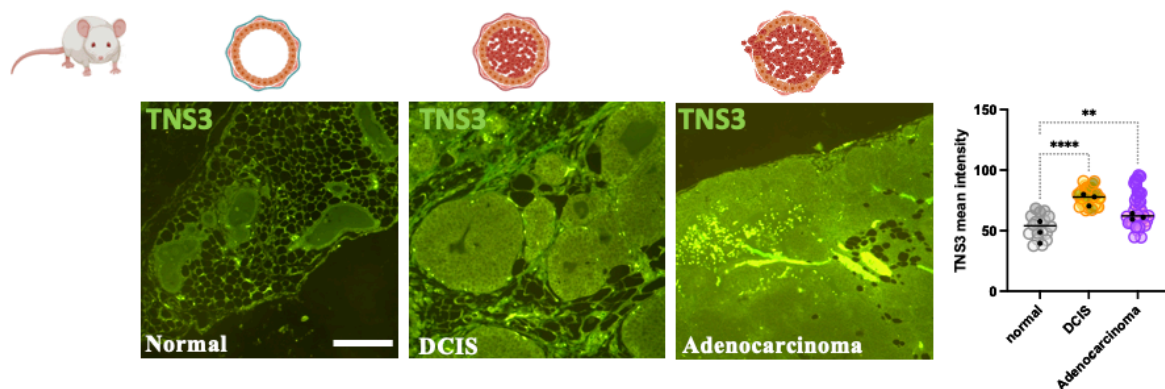


Figure 3.2: TNS3 expression is upregulated in DCIS and adenocarcinoma in a breast cancer mouse model. Tissue samples were collected from a polyoma middle T-driven mouse model (MMTV-PyMT) at 42 to 44 days old (pre-tumour initiation, normal mammary gland), at 73 days old (ductal adenocarcinoma, DCIS stage) and at 91 days old (invasive ductal adenocarcinoma). Tissues were stained for TNS3 (green). Scale bar, 100 μ m. TNS3 mean intensity was measured with ImageJ. The graph represents the mean \pm SEM of three independent experiments. The black dots represent the means of each experiment. **** p <0.0001, Kruskal-Wallis, multiple comparisons test, One-Way ANOVA.

3.2.3 TNS3 is upregulated in metastatic breast cancer cells compared to non-transformed mammary epithelial cells

TNS3 expression was examined in the well-established MCF10 series of cell lines, including MCF10A (non-transformed mammary epithelial cells), MCF10DCIS (ductal carcinoma in situ) and invasive and metastatic MCF10CA1 cells, by Western blotting and immunofluorescence microscopy. As shown in **figure 3.3A**, the expression of TNS3 was upregulated in MCF10DCIS and MCF10CA1 cells compared to MCF10A cells, indicating that TNS3 expression increased in a stage dependent manner. I then analysed the subcellular localisation of TNS3 in MCF10A, MCF10DCIS and MCF10CA1 plated on a basement membrane extract (Geltrex) using immunofluorescence microscopy. **Figure 3.3B** shows increased TNS3 staining in the ventral surface of MCF10CA1 cells, compared to MCF10DCIS and MCF10A cells. In particular, actin cables that terminate with focal adhesions were coupled with TNS3 accumulation in MCF10CA1 cells, but not in MCF10DCIS and MCF10A. These results confirmed that TNS3 expression was significantly increased in the highly invasive MCF10CA1 cells compared to MCF10A and MCF10DCIS cells, suggesting that TNS3 might play a role in controlling the invasive behaviour of breast cancer cells.

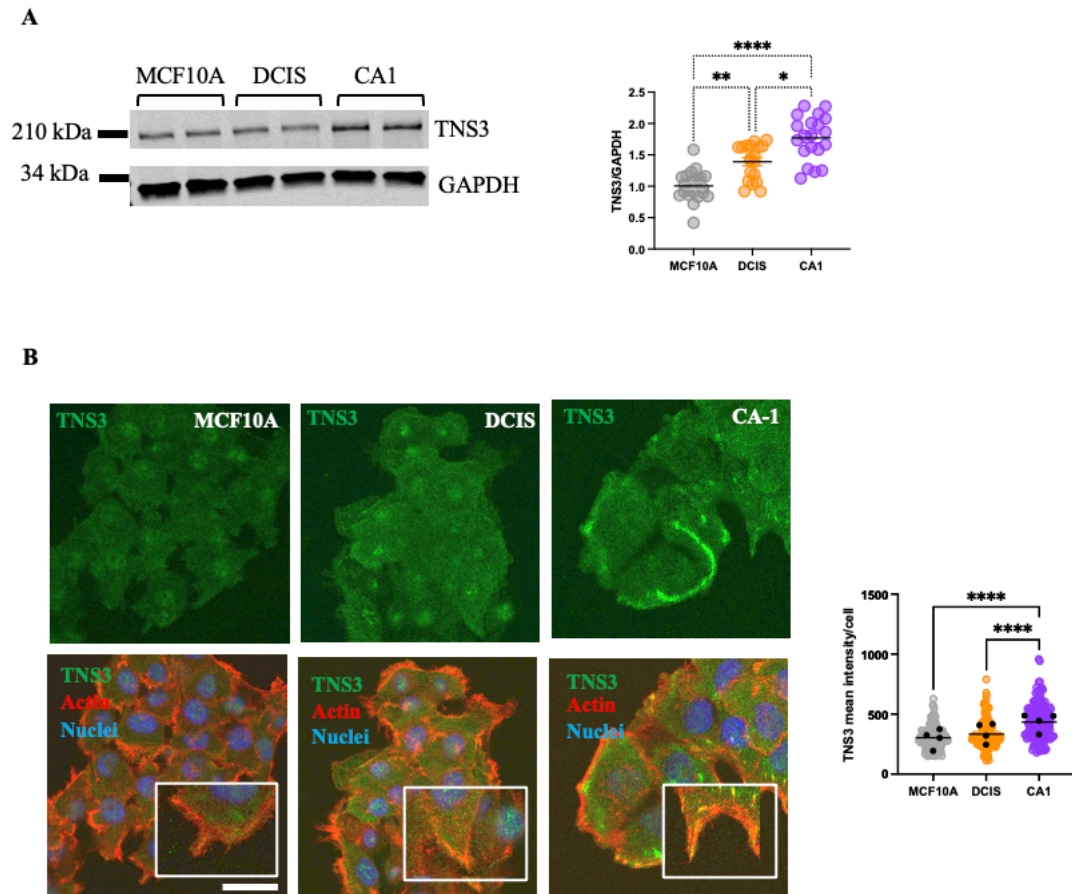


Figure 3.3: TNS3 is upregulated in metastatic breast cancer cells compared to MCF10A. (A) MCF10A, MCF10DCIS (DCIS) and MCF10CA1 (CA1) cells were plated on plastic for 24h. Cell lysates were collected and run through an SDS-PAGE gel, blotted for TNS3 and GAPDH and imaged with a Licor Odyssey Sa. Band intensities were measured with ImageStudio and normalised to GAPDH. The graph represents the mean \pm SEM of ten independent experiments. Kruskal-Wallis, multiple comparisons test, One-Way ANOVA. (B) MCF10A, MCF10DCIS (DCIS) and MCF10CA1 (CA1) cells were plated on 3.5cm glass-bottom dishes, coated with 0.25mg/ml Geltrex overnight; fixed and stained for TNS3 (green), actin (red) and nuclei (blue). Cells were imaged with a Nikon A1 confocal microscope. Scale bar, 20 μ m. Small boxes are a zoomed-in portion of the cells. TNS3 mean intensity was measured with ImageJ. The graph represents the mean \pm SEM of four independent experiments. The black dots represent the means of each experiment. **** p <0.0001, Kruskal-Wallis, multiple comparisons test, One-Way ANOVA.

3.2.4 TNS4 localises in the cytoplasm

TNS4 expression has been shown to be elevated in a variety of cancers, including breast cancer (Albasri et al., 2011; Lo, 2017). Furthermore, study has reported that in HeLa and MCF10A cells, EGF stimulation resulted in a TNS switch, with increased TNS4 expression and decreased TNS3 levels. As a result, integrin β 1 tail is released from TNS3, which reduces focal adhesion formation (Katz et al., 2007; Liao & Lo, 2021). Since we detected an increase in TNS3 expression in the more aggressive cell lines, we wanted to determine the levels of TNS4

expression in the MCF10 series of cell lines. MCF10A, MCF10DCIS, and MCF10CA1 cells were plated on Geltrex overnight, fixed, and stained for TNS4. The results show that TNS4 localised in the cytoplasm, in all three cell lines (**figure 3.4**). According to the quantification of the mean intensity, TNS4 expression was significantly lower in MCF10DCIS than MCF10A and MCF10CA1 cells, while TNS4 levels were comparable in MCF10A and MCF10CA1 cells. The findings show that the TNS switch was not detected in our experiment and TNS4 expression did not correlate with cancer cell invasiveness.

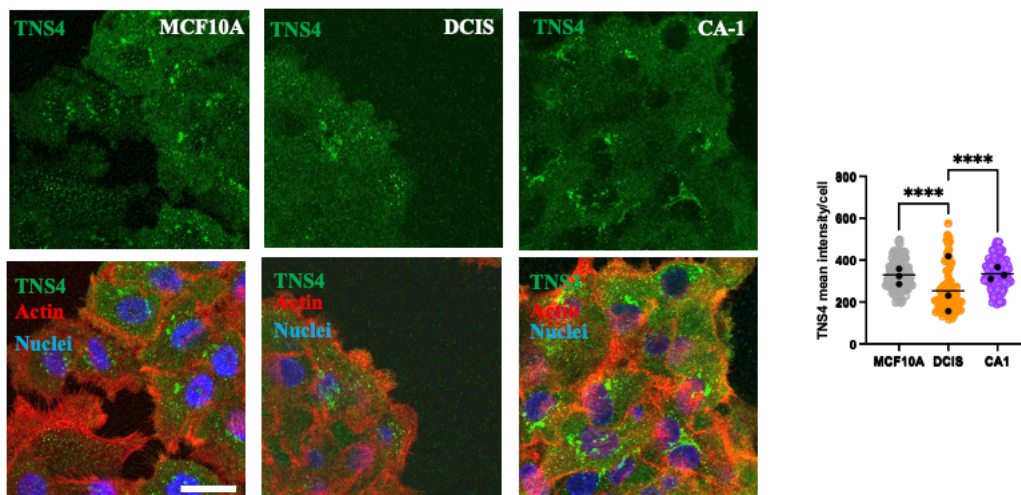


Figure 3.4: TNS4 localises in the cytoplasm. MCF10A, MCF10DCIS (DCIS) and MCF10CA1 (CA1) cells were plated on 3.5cm glass-bottom dishes, coated with 0.25mg/ml Geltrex overnight, fixed and stained for TNS4 (green), actin (red) and nuclei (blue). Cells were imaged with a Nikon A1 confocal microscope. Scale bar, 25µm. TNS4 mean intensity was measured with ImageJ. The graph represents the mean ±SEM of three independent experiments. The black dots represent the means of each experiment. ****p<0.0001, Kruskal-Wallis, multiple comparisons test, One-Way ANOVA.

3.2.5 3D culture promotes DCIS cell invasion

In order to study the role of TNS3 in breast cancer cell invasion, I aimed to establish a model in which I can study the transition from non-invasive to invasive behaviour. When DCIS cells grow in a 3D environment, they form round acini, which progress from a non-invasive to an invasive stage (Brock et al., 2019). This can be quantified by measuring the circularity of the 3D structures. A perfect circle has a circularity value equal to 1, while this decreases in the presence of protrusions. Previous research in the Rainero lab has shown that up to 3 days in culture, DCIS cells form non-invasive acini, which become invasive after 6 days. Non-invasive acini have a rounded shape (circularity ~1). In the invasive stage, cells begin to protrude out of the acinus structure, invading in the surrounding tissues, resulting in a circularity <1. To confirm these findings, MCF10A, MCF10DCIS and MCF10CA1 cells were grown in

Matrigel-based 3D cultures for up to 6 days. As shown in **figure 3.5**, non-invasive MCF10A cells formed rounded acini both at day 3 and day 6 and the size of the acini increased at day 6 compared to day 3. MCF10DCIS cells grew as non-invasive acini up to day 3, looking very similar to MCF10A acini and featuring a circular shape. Indeed, there was no significant difference in the circularity of MCF10A and MCF10DCIS acini at day 3. At day 6, MCF10DCIS cells protruded out of the acini, indicating a transition from a non-invasive to an invasive stage. Consistently, I observed a statistically significant reduction in the circularity of MCF10DCIS acini at day 6 compared to day 3. Invasive MCF10CA1 cells generated protrusions out of the acini at both day 3 and day 6, resulting in a statistically significant reduction in the circularity of MCF10CA1 acini compared with MCF10A ones. Furthermore, I detected a statistically significant increase in acini area in MCF10A and DCIS cells between day 3 and day 6, but not in CA1 cells. These results shows that 3D culture can recapitulate the invasive properties of the cell lines.

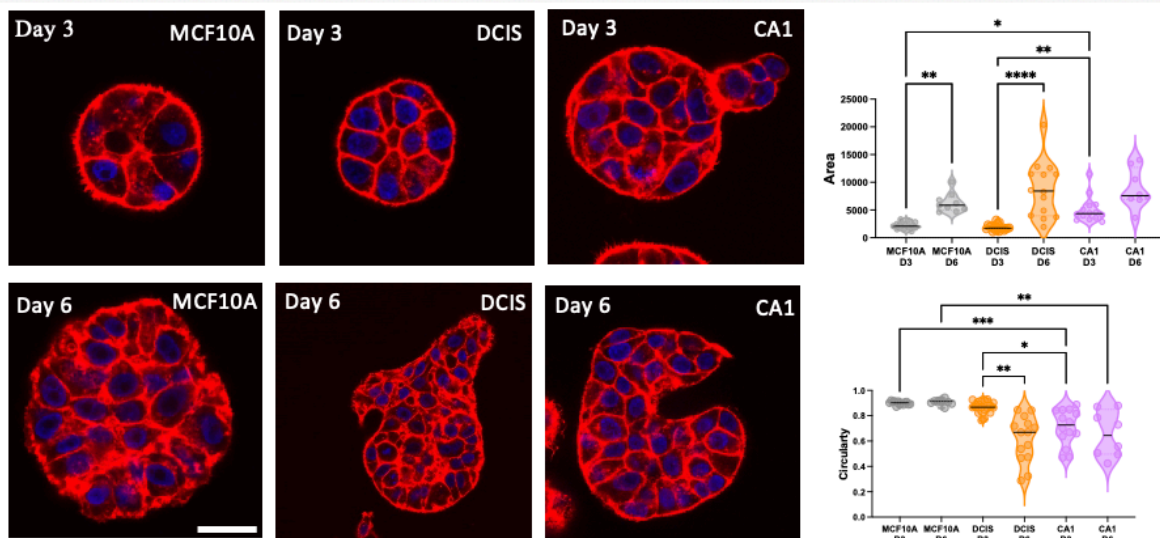


Figure 3.5: 3D culture promotes invasion in DCIS cells. Single MCF10A, MCF10DCIS (DCIS) and MCF10CA1 (CA1) cells were grown in 3D Geltrex for 3 or 6 days, fixed and stained for actin (red) and nuclei (blue). Cells were imaged by a Nikon A1 confocal microscope. Scale bar, 50µm. Area and circularity were measured in Image J. The graphs represent the mean ±SEM of three independent experiments. *p<0.05, **p<0.001, ***p<0.001, ****p<0.0001. Kruskal-Wallis, multiple comparisons test, One-Way ANOVA.

3.2.6 Characterisation of MCF10DCIS cell spheroid invasion

The 3D spheroid method is a well-established technique for studying breast cancer cell invasion *in vitro*. It has been widely used in cancer research because of its ability to mimic the environment of human tumours, allowing for the maintenance of cell-cell and cell-ECM interactions (Chang et al., 2024; Peuhu et al., 2022; Weaver et al., 2002). As a result, these characteristics make spheroids a great tool for studying the various behaviours of cancer cells, such as invasion and drug testing (Djomehri et al., 2019). While in the previous experiments acini were generated by embedding single cells in matrigel containing media (figure 5), here MCF10DCIS cell spheroids were generated by the hanging drop method first, then they were embedded in a mixture of 3mg/ml collagen I and 4mg/ml Geltrex for 4 days and imaged live every day (figure 3.6). The core size, total area and the invasion area of the

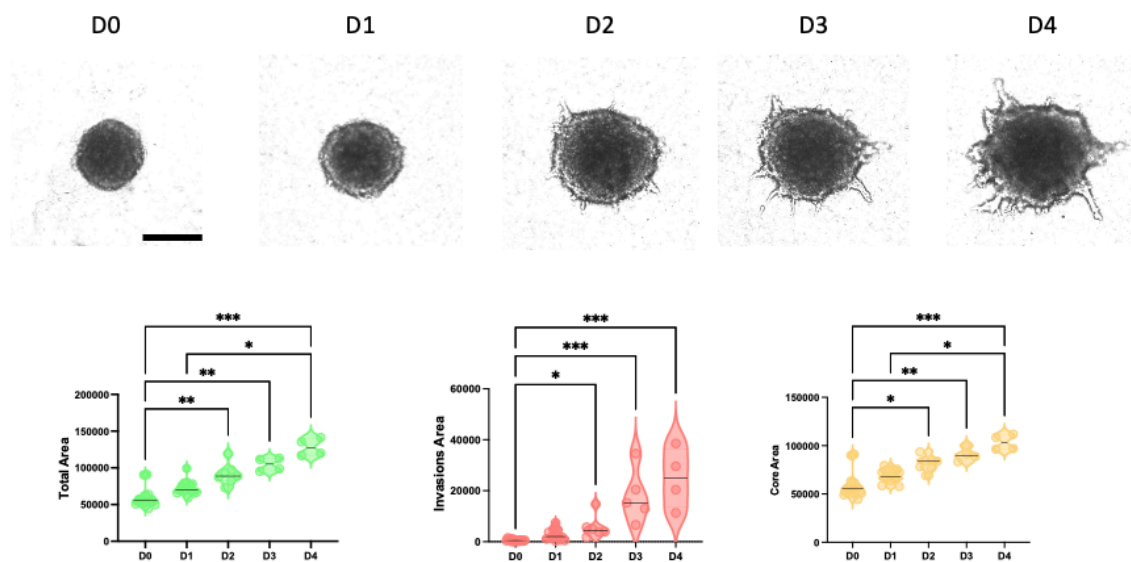


Figure 3.6: Characterisation of DCIS cell spheroid invasion. MCF10DCIS (DCIS) cells were stained with Cell Tracker Red for 40 minutes. Spheroids were formed with the hanging drop method for 48h and embedded into a mixture of 3 mg/ml Geltrix and 4 mg/ml collagen 1 for 96h. The invasion was measured Spheroids were imaged with a Nikon A1 confocal microscope at day 0 (D0), day 1 (D1), day 2 (D2), day 3 (D3) and day 4 (D4). Scale bar, 100 μ m. Total, invasion and core areas were measured with ImageJ. The graph values represent the mean \pm SEM of three independent experiments. * $p < 0.05$, ** $p < 0.001$, *** $p < 0.001$ **** $p < 0.0001$, Kruskal-Wallis, multiple comparisons test, One-Way ANOVA.

spheroids were measured with Image J. At day 0, the spheroids appear spherical. At day 1 the core size of the spheroids slightly increased but invasion was not observed. At day 2 MCF10DCIS cells started to form invasive protrusions. At day 3 the core size and invasion increased. At day 4 the cells formed protrusions and strands of collective cells invading through

the surrounding matrix. Together, this method confirms that MCF10DCIS cells acquire an invasive phenotype when cultured in 3D, allowing me to assess the effect of silencing TNS3 in DCIS cell invasion.

3.2.7 TNS3 is required for DCIS cell invasion in 3D spheroids

In order to investigate the role of TNS3 in breast cancer cell invasion, MCF10DCIS cells were transfected with a TNS3 specific si-RNA and a non-targeting siRNA as a control. Spheroids were formed with the hanging drop method for 48hr and embedded into a mixture of 4 mg/ml Geltrix and 3 mg/ml collagen 1 for 3 days. Spheroids were imaged live with a Nikon A1 confocal microscope at day 0, day 1, day 2 and day 3. The core size and the invasion area of the spheroids were measured with Image J (**figure 3.7A**). At day 0, the spheroids appear spherical, and there is no significant difference in core and invasion area between non-targeting siRNA and TNS3 specific si-RNA, while TNS3 knockdown led to a significant decrease in the core area of spheroids at day 1 and 2. Moreover, TNS3 knockdown spheroids showed a reduced number of protrusive strands compared to non-targeting siRNA ones. In addition, knocking down TNS3 resulted in a nearly 60% decrease in mean invasion area at day 1, day 2 and day 3, indicating that cell invasion, and potentially cell proliferation, in MCF10DCIS spheroids requires TNS3. To assess the efficiency of TNS3 knock-down, MCF10DCIS cells were plated in 6-well plates and transfected with either control non-targeting siRNA or an siRNA targeting TNS3. Western blotting analysis indicated that the percentage of the TNS3 knock-down was around 70% (**figure 3.7B**).

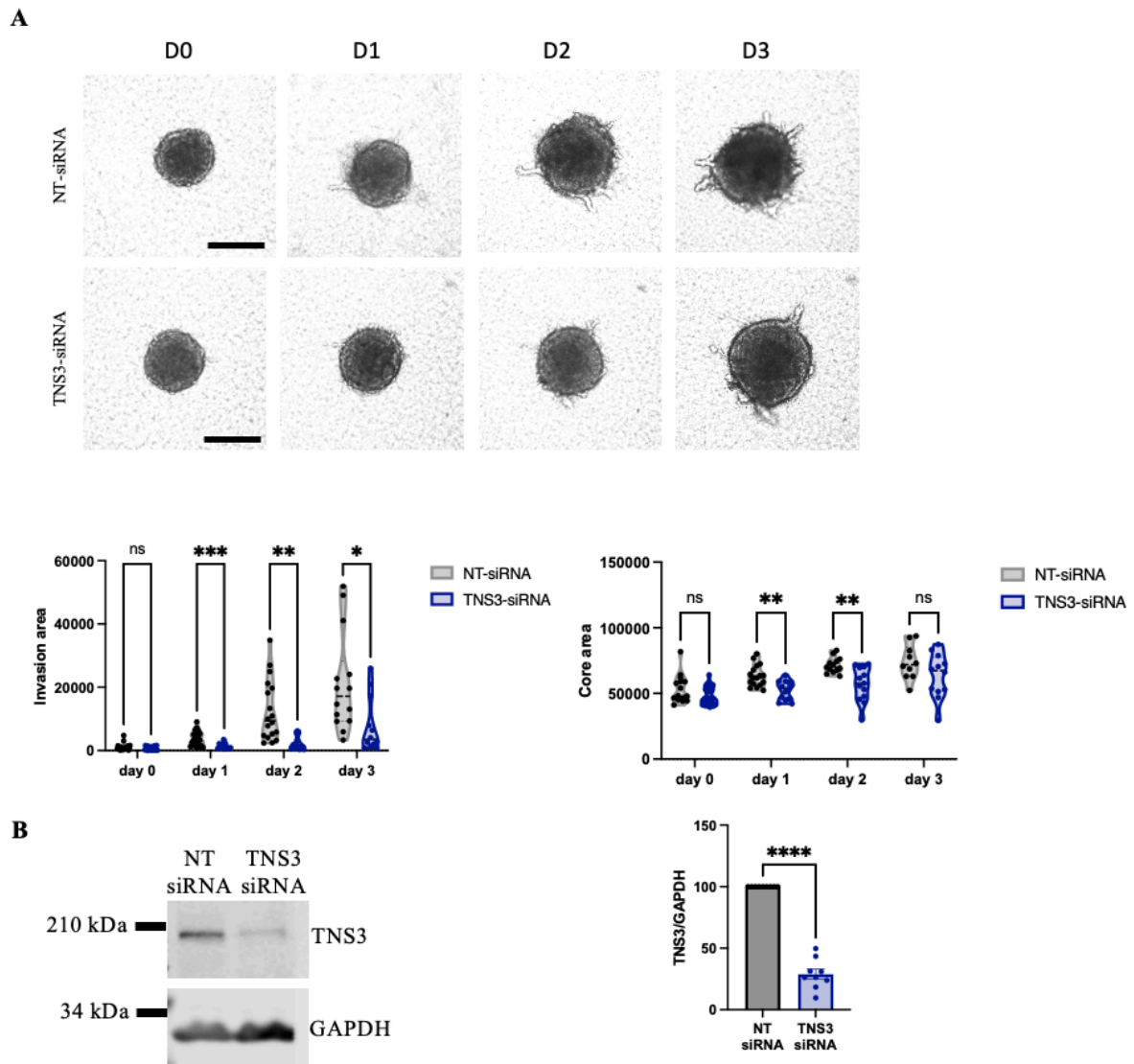


Figure 3.7: (A) TNS3 is required for DCIS cell invasion in 3D spheroids. MCF10DCIS (DCIS) cells were transfected with a TNS3 specific si-RNA (TNS3) and a non-targeting siRNA as a control (NT) and stained with Cell Tracker Red for 40 minutes. Spheroids were formed with the hanging drop method for 48hr and embedded into a mixture of 3 mg/ml Geltrex and 4 mg/ml collagen 1 for 3 days. Spheroids were imaged with a Nikon A1 confocal microscope at day 0 (D0), day 1 (D1), day 2 (D2) and day 3 (D3). Scale bar, 200 μ m. Invasion and core area were measured with ImageJ. The graphs represent the mean \pm SEM of three independent experiments. * p <0.05, ** p <0.001, *** p <0.001 **** p <0.0001, Kruskal-Wallis, multiple comparisons test, One-Way ANOVA. **(B)** MCF10DCIS (DCIS) cells were transfected as above, cell lysates were collected 2 days after transfection and run through an SDS-PAGE gel. After transfer, membranes were stained for TNS3 and GAPDH (loading control) and imaged with a Licor Odyssey Sa. Band intensity was measured with ImageStudio and normalised to GAPDH. The graph represents the mean \pm SEM of nine independent experiments. * p <0.05, ** p <0.001, *** p <0.001, **** p <0.0001. Mann-Whitney test, t-test.

3.2.8 TNS3 is required for MCF10CA1 cell in invasion.

To investigate whether TNS3 also controls the invasion of metastatic breast cancer cells, MCF10CA1 cells were transfected with TNS3-specific siRNA and a non-targeting siRNA as controls and grown from single cells in 3D Geltrex for three days. At Day 3, the

control acini developed protrusions, as expected of invasive MCF10CA1 cells. However, when TNS3 was depleted, this behaviour was significantly reduced, and acini were mostly circular (**figure 3.8A**). Indeed, quantification of acinus circularity showed a statistically significant increase upon TNS3 down-regulation. Notably, there were no notable changes in the area.

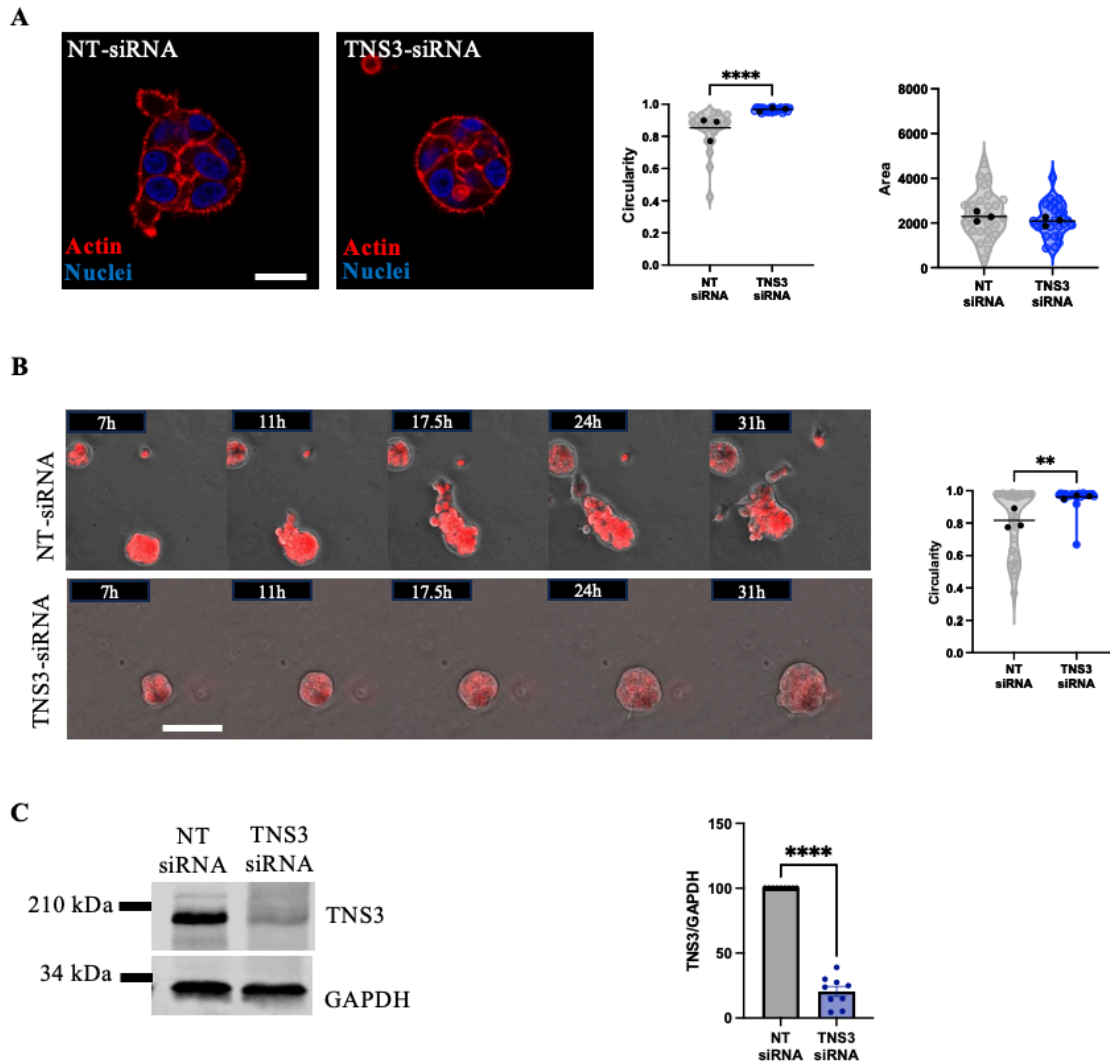


Figure 3.8: TNS3 is required for CA1 cell in invasion. (A) MCF10CA1 (CA1) cells were transfected with TNS3 specific si-RNA (TNS3 si-RNA) and a non-targeting siRNA as a control (NT-siRNA). Single CA1 cells were grown in 3D Geltrex for 3 days, fixed and stained for actin (red) and nuclei (blue). Cells were imaged by a Nikon A1 confocal microscope. Scale bar, 20 μ m. Circularity was measured in ImageJ. The graph represents the mean \pm SEM of three independent experiments. (B) CA1 cells were transfected as in (A) and grown in 3D Geltrex for 2 days. The cells were stained for nuclei (red) imaged live by time lapse microscope for 48h. Stills from a representative movie are presented. Scale bar, 50 μ m. Circularity was measured in ImageJ. The graph represents the mean \pm SEM of three independent experiments. (C) CA1 cells transfected as in A for 2 days. Cell lysates were collected, run through SDS-PAGE gels, blotted for TNS3 and GAPDH and imaged with a Licor Odyssey Sa. Band intensity was measured with ImageStudio and normalised to GAPDH. The graph represents the mean \pm SEM of nine independent experiments. * p <0.05, ** p <0.001, *** p <0.001, **** p <0.0001. Mann-Whitney test, T-test.

To gain better insights in the cell invasion dynamics, I used live imaging of MCF10CA1 cells grown in 3D Geltrex. MCF10CA1 were transfected with non-targeting siRNA or TNS3-specific siRNA and imaged from day 2 to day 4. After about 11 hours of imaging, control cells began to invade and formed multicellular protrusions. After 17.5, 24.2, and 31 hours, the invasion expanded by creating larger protrusions and the acini migrated through the matrix. The acini generated by cells transfected with TNS3-specific siRNA, on the other hand, after about 11 hours of imaging, only grew in size, but no invasion occurred. After 17.5, 24.2, and 31 hours, the size of the acini kept increasing as the cells continued to proliferate, but no invasion occurred (**figure 3.8B**). Consistent with the previous results, the circularity was significantly reduced when we silenced TNS3 compared to the control group. Western blotting analysis confirmed that the percentage of the TNS3 knock-down in MCF10CA1 cells was around 70% (**figure 3.8C**).

Altogether, we can conclude that TNS3 plays an important role in controlling breast cancer cell invasion.

3.2.9 TNS3 downregulation reduced MCF10DCIS and MCF10CA1 cell growth on Matrigel under glutamine deprivation.

Previous results showed that TNS3 knock-down in MCF10DCIS spheroids resulted in a significantly smaller core size, indicating that TNS3 may play a role in cell proliferation control. Furthermore, our lab recently found that the ECM promotes breast cancer cell growth during amino acid starvation, including glutamine (Nazemi et al., 2024). Because TNS3 plays an important role in mediating cell/ECM interaction, I wanted to investigate the effects of TNS3 knockdown on cell proliferation on plastic or matrigel, in complete media or glutamine starvation.

MCF10DCIS and MCF10CA1 cells were cultured on plastic or plastic coated with 3mg/ml Matrigel for 7 days in either full media or glutamine-free media. In **figure 3.9A**, MCF10DCIS cells cultured on plastic or Matrigel in full media showed no significant differences between control and TNS3 downregulation. Similarly, **figure 3.9B** shows that MCF10CA1 cells grown on plastic or Matrigel with full media exhibited comparable proliferation rates with and without TNS3 knock-down. Consistent with previous findings, MCF10DCIS treated with a non-targeted siRNA cells seeded in glutamine-free media grew significantly more on Matrigel than on plastic, while TNS3 downregulation significantly impaired cell proliferation on matrigel (**Figure 3.9C**). Similarly, MCF10CA1 cells plated on Matrigel in glutamine-free media

proliferated more than cells seeded on plastic in the presence of a non-targeting siRNA, while knocking down TNS3 reduced the proliferation on Matrigel without affecting cell growth on plastic (**figure 3.9D**). These findings confirmed that Matrigel supported cell proliferation under glutamine deprivation and TNS3 was required for ECM-dependent cell growth under starvation, without affecting cell proliferation in complete media.

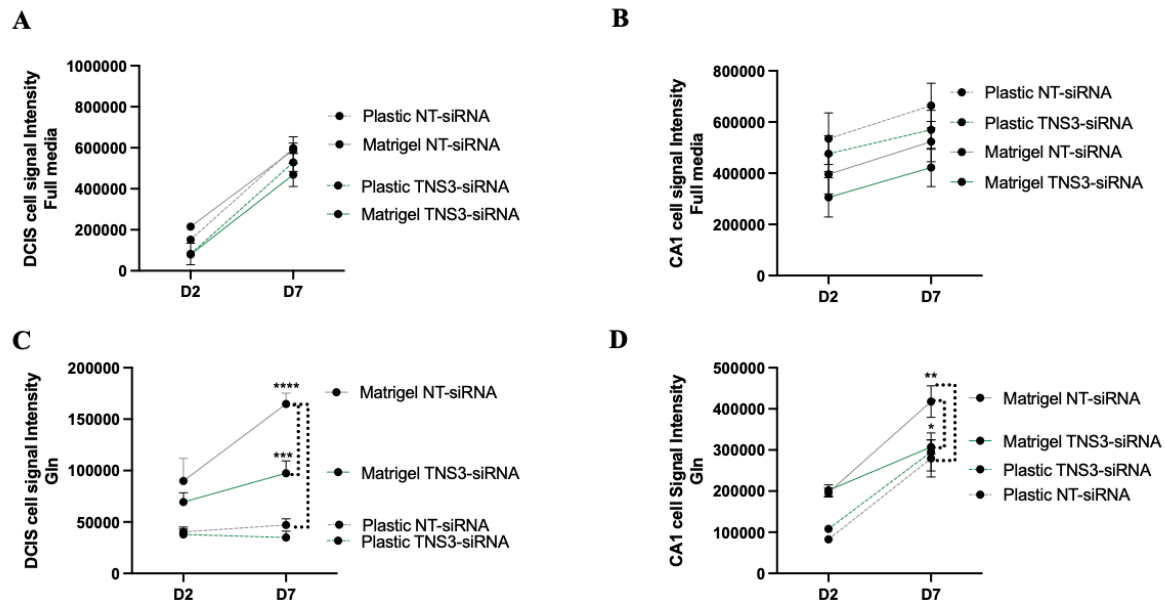


Figure 3.9: TNS3 downregulation reduced DCIS and CA1 cell growth on Matrigel under glutamine deprivation. MCF10DCIS (DCIS) and MCF10CA1 (CA1) cells were transfected with TNS3 specific si-RNA (TNS3 si-RNA) and a non-targeting siRNA as a control (NT-siRNA). MCF10DCIS (DCIS) and MCF10CA1 (CA1) were cultured on plastic or plastic coated with 3mg/ml Matrigel for 7 days, with either full media (full) or glutamine-free media (Gln). Cells were fixed, stained with DRAQ5 on day 2 and 7 and imaged with a Licor Odyssey Sa system. Data were quantified with Image Studio Lite software. The graphs represent the mean \pm SEM of three independent experiments for CA1 and two independent experiments for DCIS. * $p < 0.05$, ** $p < 0.001$, *** $p < 0.001$, **** $p < 0.0001$. Mixed effect analysis, Tukey's test, Multiple comparisons test, Two-Way ANOVA.

3.3 Discussion

Here I demonstrated that TNS3 expression increased in DCIS and IDC, compared to the healthy mammary gland, in a breast cancer mouse model. Furthermore, TNS3 expression was significantly higher in invasive and metastatic MCF10CA1 cells compared to the non-tumorigenic MCF10A cells. These data are in agreement with several publications highlighting that TNS3 levels are high in breast cancer cell lines compared to normal cell lines (Shinchi *et al.*, 20015; Qian *et al.*, 2009; Chiang *et al.*, 2005). In addition, previous *in vivo* study on FVB mice genetically modified by PyMT to produce breast cancer revealed that TNS3 is significantly more expressed in primary breast cancer tissue than in normal breast tissue (Qian

et al., 2009; Shinchi et al., 2015). Some studies indicated that TNS4 levels increased in breast cancer, while others did not. It has been documented that TNS4 exhibited high expression levels in invasive breast tumors (Liao & Lo, 2021; X. Lu et al., 2021). Following the use of an EGFR kinase inhibitor, the expression of TNS4 decreased. This finding implies that the regulation of TNS4 is dependent on EGF (Albasri et al., 2011). Another research study indicates that TNS4 and TNS3 function in contrasting manners in regulating migration. Inhibition of TNS4 led to a decrease in migration, whereas silencing TNS3 resulted in an increase in migration (Mouneimne & Brugge, 2007). Another investigation found that TNS4 decreased in various subclasses of human breast cancer obtained from a genomic database (X. Lu et al., 2021). Overexpressing TNS4 in MCF7 and human umbilical vein endothelial cells resulted in reduced cell proliferation, migration, and tube formation (X. Lu et al., 2021). In my project, I assessed TNS localisation at the adhesion level. TNS4 localization differs significantly from TNS3 in that it is located in the cytoplasm rather than at the ventral surface. Furthermore, TNS4 lacks one of the focal adhesion binding sites at the N-terminus, meaning that TNS4 can still bind to integrins via the PT domain but this is less effective at recruiting the protein to focal adhesion. It has also been reported that losing the N-terminal results in a loss of binding to focal adhesion proteins and actin filament (Liao & Lo, 2021). Here I demonstrated that MCF10DCIS cells could invade in a 3D culture setting (Brock et al., 2019). Furthermore, I was able to demonstrate that TNS3 was required for breast cancer cell invasion. This result is consistent with previous reports that TNS3 promotes cell invasion. A study was conducted to examine TNS3 and its impact on invasion in MDA-MB-231 breast cancer cells. The findings revealed that a decrease in TNS3 mRNA was linked to a reduction in invasion, but not proliferation (Shinchi et al., 2015). Another study using MDA-MB-468 breast cancer cells found that a stable reduction in TNS3 expression reduced invasion and migration (Veß et al., 2017). Furthermore, my observation that TNS3 is required for MCF10CA1 cell invasion strengthens TNS3's critical role in breast cancer progression. Additionally, it was previously reported that knocking down TNS3, but not TNS4, dramatically reduced cancer cell migration, soft agar growth *in vitro* and tumour formation *in vivo* (Qian et al., 2009). The cell lines used in this study were human non-small cell lung cancer (NSCLC) lines H1299, A549, and H358, metastatic melanoma cell lines 553B, 1088, and 568, breast cancer line MDA-MB-468, and mouse cell line Met-1. Knocking down TNS3 significantly reduced growth and migration in H1299, A549, and H358 cells, as evidenced by anchorage-independent growth in soft agar, transwell invasion assays, and the MTT assays. Similarly, 553B, 1088, and 568 melanoma cell lines showed a significant reduction in growth

and migration upon TNS3 downregulation. Met-1 cells and MDA-MB-468 breast cancer cells also exhibited decreased migration. The *in vivo* experiment was carried out in FVB/MT mice to evaluate tumour growth and metastasis. Met-1 and PyMT cells transfected with control and TNS3 targeting siRNAs were injected into the breast fat pad to assess tumour growth, as well as in the tail vein to assess metastatic potential. After four weeks, the tumours were removed from the fat pad and their volume measured. 20 days after tail vein injections, the lungs were dissected and checked for metastasis. The results showed a significant decrease in tumour growth and metastasis after TNS3 silencing. This finding suggests that TNS3 may play a critical role in the initiation and progression of breast cancer. The high level of TNS3 in DCIS may explain its role in tumour formation, whereas high levels in the metastatic stage highlight its contribution to enhanced invasion and spread to various organs.

Following my 3D spheroid experiment in MCF10DCIS cells, I noticed a reduction in cell size, implying that TNS3 might play a role in proliferation. The results I got show silencing TNS3 successfully reduced cell proliferation in both DCIS and CA1 plated on Matrigel under Gln-free media. During the growth phase, there will be intracellular interactions that drive the formation of adhesion forces, causing the cells to cluster inside the spheroids. This fact will be overcome over time. In my experiment, I observed an effect on the growth of the spheroids on days 1 and 2 because the cells were transfected with TNS3-siRNA and stained with marker, which could have a preliminary effect on their growth compared to NT-siRNA as on day 3 the spheroids core size was comparable. My proliferation results show that the cell growth significantly increased in MCF10DCIS and MCF10CA1 plated on Matrigel compared to plastic in glutamine-free media while there wasn't significant changes for both cell lines in complete media, in agreement with previous work from our lab, which demonstrated that ECM-dependent cell growth required ECM endocytosis and lysosomal degradation (Nazemi et al., 2024). Since TNS3 is needed for ligand-bound integrin internalisation, it is possible that TNS3 might regulate cell growth by modulating ECM uptake (Rainero et al., 2015).

Altogether, these findings indicate that TNS3 is upregulated during breast cancer progression and is required to promote cell invasion and ECM-dependent cell proliferation.

Chapter 4. TNS3 regulates BM organisation and filopodia formation

4.1 Introduction.

It has been reported that the deregulation of the ECM is implicated in cancer progression (Rainero, 2018; B. Sun, 2021; Walker et al., 2018). The progression of breast cancer is a multifaceted process where in the interaction between cancer cells and the ECM facilitates tumour invasion and metastasis (Guess & Quaranta, 2009). The BM possesses both tumour-inhibiting and tumour-promoting characteristics. On the one hand, the BM constrains the primary tumour and, as a result, its degradation leads to cell migration. Conversely, the association between the accumulation of certain BM components and invasive behaviours has also been recognised. Indeed, ECM components such as laminins and collagen IV have been shown to exhibit pro-invasive properties and the overexpression of laminin-332 and collagen IV correlates with the advancement of breast cancer (Chang et al., 2024; Kim et al., 2012). Laminin-332 is a glycoprotein and a principal component of the BM. It plays a crucial role in facilitating cell adhesion and migration. Laminin-332 interacts with cells through various integrins receptors, including $\alpha 3\beta 1$, $\alpha 6\beta 1$, and $\alpha 6\beta 4$ (Givant-Horwitz et al., 2005; Guess & Quaranta, 2009; Tsuruta et al., 2008). They are crucial for mediating the BM attachment, structure, assembly, and focal adhesion (Givant-Horwitz et al., 2005; Guess & Quaranta, 2009; Tsuruta et al., 2008). Extensive research has demonstrated upregulation in the expression levels of laminin-332, $\alpha 3\beta 1$, and $\alpha 6\beta 1$ during the progression of breast cancer (Faraldo et al., 2024; Gonzales et al., 1999; Kim et al., 2012; Speer et al., 2021; Yang et al., 2008; Zhou et al., 2020). Furthermore, laminin-332 binding to $\alpha 3\beta 1$ integrin has been shown to promote focal adhesion signalling (Gonzales et al., 1999; Miskin et al., 2021; Ramovs et al., 2019).

$\alpha 3$ integrin has been implicated in breast cancer metastasis. Indeed, $\alpha 3$ silencing significantly reduced the ability of triple negative MDA-MB-231 breast cancer cells to form lung metastasis in an NSGTM mouse model of breast cancer. Moreover, elevated $\alpha 3$ expression was correlated with an increase in the expression of the Brain-2 (Brn-2) transcription factor. Brn-2 is highly expressed in various types of cancer, including breast cancer and stimulates invasive behaviours (Miskin et al., 2021). The upregulation of laminin-332 and $\alpha 3\beta 1$ was also found to be associated with anoikis resistance, an essential requirement and key marker for tumour cells' ability to metastatically spread. Anoikis is a type of cell death program that begins when cells become detached from the ECM. This process maintains tissue health by preventing the spread

and growth of abnormal cells. Metastatic cancer cells typically exhibit resistance to anoikis (Dai et al., 2023). Mechanistically, laminin-332 binding to integrin $\alpha 3\beta 1$ on myofibroblasts activates a cell survival signalling pathway initiated by Akt phosphorylation, which resulted in anoikis resistance (Kim et al., 2012). Another reported study used Brca1/p53-deficient mice to study the effect of $\alpha 6$ knockout on tumour formation, which resulted in a reduction of EMT activation, thereby delaying the formation of tumours and reducing their number (Faraldo et al., 2024).

Filopodia are slender, finger-like structures that develop and extend from the cell surface (Jacquemet et al., 2017). This actin filament structure is critical to maintaining numerous cellular processes, including sensing, motility, migration, wound healing, adhesion to the ECM, and cell-cell contact (Jacquemet et al., 2017). Filopodia exhibit distinct behaviour dynamics in terms of length and density, and the quantity of these filament protrusions varies between cells (Jacquemet et al., 2017). Filopodia are composed of densely packed parallel actin filaments with barbed ends orientated towards the filopodium tip (Miihkinen et al., 2021). This shape facilitates the proximity and accumulation of molecular motors, including unconventional myosin-X (MYO10) at the tips (Miihkinen et al., 2021). It was suggested that these molecular motors facilitate the transport of proteins, such as integrins, along actin filaments to the ends of filopodia (Miihkinen et al., 2021). During migration, cells use cellular extensions, such as filopodia, to investigate their surroundings. Filopodia form special integrin-adhesion complexes to detect the ECM (Miihkinen et al., 2021). MYO10 and talin modulate $\beta 1$ -integrin activation at filopodia (Miihkinen et al., 2021). Moreover, MYO10 expression is associated with BM deposition. In addition, inhibiting MYO10 reduces BM assembly in non-invasive DCIS cells (Peuhu et al., 2022). A reported study shows both invasion ability and filopodia formation increased in a stage-dependent manner in MCF10A and MCF10DCIS cells (Jacquemet et al., 2017).

In the previous chapter, I showed that MCF10DCIS and MCF10CA1 cells expressed higher levels of TNS3 than MCF10A. Furthermore, TNS3 played a role in promoting invasion in both MCF10DCIS and MCF10CA1 cells. Therefore, I deemed it crucial to explore the underlying mechanisms through which TNS3 promoted cell invasion. According to my hypothesis, TNS3 could achieve this by controlling BM deposition and the formation of filopodia, through the modulation of integrin receptors. In this chapter, I showed that TNS3 controls the expression

of laminin-332, as well as the formation of filopodia, in both MCF10DCIS and MCF10ACA1 cells, by promoting the expression of integrin $\alpha 3\beta 1$ and $\alpha 6\beta 1$.

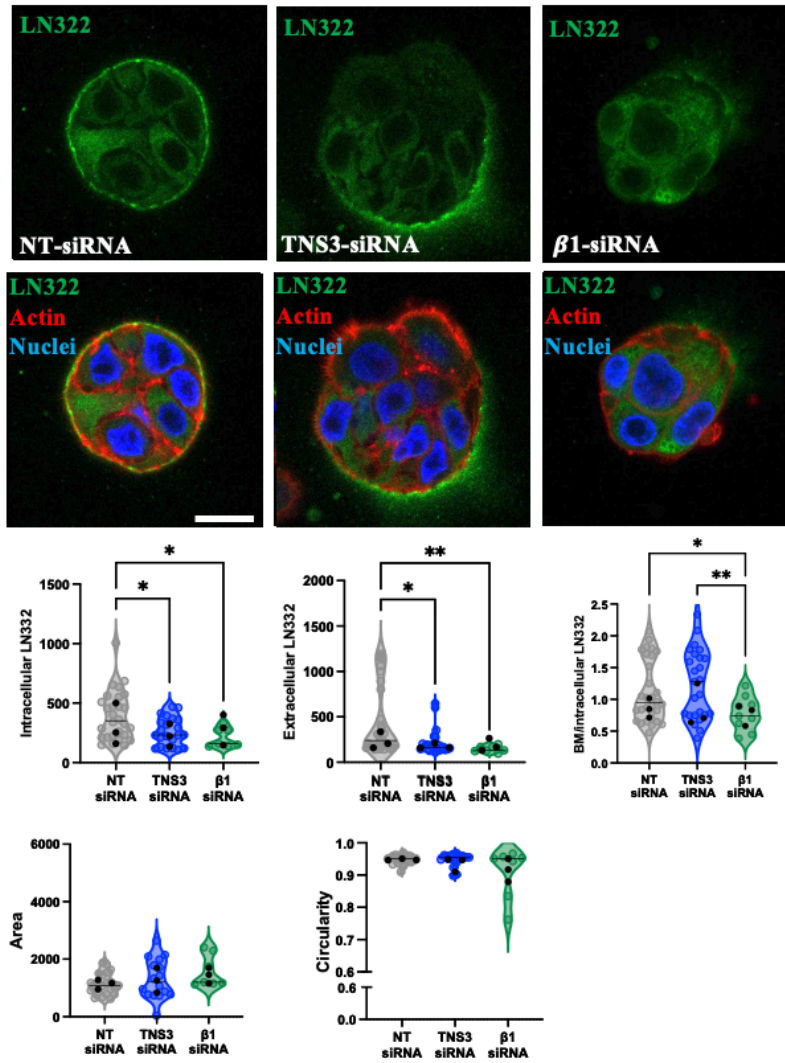
4.2 Results

4.2.1 TNS3 and $\beta 1$ integrin downregulation prevents BM deposition.

In the previous chapter, we demonstrated that TNS3 is involved in the invasion of MCF10DCIS and MCF10CA1 cells grown in 3D system. Here, I wanted to investigate the mechanisms underlying this effect by looking at how TNS3 regulates BM secretion/deposition. BM degradation is an important part of the invasion-metastasis cascade, where cancer cells begin to invade nearby tissues and travel through blood vessels to metastasis. However, localised BM component accumulation at nascent protrusion sites have been shown to drive breast cancer cell invasion (Chang et al., 2022). Therefore, I wanted to investigate the contribution of TNS3 in modulating BM organisation. MCF10DCIS cells, transfected with an siRNA targeting TNS3, $\beta 1$ integrin or a non-targeting siRNA control, were grown in Geltrex for 3 days and stained for the BM components laminin-332 (**figure 4.1A**). While control cells assembled a well-defined BM layer around the 3D acini structures, TNS3 and $\beta 1$ KD cells failed to do so, as highlighted by the quantification of the laminin-332 staining intensity in the BM (extracellular) and inside the cells. Both intracellular and extracellular laminin-332 showed a statistically significant reduction in TNS3 and $\beta 1$ KD cells when compared to the control group (**figure 4.1A**). In the presence of NT control, laminin-332 in the BM is evenly distributed around the acini, whereas silencing TNS3 leads to a more uneven distribution. In addition, silencing $\beta 1$ leads to a notable decrease in laminin-332 incorporation in the BM, resulting in a significant reduction in the laminin-332 BM/intracellular ratio. These data indicate that TNS3 and $\beta 1$ integrin might control laminin-332 levels, while $\beta 1$ integrin also plays a role in laminin-332 deposition. As the BM is crucial for tissue maintenance and influences cellular behaviour (Khalilgharibi & Mao, 2021), we assessed the consequences of TNS3 and $\beta 1$ KD on acini morphology. However, quantification of acinus circularity and area showed no significant difference between all conditions, despite a small trend towards a reduction in circularity in $\beta 1$ KD structures.

To assess the efficiency of $\beta 1$ knock-down, MCF10DCIS cells were transfected with either control non-targeting siRNA or an siRNA targeting $\beta 1$. Cells were grown in 3D Geltrex for 3 days. Then cells were fixed and stained for $\beta 1$ -integrin. As shown in **figure 4.1B**, in the control group, $\beta 1$ accumulates all around the plasma membrane, both at the cell-cell junctions

A



B

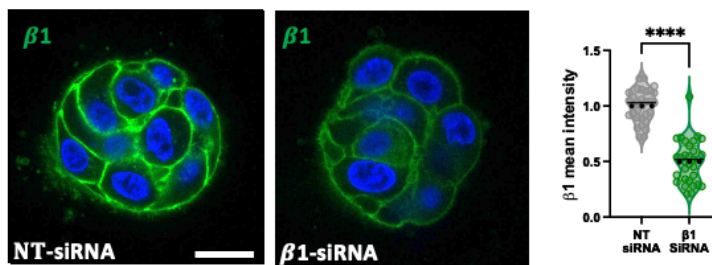


Figure 4.1: TNS3 and $\beta 1$ -integrin downregulation prevented BM deposition. (A) MCF10DCIS cells were transfected TNS3, $\beta 1$ -integrin specific si-RNA or a non-targeting siRNA control (NT-siRNA) for 24h. Cells were grown in 3D Geltrex for 3 days, were fixed and stained for actin (red), Laminin 322 (LN332, green) and nuclei (blue). Cells were imaged by a Nikon A1 confocal microscope. LN332 staining mean intensity, area and circularity of the acini were measured in ImageJ. Scale bar, 20 μ m. N=3 independent experiments. * $p < 0.05$, ** $p < 0.001$ Kruskal-Wallis, multiple comparisons test, One-Way ANOVA. (B) MCF10DCIS cells were transfected with $\beta 1$ -integrin specific si-RNA or a non-targeting siRNA control for 24h. Cells were grown in 3D Geltrex for 3 days, fixed and stained for $\beta 1$ -integrin (green) and nuclei (blue). Cells were imaged by a Nikon A1 confocal microscope. Scale bar, 20 μ m. $\beta 1$ -integrin mean intensity was measured in ImageJ. Data represent the mean \pm SEM of three independent experiments. **** $p < 0.0001$. Mann-Whitney test, T-test.

and basolaterally. However, as expected, the intensity of $\beta 1$ staining declined sharply after knocking down $\beta 1$. The analysis of $\beta 1$ intensity indicated $\sim 50\%$ reduction in integrin levels in the KD structures compared to the control.

Altogether, these data suggest that TNS3 and $\beta 1$ integrin could play a role in controlling laminin-332 levels in the BM.

4.2.2 TNS3 downregulation reduced laminin-332 expression.

Since extracellular and intracellular laminin-332 staining was reduced in TNS3 and $\beta 1$ knock-down in DCIS cells, as assessed by 3D immunofluorescence microscopy, I wanted to investigate whether overall laminin-332 expression was affected by TNS3 downregulation. MCF10DCIS cells were transfected with a TNS3 specific siRNA and a non-targeting siRNA control for 2 days. Then, the protein level of laminin-332 was determined by western blot. As shown in **figure 4.2**, laminin-332 expression was significantly decreased in TNS3 knock-down DCIS cells when compared to the non-targeting control, indicating that TNS3 controls laminin-332 protein expression.

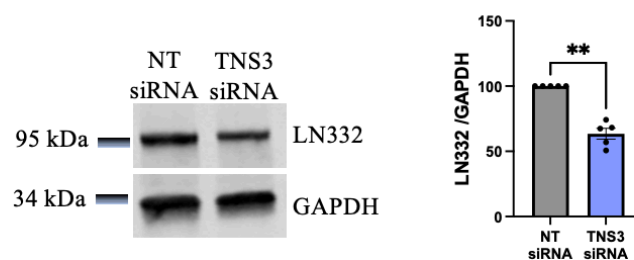


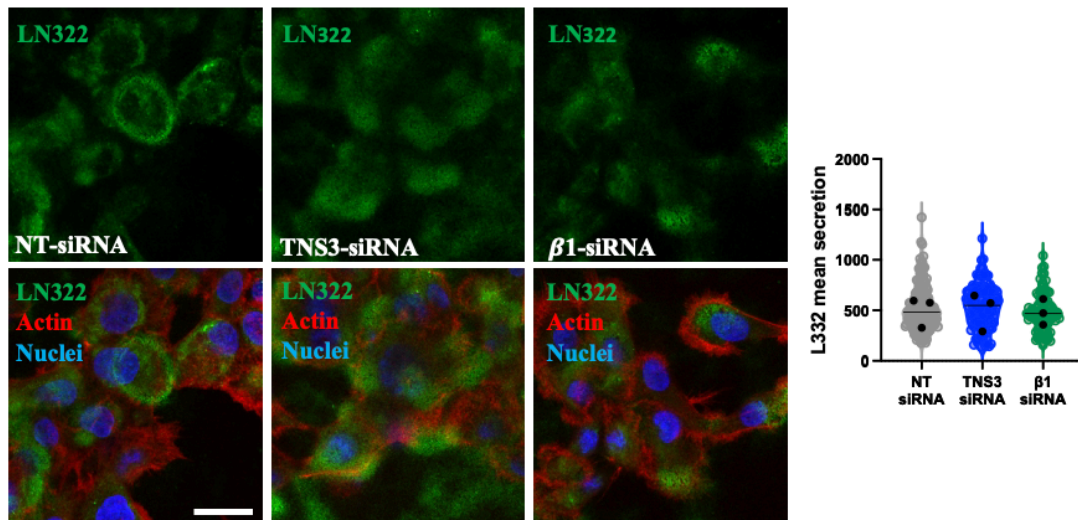
Figure 4.2: TNS3 knockdown reduced laminin-332 expression. MCF10DCIS cells were transfected with TNS3 specific si-RNA or a non-targeting siRNA control (NT-siRNA) for 2 days on plastic. Cell lysates were collected and run through SDS-PAGE gels. Membranes were stained with anti-laminin-332 (LN332) and anti-GAPDH antibodies and imaged with a Licor Odyssey system. Band intensity was measured with ImageStudio and normalised to GAPDH. Data represent the mean \pm SEM of five independent experiments. ** $p < 0.001$ Mann-Whitney test, T-test.

4.2.3 TNS3 and $\beta 1$ integrin down regulation did not affect laminin-332 secretion/deposition in 2D.

As $\beta 1$ integrin downregulation affected laminin-332 BM deposition, I wanted to examine if TNS3 and $\beta 1$ -integrin were affecting laminin-332 secretion/deposition in 2D systems, alongside a decrease in overall expression. MCF10DCIS cells, transfected with an siRNA targeting TNS3, $\beta 1$ -integrin or a non-targeting siRNA control were plated on glass-bottom dishes, coated with 0.25mg/ml Geltrex for 48h. Cells were then fixed and stained for laminin-

332 and $\beta 1$ -integrin. Z-stacks were acquired to be able to measure laminin-332 intensity below the ventral surface of the cells.

A



B

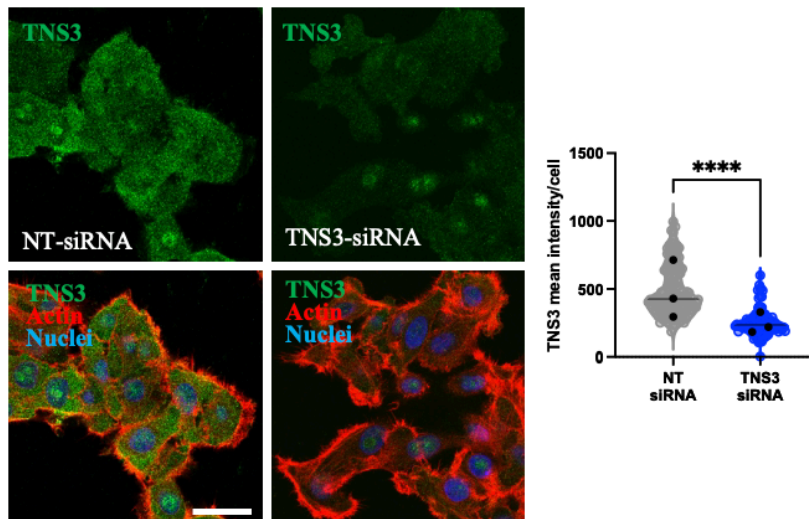


Figure 4.3: TNS3 and $\beta 1$ integrin down regulation did not affect laminin-332 secretion/deposition in 2D. MCF10DCIS cells were transfected with TNS3 specific siRNA, $\beta 1$ -integrin specific siRNA or a non-targeting siRNA control (NT-siRNA) for 24h. Cells were plated on glass-bottom 3.5cm dish, coated with 0.25mg/ml Geltrex, overnight, fixed and stained for Laminin 322 (LN322, green), actin (red) and nuclei (blue). Cells were imaged with a Nikon A1 confocal microscope. Scale bar, 25 μ m. Laminin 322 mean intensity in the ventral surface of the cells was measured with ImageJ. N=3 independent experiments. The black dots represent the mean of each experiment. **(B)** MCF10DCIS cells were transfected with TNS3 specific siRNA or a non-targeting siRNA for 24h. Cells were plated on glass-bottom 3.5cm dish, coated with 0.25mg/ml Geltrex, overnight, fixed and stained for TNS3 (green), actin (red) and nuclei (blue). Cells were imaged by a Nikon A1 confocal microscope. Scale bar, 25 μ m. TNS3 mean intensity was measured in ImageJ. N=3 independent experiments. The black dots represent the mean of each experiment. ****p<0.0001. Mann-Whitney test, T-test.

The results in **figure 4.3** show that the amount of the laminin-332 present in the BM was the same in the control compared to si-TNS3 and si- $\beta 1$ -integrin. To validate the downregulation of TNS3 upon knockdown, cells transfected with a non-targeting siRNA control or an siRNA

against TNS3 were fixed and stained for TNS3. TNS3 intensity was reduced by approximately 60% in the knocked down cells compared to non-targeting siRNA. The signal in the nucleus is non-specific, as we have previously observed using this TNS3 antibody (**figure 4.3B**). These data suggests that TNS3 and β 1-integrin are not controlling the secretion of laminin-332 to the BM in 2D system.

4.2.4 Filopodia formation precedes laminin deposition.

Considering there was an effect on the overall laminin-332 levels, I wanted to examine the deposition of laminin-332 at different time points in 3D. Therefore, MCF10DCIS cells were grown in 3D Geltrex for up to 3 days, fixed and stained for laminin-332 and actin. The findings indicate that on day 1, there was no detectable laminin-332 in the BM around the acini. However, on day 2, a clear ring of laminin-332 became visible. On the third day the BM accumulation of laminin-332 was increased. The intracellular laminin-332 levels appeared constant over the three days. Image analysis show that extracellular laminin-332 increased significantly on Day 2 and 3 compared to Day 1, while, the intracellular laminin-332 remain constant over three days. Consequently, the BM to intracellular ratio of laminin-332, which reflects BM incorporation, progressively increased during the time course (**figure 4.4**).

A recent study has demonstrated that MYO10, which is situated in the filopodia and is a master regulator of filopodia formation, is associated with BM deposition in MCF10DCIS cells. The expression of this protein was elevated in DCIS in comparison to the normal mammary gland and the loss of filopodia resulting from MYO10 knock-down impaired BM deposition in MCF10DCIS cells (Peuhu et al., 2022). Therefore, I quantified filopodia formation in MCF10DCIS cells grown in Geltrex for up to 3 days. The filopodia appeared dense and long, as the size of the acini increased over time, so did the number of filopodia per acinus. The results show that filopodia number and area grew on day 3 compared to days 1 and 2. Additionally, the filopodia lengths remained constant over the three days (**figure 4.4**). This suggests that the filopodia form first, followed by laminin-332 deposition in the BM, while the acini grow in size over time. This is consistent with the observation that filopodia are required for BM deposition (Peuhu et al., 2022).

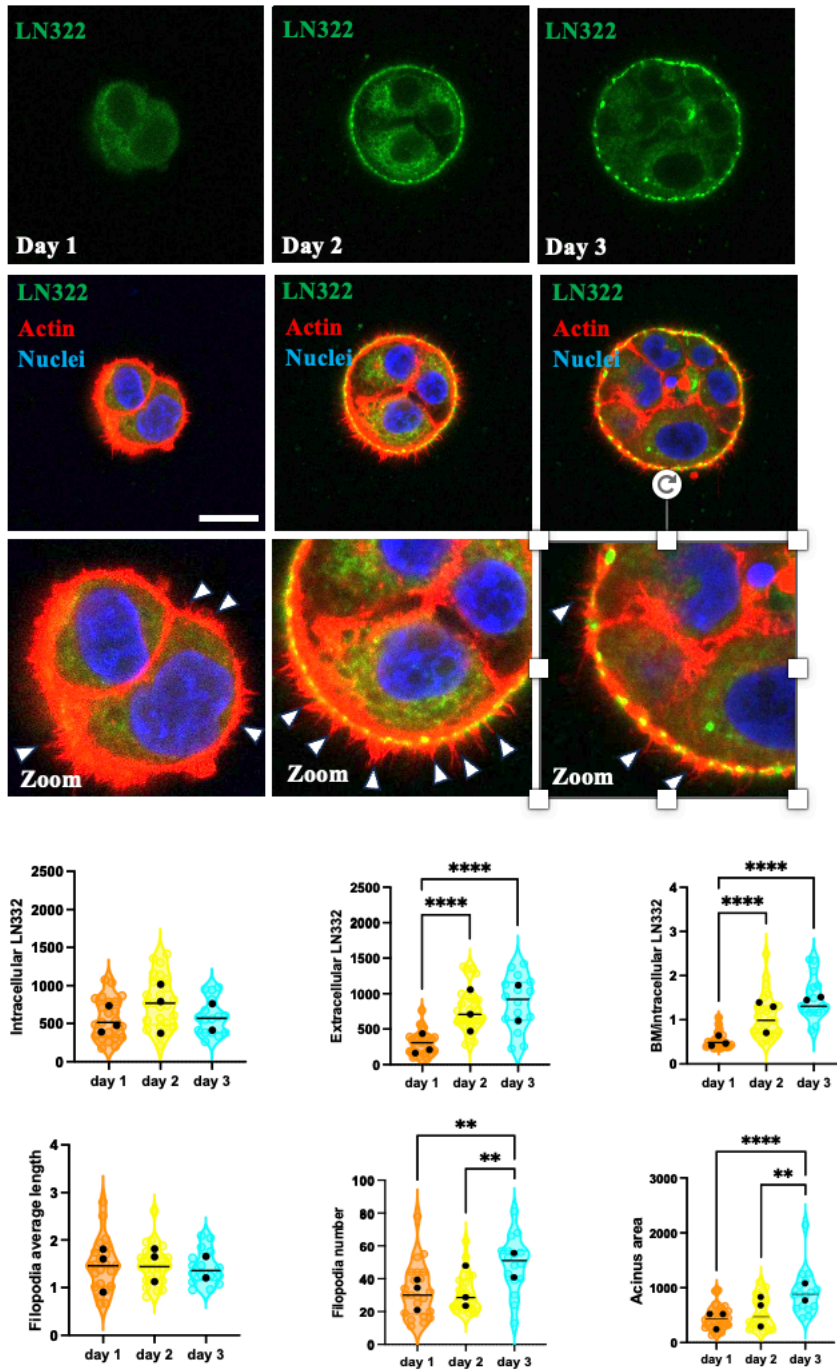


Figure 4.4: Filopodia formation preceded laminin-332 deposition. MCF10DCIS cells were grown in 3D Geltrex for up to 3 days. Cells were fixed at day 1, day 2 or day 3 and stained for actin (red), Laminin 322 (LN332, green) and nuclei (blue). Cells were imaged by a Nikon A1 confocal microscope. Laminin 332 mean intensity was measured in ImageJ. Scale bar, 20 μ m. N \geq 2 independent experiments. The black dots represent the mean of each experiment. * p <0.05, ** p <0.001, *** p <0.001, **** p <0.0001. Kruskal-Wallis, multiple comparisons test, One-Way ANOVA.

4.2.5 TNS3 and β 1-integrin downregulation reduced filopodia formation.

It was reported that active β 1-integrin accumulates at the leading edge of filopodia whereas inactive ones are distributed evenly (Miihkinen et al., 2021). Reportedly, the formation of filopodia was hindered when β 1-integrin was suppressed, suggesting that β 1-integrin is necessary for the formation of filopodia (Kren et al., 2007). To study the effects of suppressing TNS3 and β 1-integrin on filopodia formation, MCF10DCIS cells were transfected with TNS3, β 1-integrin specific siRNA or a non-targeting siRNA control for 24h. Then, cells were grown in 3D Geltrex for 3 days, fixed and stained for actin and nuclei. Filopodia are readily visible in the non-targeting siRNA group (**figure 4.5**). In the acini where TNS3 or β 1-integrin were silenced, fewer filopodia were present, which were smaller and less dense. The quantification shows that the average length and number of filopodia was significantly reduced in TNS3 or β 1-integrin specific siRNA when compared to the non-targeting control (**figure 4.5**). These results indicate that TNS3 and β 1-integrin are required for filopodia formation in 3D systems.

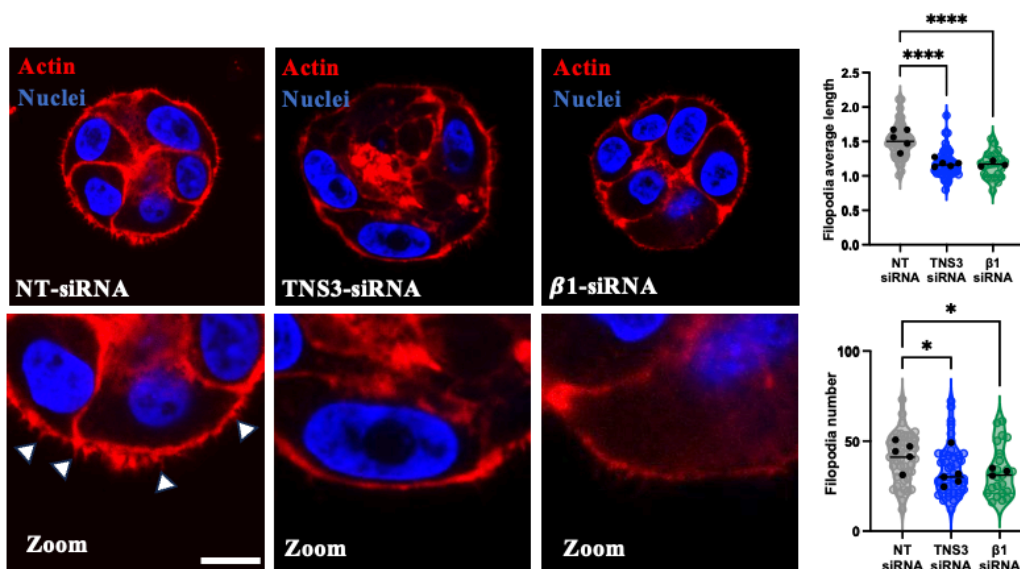


Figure 4.5: TNS3 β 1-integrin knockdown reduced filopodia formation. MCF10DCIS cells were transfected with TNS3 specific siRNA, β 1-integrin specific siRNA or a non-targeting siRNA (NT-siRNA) as a control for 24h. Cells were grown in 3D Geltrex for 3 days, fixed and stained for actin (red) and nuclei (blue). Cells were imaged with a Nikon A1 confocal microscope. Scale bar, 25 μ m. Filopodia length and number were quantified in ImageJ. N \geq 3 independent experiments. The black dots represent the mean of each experiment. * p <0.05, **** p <0.0001. Kruskal-Wallis, multiple comparisons test, One-Way ANOVA.

4.2.6 TNS3 knockdown did not affect β 1-integrin distribution in MCF10DCIS cells.

It has been demonstrated that filopodia function is regulated by β 1-Integrin (Miihkinen et al., 2021). In an integrin-dependent manner, it has been demonstrated that upregulating MYO10 expression promotes filopodia production and elongation (Miihkinen et al., 2021; Zhang et al.,

2004). Moreover, TNS3 expression has previously been shown to be required for $\beta 1$ -integrin activation. In fibroblast cells, higher TNS3 levels were associated with higher $\beta 1$ -integrin activation (Georgiadou et al., 2017). It is possible to speculate that TNS3, being an integrin-binding protein, could regulate the formation of filopodia by modulating the localisation of integrin at the basolateral surface. To study the effect of silencing TNS3 on $\beta 1$ -integrin localisation, MCF10DCIS cells were transfected with TNS3 specific siRNA or a non-targeting siRNA and grown in 3D Geltrex for 3 days, fixed and stained for $\beta 1$ -integrin. $\beta 1$ -integrin localised at cell-cell junctions and in the basolateral surface in both the control and TNS3-KD groups. There was no apparent variation in observable intensity. The mean intensity of extracellular, intracellular and the ratio of BL/intracellular $\beta 1$ integrin staining was measured by ImageJ. The results show that the extracellular and intracellular $\beta 1$ -integrin expression levels remained unchanged in both the TNS3 siRNA and non-targeting siRNA groups (**figure 4.6**). Thus, result suggest that the total expression of $\beta 1$ -integrin and its localisation are not affected by TNS3 downregulation.

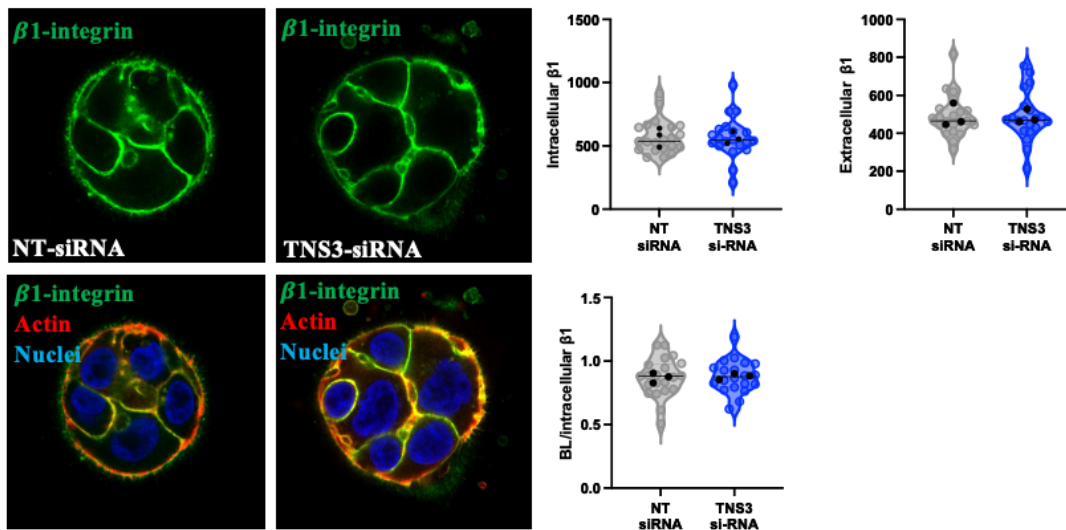


Figure 4.6: TNS3 knockdown did not affect $\beta 1$ -integrin distribution. MCF10DCIS cells were transfected by with TNS3 specific si-RNA or a non-targeting siRNA as a control for 24h. Cells were grown in 3D Geltrex for 3days, fixed and stained for actin (red), $\beta 1$ -integrin (green) and nuclei (blue). Cells were imaged by a Nikon A1 confocal microscope. Scale bar, 20 μ m. $\beta 1$ -integrin mean intensity was measured in ImageJ. N=3 independent experiments. The black dots represent the mean of each experiment.

4.2.7 TNS3 knock-down reduced $\alpha 3$ and $\alpha 6\beta 1$ integrin levels in MCF10DCIS cells.

Two main laminin-332 receptors are $\alpha 3\beta 1$ and $\alpha 6\beta 1$. According to reports, integrins regulate laminin deposition, through the activation of Rho GTPase signalling pathway (Hamill et al., 2009). This pathway also promotes the invasion and metastatic spread of cancer (Hamill et al.,

2009). In addition, it has been suggested that Tiam1, a Rho GTPase guanine nucleotide exchange factor, could promote the laminin-332 deposition (Dehart et al., 2003). Furthermore, another study demonstrates that $\alpha 3$ regulates the organization of laminin-332 in the extracellular matrix in keratinocytes, as suppressing $\alpha 3$ has been shown to impair laminin-332 deposition (Dehart et al., 2003). While I did not detect changes in $\beta 1$ level, it is possible that TNS3 controls the expression levels of the specific laminin-332 receptors, $\alpha 3$ and $\alpha 6$ integrin. To investigate this, MCF10DCIS cells were transfected with TNS3 specific siRNA or a non-targeting siRNA as a control for 24h, grown in 3D Geltrex for 3 days and stained for $\alpha 3$ or $\alpha 6$. $\alpha 3$ is expressed at low levels and localised at the plasma membrane as well as in the cytosol. The quantification shows that $\alpha 3$ basolateral and intracellular expression was significantly lower in TNS3 silenced acini than in the control group, but the BL/intracellular ratio remained constant (**Figure 4.7A**). Similarly, when TNS3 was downregulated the intensity of $\alpha 6$ integrin dropped significantly, from both intracellularly and in the basolateral surface, while the BL/intracellular ratio remained the same (**Figure 4.7B**). These findings suggest that TNS3 may control laminin-332 in the BM via the modulation $\alpha 3$ and $\alpha 6$ levels.

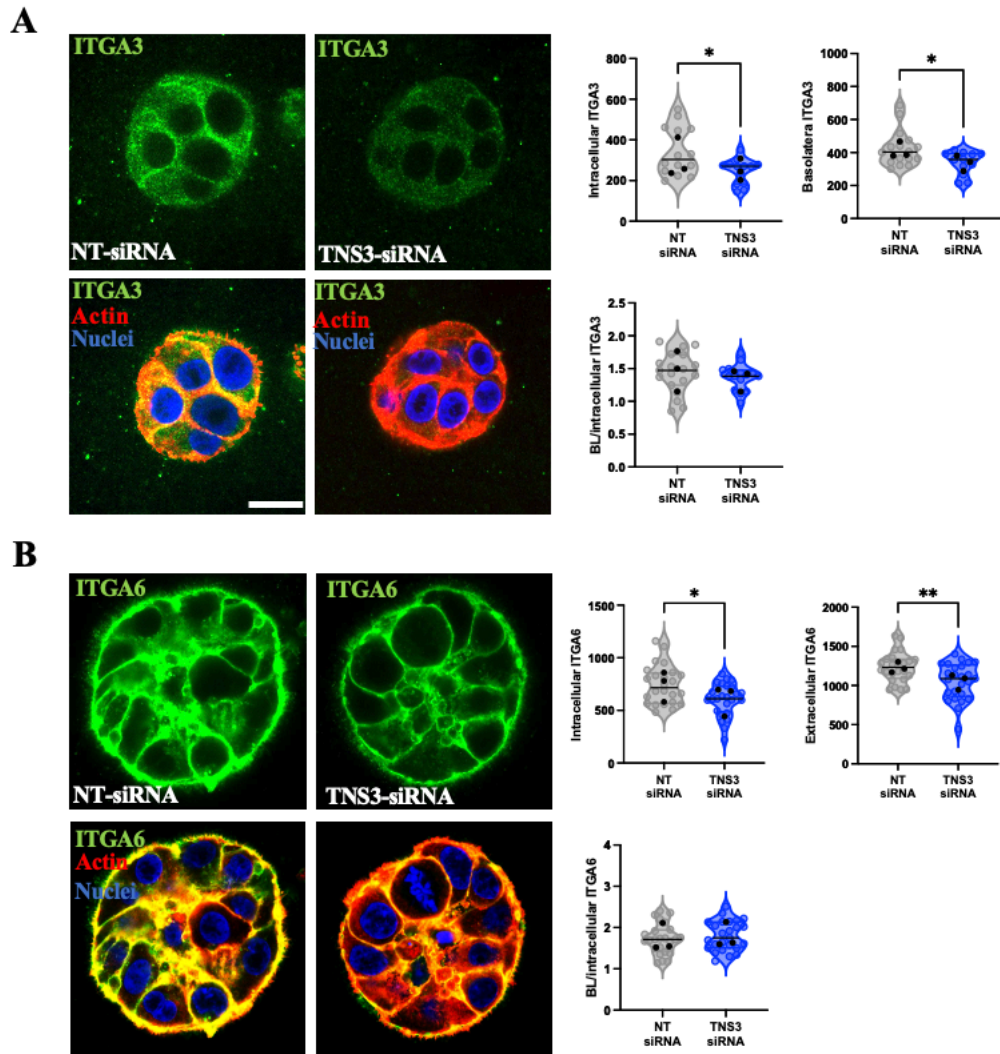


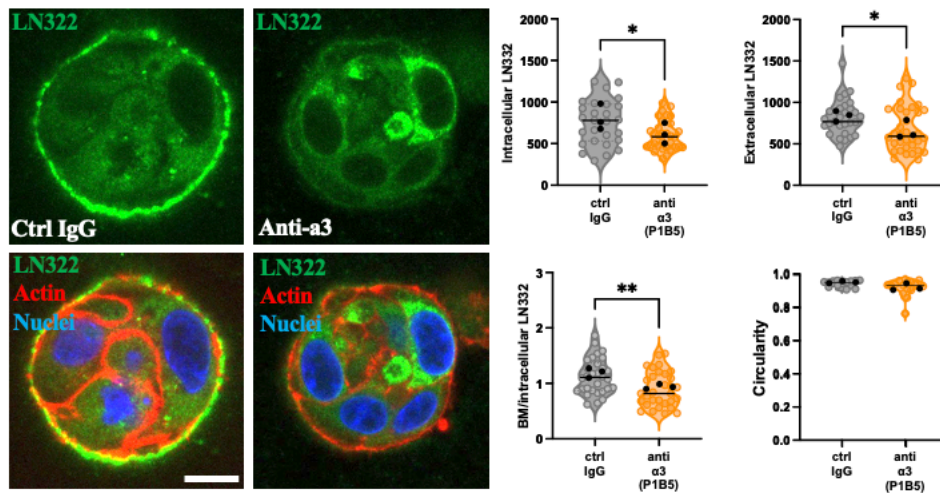
Figure 4.7: TNS3 knock-down reduced $\alpha 3$ and $\alpha 6$ integrin levels in 3D systems. MCF10DCIS cells were transfected with TNS3 specific siRNA or a non-targeting siRNA (NT-siRNA) as a control for 24h. Cells were grown in 3D Geltrex for 3days, fixed and stained for actin (red), $\alpha 3$ integrin (ITGA3, green) or $\alpha 6$ integrin (ITGA6, green) and nuclei (blue). Cells were imaged by a Nikon A1 confocal microscope. Scale bar, 20 μ m. $\alpha 3$ and $\alpha 6$ mean intensity was measured in ImageJ. N=3 independent experiments. The black dots represent the mean of each experiment. * $p < 0.05$, ** $p < 0.001$. Mann-Whitney test.

4.2.8 $\alpha 3$ integrin inhibition prevented laminin-332 deposition and filopodia formation in MCF10DCIS cells.

Studies have demonstrated the localisation of $\alpha 3$ integrin to filopodia in migrating epithelial cells (Underwood et al., 2009), implying its potential involvement in the formation of filopodia and the deposition of laminin-332. To test this, I used a specific anti-integrin $\alpha 3$ blocking antibody ((Byron et al., 2009), clone P1B5). MCF10DCIS cells were grown in 3D Geltrex in the presence of the $\alpha 3$ integrin blocking antibody or an IgG control for 3 days, fixed and stained for laminin 322. In the presence of the IgG control, laminin-332 formed a thick, strong layer

in the BM around the acini. This accumulation in the BM was strongly reduced when $\alpha 3$ was blocked. The quantification shows that blocking $\alpha 3$ significantly reduced the intensity of intracellular and extracellular laminin-332 when compared to the control group (**figure 4.8A**). Moreover, the ratio of extracellular to intracellular laminin-332 was reduced in the presence of the anti- $\alpha 3$ blocking antibody compared to the control group, suggesting that $\alpha 3$ might control both laminin-332 levels and its incorporation in the BM. Furthermore, the circularity of the acini was not affected by $\alpha 3$ blocking. Interestingly, I found that blocking $\alpha 3$ resulted in a significant reduction in the number and length of filopodia when compared to the control. The filopodia in the control group are long, thin actin protrusions present all around the acini, whereas in the group treated with $\alpha 3$ blocking antibodies, very few filopodia are detectable (**figure 4.8B**). These findings indicate that $\alpha 3$ plays a role in controlling filopodia formation and laminin-332 expression/deposition in DCIS cells.

A



B

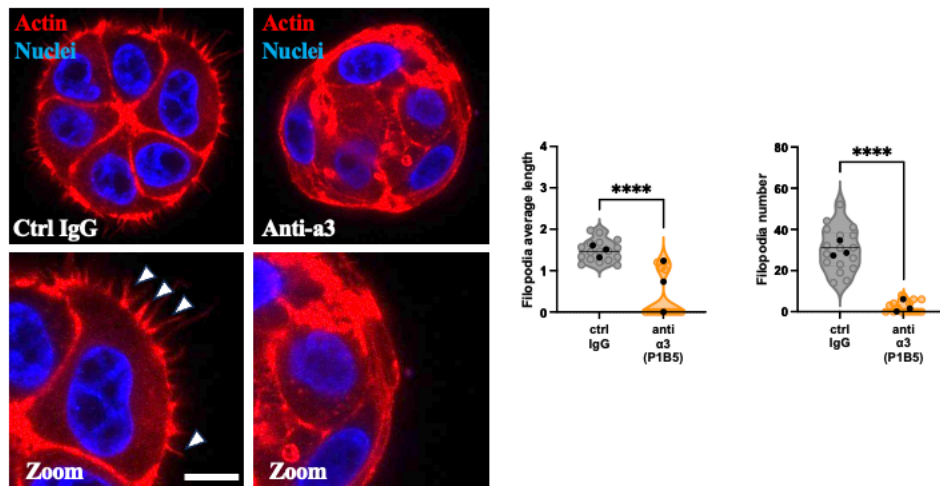


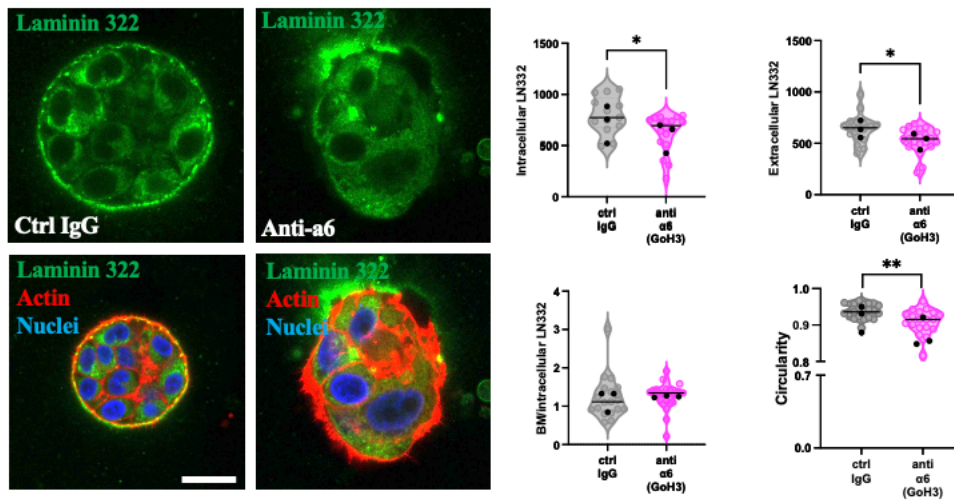
Figure 4.8: $\alpha 3$ integrin blocking antibody prevented laminin-332 deposition and filopodia formation. MCF10DCIS cells were grown in 3D Geltrex in the presence of 5 $\mu\text{g}/\text{ml}$ $\alpha 3$ integrin blocking antibody P1B5 or an IgG control. Cells were left to grow for 3 days, fixed and stained for actin (red), Laminin 322 (LN332, green) and nuclei (blue). Cells were imaged by a Nikon A1 confocal microscope, Scale bar, 20 μm . LN332 mean intensity was measured in ImageJ. N=3 independent experiments. * $p < 0.05$, ** $p < 0.001$, **** $p < 0.0001$ Mann-Whitney test, T-test.

4.2.9 $\alpha 6$ integrin inhibition prevented laminin-332 deposition and filopodia formation in MCF10DCIS cells.

In addition to $\alpha 3\beta 1$ -integrin, $\alpha 6\beta 1$ -integrin is a laminin-332 receptor which is also required for laminin assembly (Bajanca et al., 2006; Speer et al., 2021; Tsuruta et al., 2008). To investigate the role of $\alpha 6$ in laminin-332 incorporation in the BM and filopodia formation in breast cancer cells, I inhibited $\alpha 6$ function with a specific blocking antibody (Speer et al., 2021). MCF10DCIS cells were grown in 3D Geltrex in the presence of the $\alpha 6$ integrin blocking antibody or an IgG control for 3 days and stained for laminin-322. The acini in the control group formed a well-organised circular structure, with an accumulation of laminin-332 in the BM, appearing as a ring around the acini. However, when $\alpha 6$ was blocked, laminin-332

staining in the BM was reduced, and the structure of the acini appeared disorganised (**figure 4.9A**). The quantifications show that blocking $\alpha 6$ significantly reduced the intensity of extracellular laminin-332 when compared to the control group. Similarly, intracellular laminin-332 intensity decreased in the $\alpha 6$ blocked group compared to the control. Furthermore, when $\alpha 6$ is blocked, the circularity of the acini was diminished compared to the control groups (**figure 4.9A**), suggesting that $\alpha 6$ might be required to maintain the integrity of the acini. Moreover, blocking $\alpha 6$ significantly reduced the number and length of filopodia compared to control. Filopodia appear extended and abundant in the control group but were reduced in the group treated with $\alpha 6$ blocking antibodies (**figure 4.9B**). The findings suggest that $\alpha 6$ may influence filopodia formation and BM secretion in MCF10DCIS cells in 3D systems.

A



B

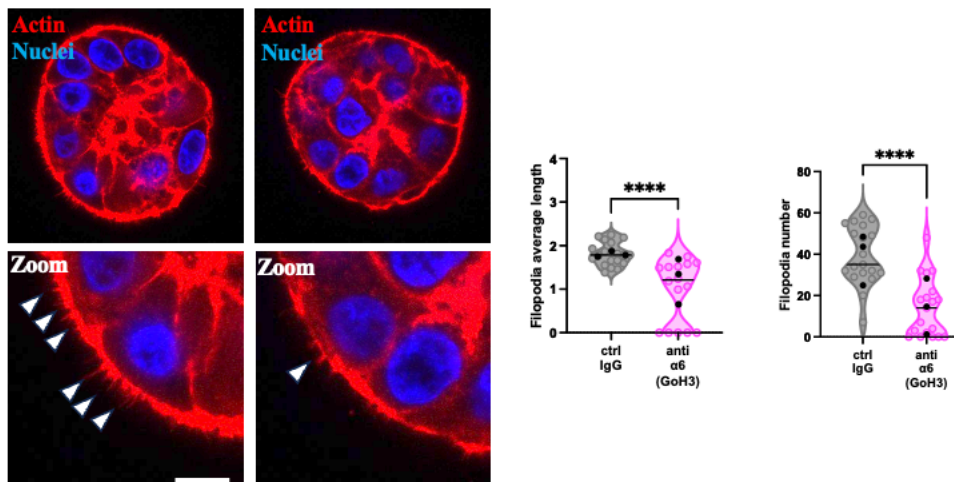


Figure 4.9: $\alpha 6$ integrin blocking antibody prevented laminin-332 deposition and filopodia formation in DCIS. MCF10DCIS cells were grown on 3D Geltrex in the presence of 10 $\mu\text{g}/\text{ml}$ $\alpha 6$ integrin blocking antibody (clone GoH3) or an IgG control for 3 days. Cells were fixed, stained for actin (red), laminin 322 (green) and nuclei (blue) and imaged by a Nikon A1 confocal microscope. Scale bar, 20 μm . Laminin-332 mean intensity, filopodia number and length were measured in ImageJ. N=3 independent experiments. * $p < 0.05$, ** $p < 0.001$, **** $p < 0.0001$. Mann-Whitney test.

4.2.10 Downregulation of TNS3 in MCF10CA1 cells reduced laminin-332 levels.

In addition to MCF10DCIS cells, TNS3 was also found to be unregulated in MCF10CA1 cells and IDC tumours in the mice. Consequently, I was interested in exploring whether TNS3 was also controlling BM dynamics in invasive and metastatic breast cancer cells. MCF10CA1 cells were transfected with TNS3 specific siRNA or a non-targeting siRNA as a control, grown in 3D Geltrex for 3 days and stained for laminin-322. It has been demonstrated that laminin-332 accumulates at the invasive protrusion of migrating cells during 3D invasion (Chang et al., 2022). Consistently, the staining of laminin-332 appeared strong in the control group and accumulated in areas where the cancer cells were forming invasive protrusions; however, this

was not the case in the group where TNS3 was downregulated. The quantifications show that extracellular laminin-332 intensity was significantly reduced in the TNS3-siRNA group when compared to the non-targeted. Similarly, intracellular laminin-332 intensity decreased in the TNS3-siRNA group compared to the control. However, the BL/intracellular ratio remained unchanged (**Figure 4.10A**), suggesting that TNS3 might control laminin-332 overall levels, similarly to what I observed in MCF10DCIS cells. To assess this, western blot was used to measure laminin-332 expression in MCF10CA1 cells transfected with TNS3 specific siRNA and a non-targeting siRNA control for 2 days. **Figure 4.10B** shows a significant reduction, nearly 50%, in laminin-332 levels in MCF10CA1 cells following TNS3 knock-down, as compared to the non-targeting control. These findings indicate that TNS3 may play a role in controlling laminin-332 overall protein levels in the invasive MCF10CA1 cells.

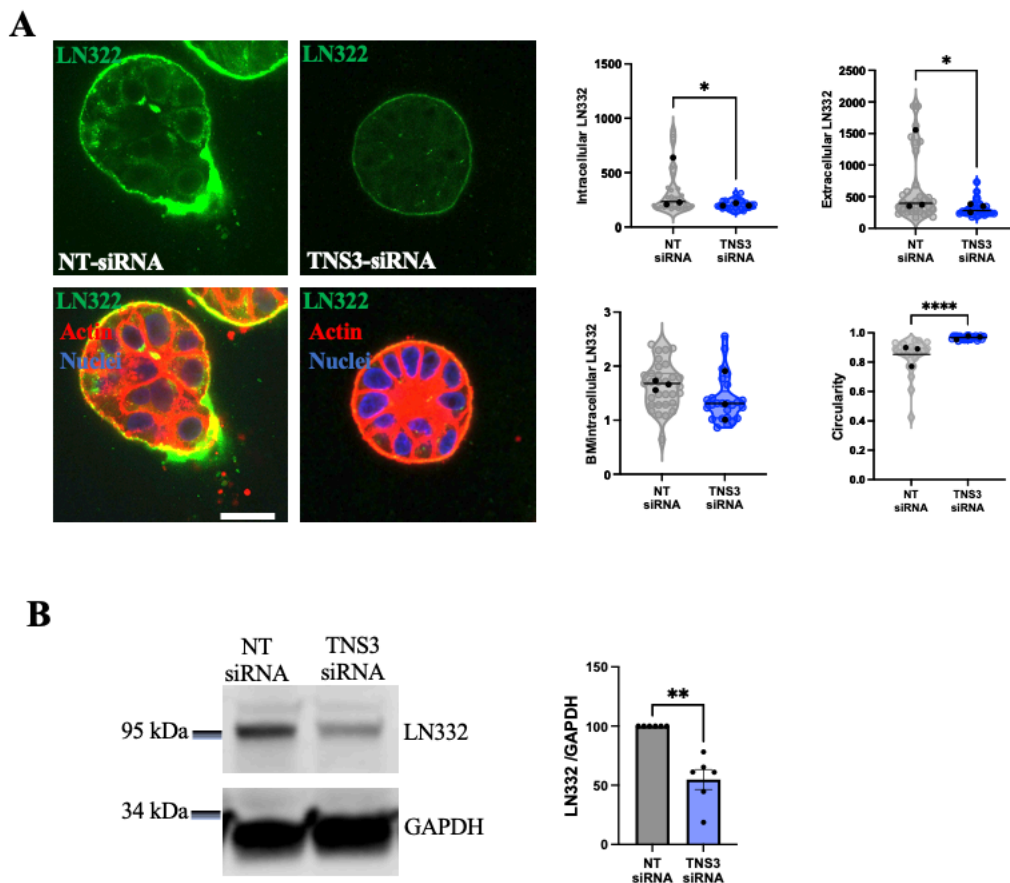


Figure 4.10: Downregulation of TNS3 in MCF10CA1 cells reduced Laminin 332 levels. (A) MCF10CA1 cells were transfected with TNS3 specific si-RNA on a non-targeting siRNA control (NT-siRNA) for 24h. Cells were grown in 3D Geltrex for 3 days, fixed and stained for actin (red), laminin 322 (LN332, green) and nuclei (blue). Cells were imaged by a Nikon A1 confocal microscope. Scale bar, 20 μ m. Laminin 332 mean intensity was measured in ImageJ. N=3 independent experiments. (B) MCF10CA1 cells were transfected as in A. The protein level of LN332 was determined using western blotting. Cell lysates were collected, run through SDS-PAGE gels, membranes were stained with anti-LN332 and anti-GAPDH antibodies and imaged with a Licor Odyssey system. Band intensities were measured with ImageStudio and normalized to GAPDH. The graph represents the mean \pm SEM of six independent experiments. * p <0.05, ** p <0.001, **** p <0.0001 Mann-Whitney test.

4.2.11 Downregulation of TNS3 reduced filopodia formation in MCF10CA1 cells.

My previous findings indicate that the downregulation of TNS3 diminished both the length and number of filopodia, while concurrently reducing the deposition of laminin-332 in non-invasive MCF10DCIS cells. I aimed to assess whether the same was true in the invasive MCF10CA1 cell line. Therefore, the total number and length of filopodia were examined after suppressing TNS3 expression in MCF10CA1 cells. As shown in **figure 4.11**, the control group exhibited elongated and dense filopodia, but this was reduced in the group that received treatment with TNS3-siRNA. Indeed, TNS3 downregulation substantially decreased the quantity and length of filopodia in comparison to the non-targeting siRNA. The results indicate that TNS3 is required for the formation of filopodia in the metastatic MCF10CA1 cells.

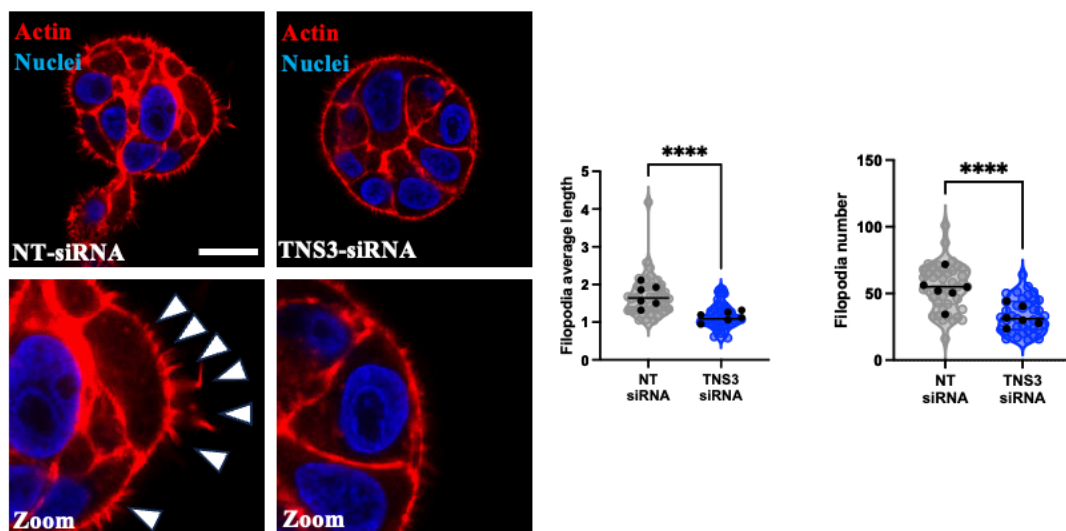


Figure 4.11: Downregulation of si-TNS3 in MCF10CA1 reduced filopodia formation. MCF10CA1 cells were transfected with TNS3 specific si-RNA and a non-targeting siRNA control (NT-siRNA) for 24h. Cells were grown in 3D Geltrex for 3 days, fixed and stained for actin (red) and nuclei (blue). Cells were imaged by a Nikon A1 confocal microscope. Scale bar, 20 μ m. Filopodia number and length were measured in ImageJ. N =6 independent experiments. ****p<0.0001. Mann-Whitney test.

4.2.12 TNS3 downregulation reduced α 3 integrin levels in MCF10ACA1 cells.

In non-invasive MCF10DCIS cells, knocking down TNS3 resulted in a significant reduction in the intracellular and basolateral expression of the α 3 integrin receptor. To assess TNS3 also controlled the level of expression of α 3 integrin in invasive MCF10CA1 cells, cells were transfected with either TNS3 specific or non-targeting siRNA, grown in 3D Geltrex for 3 days and stained for α 3 integrin. In the control group, α 3 integrin localised at cell-cell junctions and at the basolateral surface of the acini (**figure 4.12**). However, silencing TN3 resulted in a weaker and barely visible signal at the basolateral surface and cell-cell junctions compared to

the control group, resulting in a small but statistically significant reduction in $\alpha 3$ integrin intensity. These findings suggest that TNS3 may control laminin deposition and filopodia formation through the modulation of $\alpha 3$ integrin levels.

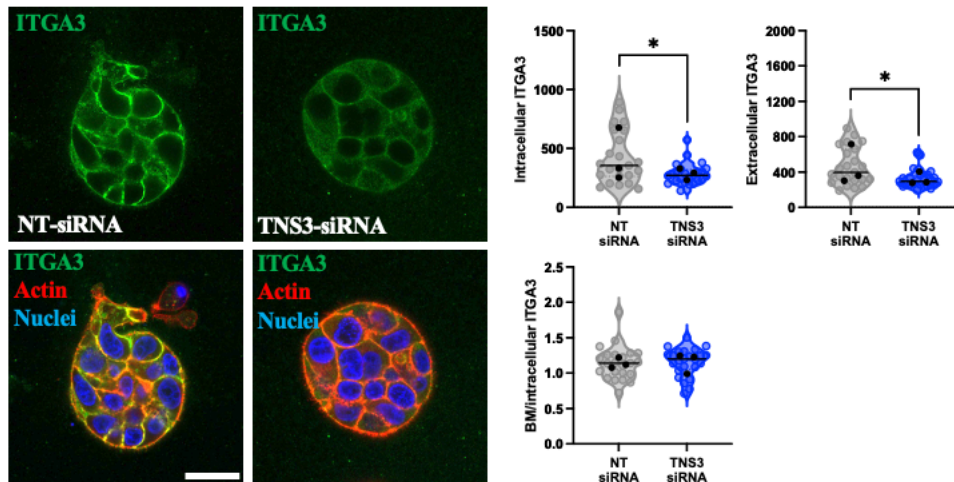


Figure 4.12: TNS3 knockdown slightly reduced $\alpha 3$ integrin levels in MCF10CA1 cells. MCF10CA1 cells were transfected with TNS3 specific si-RNA or a non-targeting siRNA (NT-siRNA) as a control for 24h. Cells were grown in 3D Geltrex for 3 days, fixed and stained for actin (red), $\alpha 3$ integrin (ITGA3, green) and nuclei (blue). Cells were imaged by a Nikon A1 confocal microscope. Scale bar, 20 μ m. $\alpha 3$ integrin mean intensity was measured in ImageJ. N=3 independent experiments. * $p < 0.05$ Mann-Whitney test.

4.3 Discussion

In this chapter, I demonstrated that the silencing of TNS3 and $\beta 1$ -integrin leads to a defect in BM deposition, assessed by measuring the basolateral and intracellular levels in 3D in MCF10DCIS. Furthermore, there was a decrease in the expression level of laminin-332 in 2D cultures upon TNS3 downregulation. Similarly, TNS3 silencing reduced laminin-332 levels in MCF10CA1 cells and opposed filopodia formation in both cell lines. Moreover, there was a significant decline in the expression level of $\alpha 3$ and $\alpha 6$ at both the basolateral and intracellular sites in MCF10DCIS cells and in the expression level of $\alpha 3$ in MCF10CA1 cells. Inhibition of both $\alpha 3$ and $\alpha 6$ integrins impaired both laminin-332 BM accumulation and filopodia formation.

BM remodelling plays a key role in controlling cancer invasion. It has been recently reported that laminin-332 deposition at the tumour's leading edge is needed for collective cell migration (Hwang et al., 2023; Chang et al., 2022). Laminin-332 is essential for cell adhesion, migration, and differentiation (Hwang et al., 2023; Rousselle & Scoazec, 2020; Troughton et al., 2022; Yin et al., 2022; Zhou et al., 2020). Some cancer types, most notably breast and colorectal cancer, have been shown to overexpress laminin-332 and collagen IV (Lindgren et al., 2021;

Tsuruta et al., 2008). It is widely established that laminin-332 and collagen IV stimulate breast cancer cell migration via interaction with β 1-containing integrin heterodimers, and are linked to breast cancer metastasis and invasiveness (Desgrosellier & Cheresch, 2010; Pan et al., 2018; Zhou et al., 2020). This is believed to occur in response to the increased expression of α 3 β 1 and α 6 β 1 integrin receptors, which subsequently activate the PI3K-Akt signalling pathway, thereby enhancing the survival and proliferation of cancer cells in response to laminin-332 (Bajanca et al., 2006; Faraldo et al., 2024; Miskin et al., 2021; Ramovs et al., 2019; Tsuruta et al., 2008). It was reported that silencing α 3 β 1-integrin in MDA-MB-231 breast cancer cells and injecting them into fat pad mice reduced tumour growth while silencing α 3 β 1-integrin in MDA-MB-231 cells plated on matrigel reduced invasion compared to the control (Mitchell et al., 2010). The laminin-332 receptor α 3 β 1 integrin triggers the activation of intracellular cellular signalling pathways, promoting the invasion of cancers such as colorectal adenocarcinoma, head, neck, and pancreatic carcinoma (Tsuruta et al., 2008). Furthermore, studies have linked α 6 β 1-integrin to breast cancer progression and a poor prognosis (Faraldo et al., 2024; Yang et al., 2008). When laminin-332 binds to the integrin receptor α 3 and α 6, it activates the integrins by clustering them and initiates downstream signalling pathways (Cooper & Giancotti, 2019; Givant-Horwitz et al., 2005; Halder et al., 2022; Zhou et al., 2020). One of the well-studied pathways is FAK/SRC/MAPK/c-Jun, which will result in increased invasion and migration (Cooper & Giancotti, 2019; Givant-Horwitz et al., 2005; Gonzales et al., 1999; Zhou et al., 2020).

Here I found a significant reduction in basolateral and intracellular laminin-332 staining after TNS3 silencing in 3D culture systems in both MCF10DCIS and MCF10CA1 cells. Furthermore, western blot experiments demonstrated a reduction in laminin-332 levels upon TNS3 downregulation in comparison to the control group. However, in 2D immunofluorescence microscopy experiments to examine laminin-332 secretion level in TNS3 and β 1-integrin knocked down cells, the result showed no differences between the three groups, which is not consistent with the western blotting results. This observation could be explained by the fact that for the 2D western blot cells were grown on plastic while in 2D immunofluorescence microscopy the cells were plated on Geltrex. Another point to note is that western blot was performed two days after transfection, whereas for the immunofluorescence microscopy the cells were stained 24hr after transfection.

Recent research has indicated a correlation between filopodia formation and the advancement of invasive breast carcinoma (IBC) as well as the invasion of the surrounding region (Peuhu et al., 2022). Both DCIS and IBC from patient samples were used to quantify the presence of filopodia. The results indicated a notable upregulation in filopodia formation in both samples when compared with normal mammary epithelium. In addition, silencing the key filopodia regulator MYO10 was linked to a decrease in BM accumulation, filopodia number and length in DCIS cells. Furthermore, the production of MYO10-filopodia was increased in DCIS, which enhances their invasive capabilities when compared to the control group (Peuhu et al., 2022). Consistently, compared to the non-transformed MCF10A cells, the metastatic MCF10CA1 cells exhibited greater length and density of filopodia (Kyykallio et al., 2020), while a significant increase in the density and length of the filopodia was observed in MCF10DCIS cells when compared to MCF10A cells (Jacquemet et al., 2017).

My data show that filopodia formation preceded BM assembly in non-invasive MCF10DCIS cells, supporting published observations that filopodia were required for BM assembly. Moreover, I observed a significant reduction in filopodia length and number when TNS3 and β 1-integrin were silenced, suggesting that TNS3 and β 1 integrin might control laminin-332 by modulating filopodia formation. To note, only few 3D MCF10DCIS acini grew upon β 1 integrin knockdown, in line with the fact that β 1 integrin KD has been shown to hinder cell growth in 3D (Kren et al., 2007). This is consistent with the fact that silencing β 1 in cancer cells both *in vivo* and *in vitro* has been shown to reduce tumour growth and colony formation (M. B. Chen et al., 2016). In pancreatic cell lines, β 1 downregulation resulted in a significant reduction in cell proliferation, migration, and adhesion *in vitro*, while it was found to reduce primary tumour growth while also preventing metastatic spread *in vivo* (Grzesiak et al., 2011).

As TNS3 can bind to β 1-integrin (Zuidema et al. 2022) and control integrin function (Q. Huang et al., 2024), it is possible that TNS3 controlled filopodia formation by controlling β 1 integrin. However, TNS3 knockdown did not affect β 1-integrin localisation and levels in MCF10DCIS cells. This could be due to the fact that TNS3 might control only a subset of β 1-containing integrin heterodimers. In addition, that there may still be subtle differences in terms of β 1 targeting to the filopodia, which I cannot resolve at the magnification used in my experiments. Future research could use super-resolution microscopy to determine whether TNS3 is necessary for the targeting of β 1 integrin to the filopodia tip. Indeed, my data suggest that TNS3 might control laminin-332 deposition via modulating α 6 β 1 and/or α 3 β 1 integrin

receptors. Silencing $\alpha 3\beta 1$ integrin was found to reduce invasion in MDA-MB-231 cells (Miskin et al., 2021). Furthermore, RNAseq data analysis of patient samples revealed that high $\alpha 3$ expression correlated with poor survival (Ramovs et al., 2019). Interestingly, laminin-332 was shown to influence cell proliferation by binding to $\alpha 3$ integrin (Gonzales et al., 1999), while $\alpha 3\beta 1$ integrin was shown to mediate the formation of filopodia in the MDA-MB-435 breast carcinoma cell line (Subramaniam Chandrasekaran, 1998). Consistently, we demonstrated that inhibiting $\alpha 3$ reduced BM deposition in MCF10DCIS cells. It has been widely reported that $\alpha 6$ is pro-tumorigenic, and high expression is linked to poor survival (Faraldo et al., 2024). $\alpha 6$ has been observed to be elevated in different breast cancer cell lines including: MCF7, BT474, SKBR-3, MDA-MB-231, BT549, and HCC1937 (Faraldo et al., 2024). A report found that $\alpha 6$ -deficient Brca1/p53 mutant mice had lower tumour initiation rates. However, the loss of $\alpha 6$ after tumour formation had no effect on tumour growth (Faraldo et al., 2024; Hu et al., 2016), suggesting that $\alpha 6$ might play a prominent role in tumour initiation. Our findings indicate that the inhibition of $\alpha 6$ decreased laminin-332 levels in the BM in MCF10DCIS cells. These results are consistent with previous research indicating that inhibiting $\alpha 3$ and $\alpha 6$ decreased BM assembly alongside the filopodia density and length.

It has been previously reported that laminin accumulated on sites where the invasion occurs, and the thickness of the BM enhanced the invasion (Ghannam et al., 2022; Peuhu et al., 2022). Consistently, my data show that laminin-332 accumulated around invasive protrusions in MCF10CA1 acini, in a TNS3-dependent manner. However, laminin-332 basolateral-to-intracellular ratio was not affected by TNS3 downregulation. This could be explained by the fact that in the control group, laminin-332 is mostly polarised in areas of protrusions. Importantly, my data show that TNS3 regulates laminin-332 levels, rather than BM accumulation, in both MCF10DCIS and MCF10CA1 cells. Previous research has shown that MAPK/ERK signalling pathways regulate laminin expression. In particular, the transcription factor c-Jun has been shown to regulate the expression of LAMB1 (H. Lee et al., 2021). I can therefore hypothesise that TNS3 might regulate the expression of laminin 332 by activating MAPK/ERK signalling pathways downstream of integrin $\alpha 6\beta 1$ or $\alpha 3\beta 1$.

Chapter 5. TNS3 restricts transformation in normal epithelial cells.

5.1 Introduction.

The majority of human cancers develop as a result of epithelial cell transformation. The process starts when a single normal epithelial cell acquires genetic mutations, which lead to the activation of cancer-causing genes or the suppression of tumour suppressor genes (Hogan, 2012). When genetic mutations occur, it causes the formation of a primary tumour. This process is promoted by various factors, including the remodelling of the ECM, resulting in the degradation of the BM and metastasis formation (Chua et al., 2016; Hogan, 2012; Hynes, 2009). RAS GTPases play a crucial role in the progression of various cancers. Activating RAS mutations initiate downstream signalling cascades. This regulates numerous cellular processes that are responsible for the proliferation and survival of cancer cells (Boutin et al., 2017; Martínez-Abarca Millán et al., 2023). This pathway includes the phosphoinositide 3-kinase (PI3K) and MAP kinase pathways (Boutin et al., 2017). Genetically modified animal models provided an effective tool for studying tensin roles in various diseases. Different models, including *Drosophila melanogaster* and *Caenorhabditis elegans*, have a single tensin, whereas mammals have four different ones (Lo, 2017; Torgler et al., 2004).

Drosophila melanogaster genome is 60% similar to the human one and approximately 75% of genes encoding for human diseases share similarity in flies. These characteristics, combined with a short generation time and low maintenance costs, make the *Drosophila* model capable of studying complex pathways related to medical research, such as cancer (Mirzoyan *et al.*, 2019). *Drosophila* models provide useful information about different cancers. These models offer a good foundation from which we can analyse tumour progression and look for underlying mechanisms. We can use *Drosophila* to study various cancer models, such as gut, brain, lung, prostate, thyroid, and haematologic cancers (Mirzoyan et al., 2019). Recently, researchers developed a model for colorectal cancer in *Drosophila* (Campbell et al., 2019). Colorectal cancer (CRC) affects approximately 4% of people, and it begins with a loss of function in the tumour-suppressor gene adenomatous polyposis coli (APC), resulting in the activation of the WNT signalling pathway. Activating mutation in the oncogene Ras is another common feature in CRCs. The mammalian and *Drosophila* gut share striking similarities. To model CRC in *Drosophila*, Wnt and Ras signalling pathways are activated clonally in the adult midgut. This is achieved by inactivating *Apc1* and *Apc2*; while UAS-RasV12 is used to overexpress a constitutive active form of Ras. It has been shown that these genetic changes resulted in the formation of intestinal tumours (Campbell et al., 2019). An increase in cell proliferation,

decreased cell polarity, and the expression of tumour markers similar to those found in human CRC validated these findings. These findings emphasise the similarities in CRC development between *Drosophila* and humans, making *Drosophila* an ideal model for studying cancer progression mechanisms (Martorell et al., 2014).

Moreover, it has been shown that cancer cells take advantage of the epithelial-to-mesenchymal transition (EMT) to become invasive during the initial stages of the metastatic cascade. It is a process that causes epithelial cells to lose their characteristics and become mesenchymal, which promotes invasive behaviour. This process is driven by transcription factors such as Twist, Snail and ZEB, which promote the expression of mesenchymal markers, the loss of epithelial markers, and the production of ECM-degrading enzymes such as metalloproteases (Kalluri & Weinberg, 2009). The transcription factor SNAIL (Sna in *Drosophila*) is a key regulator of EMT. To recapitulate the metastatic spread of CRC, an activating Sna mutation was introduced in the Apc/Ras model. Noticeably, within 2-3 weeks, metastasis formation could be observed in different locations, including abdomen, thorax, head, the ovaries, legs and the brain (Campbell et al., 2019).

The alignment of the four different TNS proteins in humans shows approximately 54% similarity with the SH2 and PTB domains to *Drosophila* TNS. The tensin protein in *Drosophila* connects integrin to actin and initiates signalling pathways like FAK signal transduction (Torgler et al., 2004). Researchers have extensively studied Tensin in *Drosophila*, uncovering its significant roles in cellular processes like cell adhesion, migration, wing development, and signalling pathways including JNK and FAK/Scr signalling (Cha et al., 2017; S. B. Lee et al., 2003; Torgler et al., 2004). Another study examined the relationship between tensin and integrin. They created a tensin null mutation, which resulted in wing blister formation. This phenotype results from a loss of integrin adhesion (Torgler et al., 2004). These *in vivo* results suggested that tensin plays a role in linking integrins and the cytoskeleton, similarly to its role in mammalian cells.

Here I used non-transformed MCF10A cells and a *Drosophila* cancer model to study how tensin affects tumour formation and metastasis. I showed that silencing TNS3 in MCF10A significantly increased cell invasion and proliferation. Mechanistically, TNS3 downregulation significantly increased laminin-332 expression, filopodia formation, and $\alpha 3$ integrin expression. *In vivo*, tensin overexpression significantly impaired tumour growth in both

Apc/Ras and Apc/Ras/Sna background, while it also opposed metastasis formation in the Apc/Ras/Sna model, indicating that tensin act as a tumour suppressor during tumour initiation.

5.2 Results

5.2.1 TNS3 knockdown increased invasiveness and cell proliferation in MCF10A cells.

In non-transformed mammary epithelial cells, the BM provides tissue support and plays an essential role in maintaining tissue homeostasis (Ghannam et al., 2022). Integrin β 1 has been shown to control mammary gland development and to be required to maintain mammary architecture integrity (Nisticò et al., 2014). Here I set out to investigate the role of TNS3 in non-transformed mammary epithelial cells. MCF10A cells were transfected with an siRNA targeting TNS3 or a non-targeting siRNA control, grown in 3D Geltrex for 3 days and stained for actin. On day 3, the control acini appear round and do not exhibit any invasive behaviour. However, the depletion of TNS3 promoted the formation of protrusions, as cells started to invade out of the acini (**Figure 5.1A**). Indeed, the quantification of acinus circularity revealed a statistically significant decrease due to TNS3 down-regulation. Importantly, that there were no significant changes in the area (**Figure 5.1A**).

To gain better insights in the cell invasion dynamics, I used live cell imaging of MCF10A cells grown in 3D Geltrex. MCF10A were transfected with non-targeting siRNA or TNS3-specific siRNA for 48h and imaged from day 2 to day 4. After nearly 7 hours of imaging, control cells appeared spherical and uniform. After nearly 11 hours of imaging, there was only an increase in size, with no invasion observed. During 17.5, 24.2, and 31 hours, the acini size consistently increased in a regular pattern as cellular proliferation kept going, yet no invasion occurred. Conversely, the acini generated by cells transfected with TNS3-specific siRNA began to assume an irregular shape from 7 hours of imaging. Subsequently, after 11 hours of imaging, TNS3 knockdown acini began to invade and developed protrusions. Following 17.5, 24.2, and 31 hours, the invasion progressed by forming multicellular protrusions (**figure 5.1B**). Consistent with the previous results, the circularity was significantly reduced when we silenced TNS3 compared to the control group (**figure 5.1B**). Western blotting analysis confirmed that the percentage of TNS3 knockdown in MCF10A cells was approximately 70%. (**figure 5.1C**). Overall, these data indicate that TNS3 prevents normally mammary epithelial cell invasion in 3D systems.

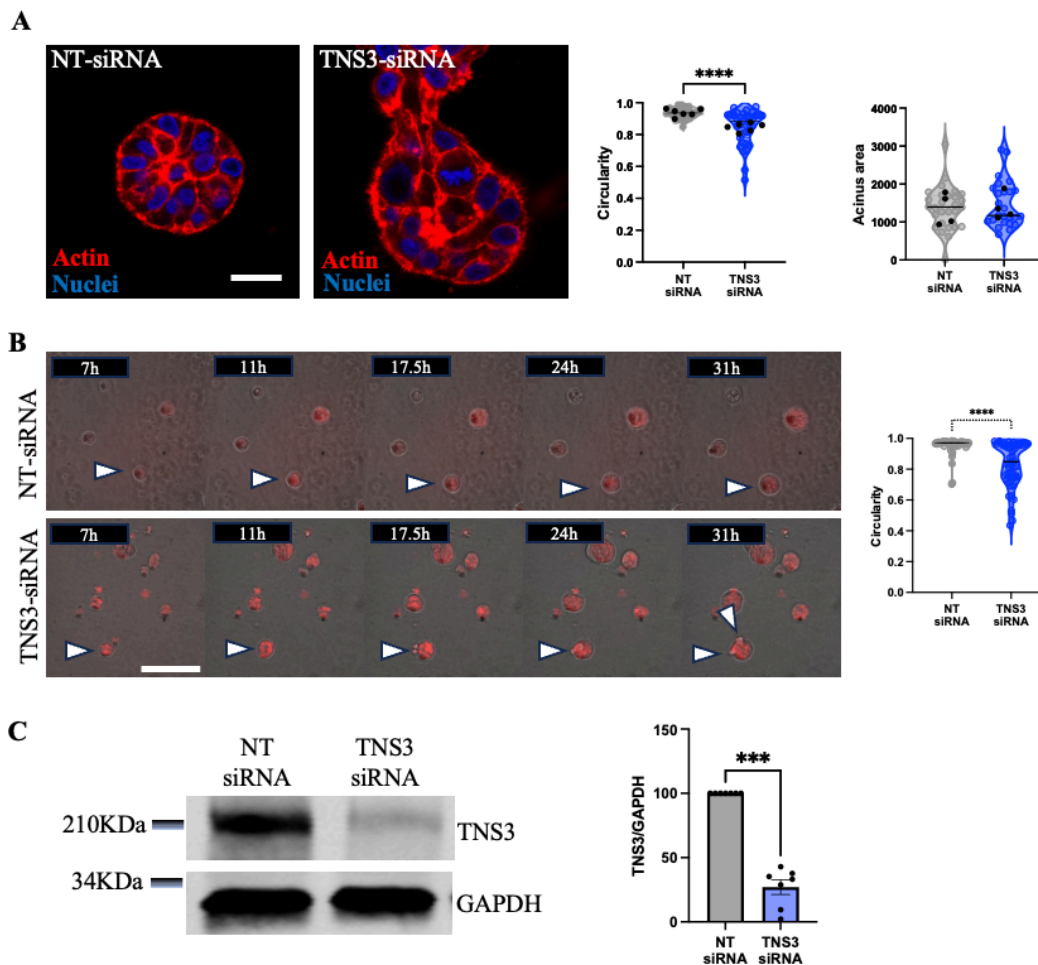


Figure 5.1: Suppressing TNS3 promotes MCF10A cell invasion. (A) MCF10A cells were transfected with TNS3 specific siRNA (TNS3-siRNA) and a non-targeting siRNA as a control (NT-siRNA) and grown in 3D Geltrex for 3 days, fixed and stained for actin (red) and nuclei (blue). Cells were imaged by a Nikon A1 confocal microscope. Scale bar, 20 μ m. Area and circularity of individual acini were measured in ImageJ. $N \geq 4$ independent experiments. (B) MCF10A cells were transfected as in A, grown in Geltrex for 2 days, stained for nuclei (red) and imaged live by time lapse microscopy for 48h. Stills from a representative movie are presented. Scale bar, 50 μ m. Circularity was measured in ImageJ. $N=3$ independent experiments. (C) MCF10A cells transfected as in A for 2 days. Cell lysates were collected, run through SDS-PAGE gels, blotted for TNS3 and GAPDH and imaged with a Licor Odyssey Sa. Band intensity was measured with ImageStudio and normalised to GAPDH. The graph represents the mean \pm SEM of seven independent experiments. *** $p < 0.001$, **** $p < 0.0001$. Mann-Whitney test.

To investigate the effects of TNS3 knockdown on cell proliferation, MCF10A cells were transfected with non-targeting siRNA or TNS3 specific siRNA and grown for 7 days. As shown in **figure 5.2**, TNS3 knockdown MCF10A cells grew significantly more when compared to the non-targeting siRNA cells. These data indicate that TNS3 prevents cell growth in non-transformed mammary epithelial cells.

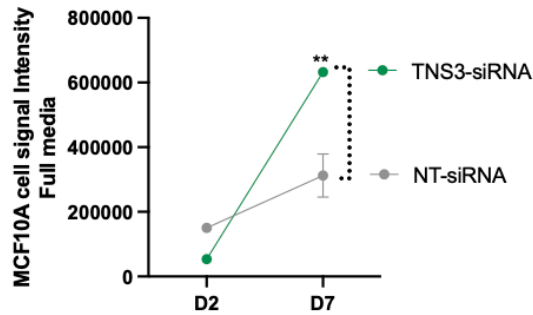


Figure 5.2: TNS3 knockdown increased the growth of MCF10A cells. MCF10A cells were transfected with TNS3 specific si-RNA (TNS3 si-RNA) and a non-targeting siRNA as a control (NT-siRNA). MCF10A cells were cultured on plastic for 7 days, with full media (full). Cells were fixed, stained with DRAQ5 on day 2 and 7. Cells were imaged with a Licor Odyssey Sa system. Data were quantified with Image Studio Lite software. The graphs represent the mean \pm SEM of three independent experiments. ** $p < 0.001$, Mixed effect analysis, Tukey's test, Multiple comparisons test, Two-Way ANOVA.

5.2.2 TNS3 knockdown increased laminin-332 deposition in MCF10A cells.

While on the one hand the BM inhibits cancer cell invasion by serving as a barrier that retains the cells within it (Ghannam et al., 2022), on the other hand a correlation between cell invasion and the accumulation and densification BM components have been reported (Chang et al., 2022). Therefore, I hypothesised that losses TNS3 might promote cell invasion by modulating laminin expression.

MCF10A cells were transfected with an siRNA targeting TNS3 or a non-targeting siRNA control, grown in Geltrex for 3 days and stained for laminin-332. In the control acini, laminin-332 in the BM was deposited around the acini in a thin, even layer. However, upon TNS3 downregulation, the laminin-332 staining around the acini became stronger and thicker. The quantification of laminin-332 staining intensity in the BM (extracellular) and inside the cells showed a statistically significant increase in both intracellular and extracellular laminin-332 in TNS3 KD cells compared to the control group (**Figure 5.3A**), while the BM/intracellular ratio remained the same. These data indicate that TNS3 could regulate the levels of laminin-332 in MCF10A cells, rather than its BM deposition.

To validate this, MCF10A cells were transfected with a TNS3 specific siRNA, or a non-targeting siRNA control and the laminin-332 protein level was determined by western blotting. **Figure 5.3B** demonstrates that TNS3-depleted MCF10A cells expressed significantly more laminin-332 compared to the non-targeting control. This suggests that TNS3 prevents the accumulation of laminin-332 in non-transformed mammary epithelial cells.

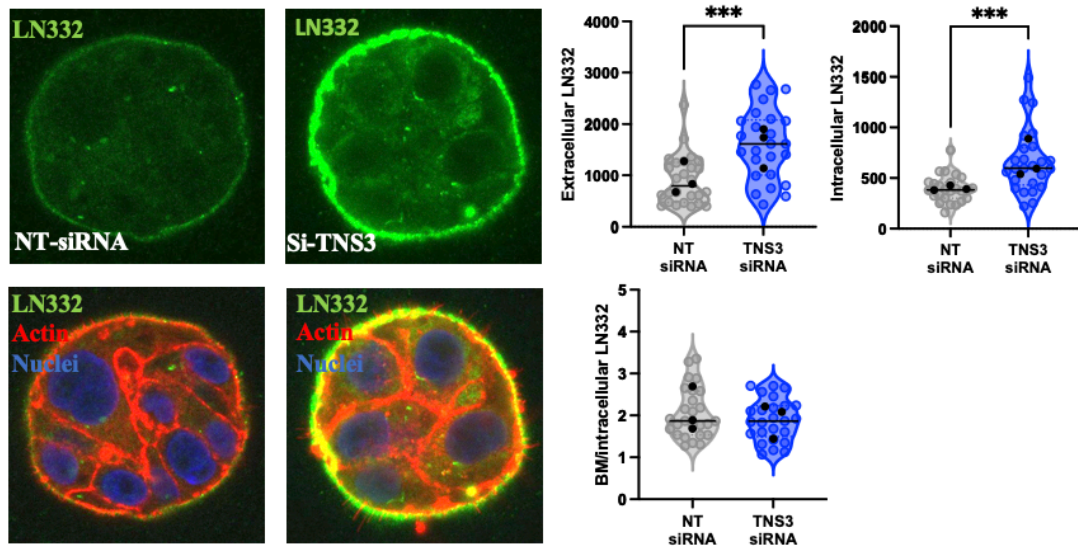
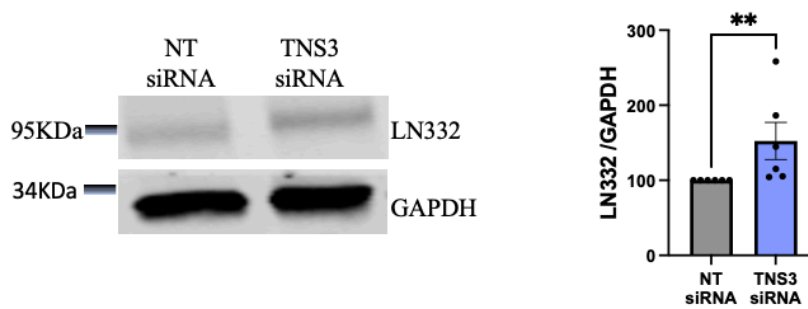
A**B**

Figure 5.3: TNS3 downregulation increased laminin-332 expression in MCF10A cells. (A) MCF10A cells were transfected with a TNS3 specific siRNA and a non-targeting siRNA (NT-siRNA) as a control for 24h. Cells were grown in 3D Geltrex for 3days, fixed and stained for actin (red), laminin 322 (LN332, green) and nuclei (blue). Cells were imaged by a Nikon A1 confocal microscope. Scale bar, 25 μ m. Laminin 332 mean intensity was measured in ImageJ. N=3 independent experiments ***p<0.001, Mann-Whitney test **(B)** MCF10A cells were transfected with a TNS3 specific siRNA and a non-targeting siRNA (NT-siRNA) as a control for 2 days. Cell lysates were collected and run through SDS-PAGE gel. Membranes were stained with anti-laminin 332 (LN332) and anti-GAPDH antibodies and imaged with a Licor Odyssey Sa system. Band intensity was measured with ImageStudio and normalized to GAPDH. The graph shows the mean \pm SEM of six independent experiments. **p<0.001, Mann-Whitney test.

5.2.3 TNS3 silencing increased the number and length of filopodia in MCF10A cells

Reports link the formation of filopodia to the assembly of the BM. Furthermore, as breast cancer progresses, the length and density of filopodia increase (Jacquemet et al., 2017; Peuhu et al., 2022). To assess whether suppressing TNS3 affected the length and quantity of filopodia, MCF10A cells were transfected with an siRNAs targeting TNS3 or a control siRNA for 24 hours. Cells were then grown in 3D Geltrex for 3 days, fixed and stained for actin. Compared to the control, filopodia appeared longer and more abundant in cells in which TNS3 was silenced (**figure 5.4**). Image analysis indicated that TNS3-specific siRNA significantly increased the average length and number of filopodia compared to the non-targeting group. These results suggest that in non-transformed cells TNS3 might suppress filopodia formation.

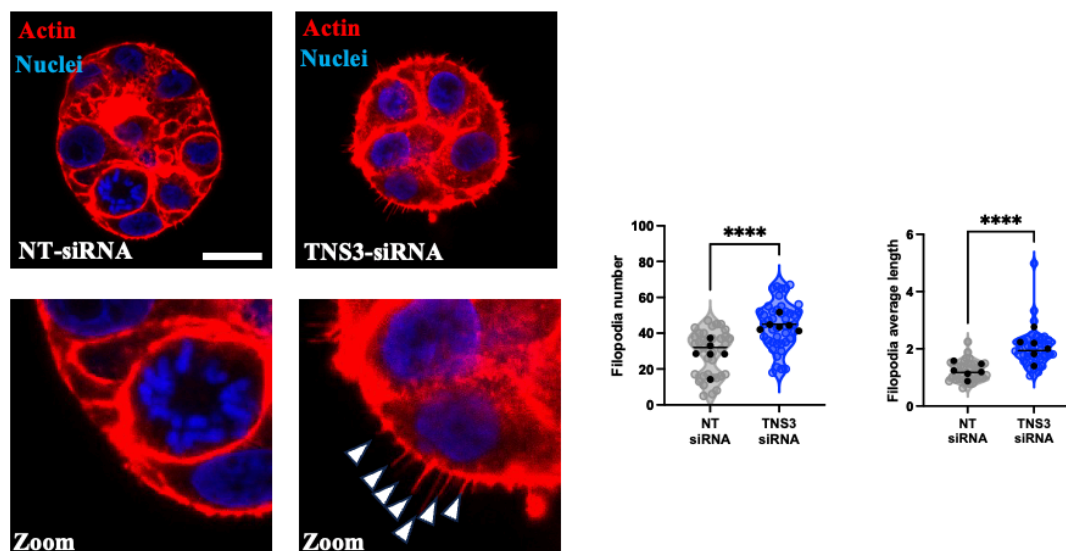


Figure 5.4: TNS3 silencing increased the number and length of filopodia in MCF10A cells. MCF10A cells were transfected with a TNS3 targeting siRNA or a non-targeting siRNA (NT-siRNA) as a control for 24h. Cells were grown in 3D Geltrex for 3 days, fixed and stained for actin (red) and nuclei (blue). Cells were imaged by a Nikon A1 confocal microscope. Scale bar, 25 μ m. Filopodia number and length were measured in ImageJ. N=6 independent experiments. ****p<0.0001. Kruskal-Wallis, multiple comparisons test, One-Way ANOVA.

5.2.4 TNS3 knock-down increased α 3 integrin levels in 3D systems

I determined in my previous chapter that α 3 is essential for the formation of filopodia and the expression/stabilization of laminin-332 in cancer cells. Therefore, I aimed to explore the impact of TNS3 knockout on the expression of α 3 integrin in non-transformed cells. MCF10A cells were transfected with a TNS3 specific siRNA or a non-targeting siRNA as a control, grown in

3D Geltrex for 3 days and stained for $\alpha 3$. The results show that $\alpha 3$ staining was very faint in the control group, but after silencing TNS3, the staining became stronger. The quantification shows a significant increase in the basolateral and intracellular $\alpha 3$ level in the TNS3 knockdown group when compared to the control, however, the BL/intracellular ratio stayed the same (**Figure 5.5**). These findings suggest that the downregulation of TNS3 may promote laminin-332 expression and filopodia formation by increasing $\alpha 3$ integrin expression. Overall, we can conclude that TNS3 is tumour suppressor gene in non-transformed mammary epithelial cells.

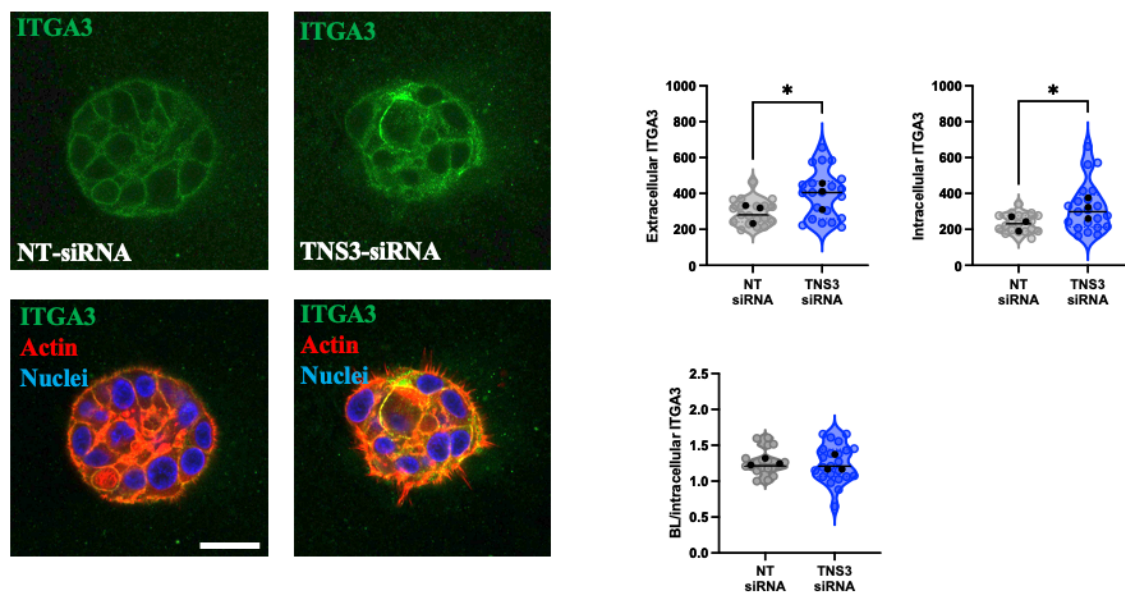


Figure 5.5: TNS3 knock-down increased the ITGA3 levels in 3D systems. MCF10A cells were plated on plastic dish for 24h. Cells were transfected by DharmaFECT with TNS3 specific si-RNA and a non-targeting siRNA as a control for 24h. Cells were grown in 3D Geltrex for 3days. Then cells were fixed and stained for actin (red), ITGA3 (green) and nuclei (blue). Cells were imaged by a Nikon A1 confocal microscope. Scale bar, 25 μ m. mean intensity was measured in ImageJ. The graph values represent the mean \pm SEM of three independent experiments. * $p < 0.05$, ** $p < 0.001$, *** $p < 0.001$, **** $p < 0.0001$. Mann-Whitney test, T-test.

5.2.5 TNS overexpression in the Apc/Ras background reduced tumour formation

To assess the role of tensin in cancer formation and progression *in vivo*, we took advantage of the Apc/Ras Drosophila cancer model, whereby Apc1 and Apc2 are inactivated, and active Ras is expressed in Lgr5-positive intestinal stem cells (**figure 5.6A**, collaboration with Dr Jamie Adams). We analysed tumour formation in flies expressing GFP control, Apc/Ras and Apc/Ras/TNS. Consistent with previous data, we can detect tumours in the Apc/Ras, while mostly small clones of stem cells are present in the GFP only condition (**figure 5.6B**).

Strikingly, the overexpression of TNS profoundly reduced tumour formation, as measured the the % GFP coverage in the intestine. When assessing overall tumour burden by measuring the luciferase signal in the whole body of the flied, we detected a reduction upon TNS

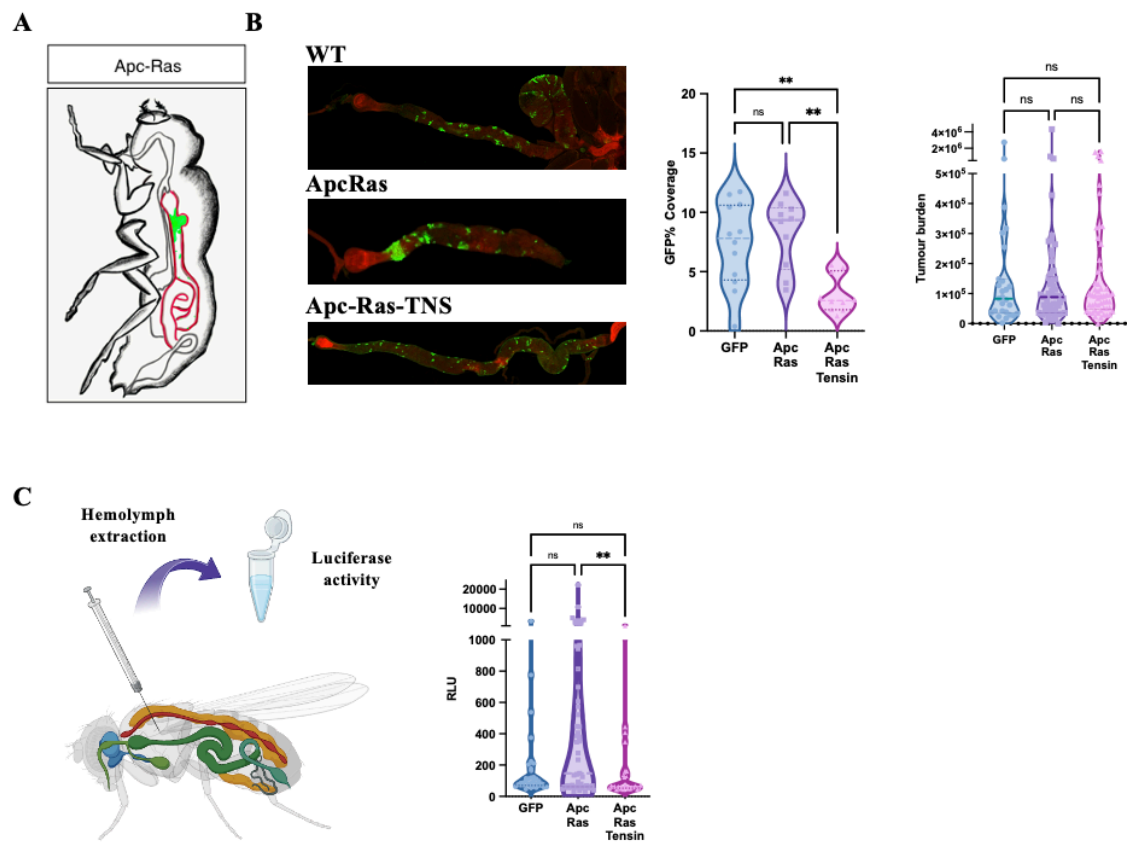


Figure 5.6: TNS overexpression in the Apc/Ras background reduced tumour formation. (A) Schematic representation of Apc-Ras tumours (green) confined in the midgut (red). Adapted from Campbell et al., 2019. (B) Adult midgut representing wild type (WT), Apc-Ras and Apc-Ras-TNS clones marked with GFP (green). % GFP coverage and tumour burden were quantified with Image J. (C) The hemolymph was extracted from individual flies and levels of luciferase activity were measured. **p<0.001 Kruskal-Wallis, multiple comparisons test, One-Way ANOVA.

overexpression, but this was not statistically significant. To assess metastatic burden, the hemolymph was extracted from the flies and the levels of luciferase in circulation were monitored. Consistent with the fact that the Apc/Ras is mostly a non-metastatic models, we detected low luciferase levels, and these were further reduced in the presence of TNS overexpression, indicating that TNS has tumour suppressive functions in this context.

5.2.6 TNS overexpression in the Apc/Ras/Sna background reduced tumour formation and metastasis

Next we wanted to investigate the effect of TNS overexpression in the metastatic Apc/Ras/Sna model (figure 5.7A). In agreement with published data, big tumours were detected throughout the gut of Apc/Ras/Sna flies. Consistent with our results in the Apc/Ras background, TNS

overexpression almost abrogated tumour formation in the gut. Analysis of 5GFP coverage of the intestine and whole body luciferase signal showed a statistically significant reduction in TNS overexpressing flies compared to control (**figure 5.7B**). Consistent with published data, metastatic dissemination is easily detectable in Apc/Ras/Sna flies. Indeed, we detected ~10fold increase in the luciferase signal in the circulation of APC/Ras/Sna flies compared to Apc/Ras (see figure 5.6B), and TNS overexpression resulted in a significant reduction (**figure 5.7B**). Altogether, these data support the hypothesis that TNS is a tumour suppressor gene in this context.

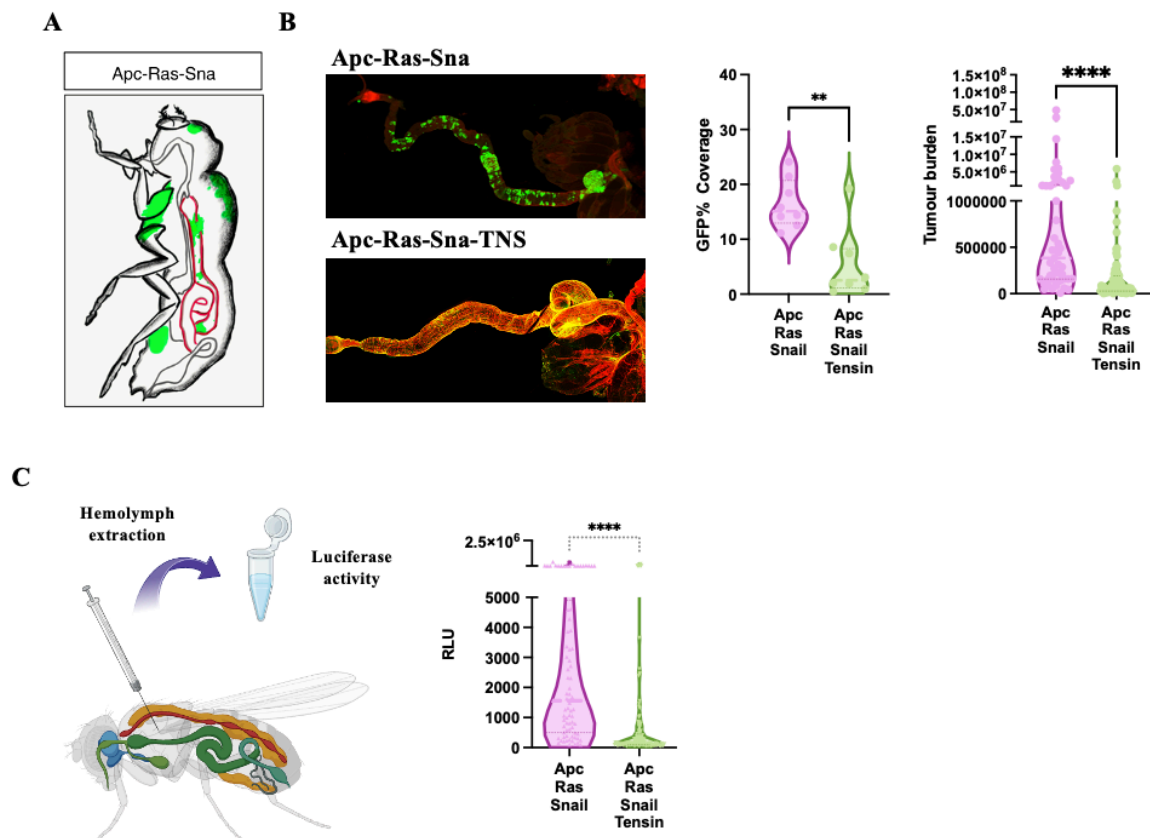


Figure 5.7: TNS overexpression in the Apc/Ras/Sna background reduced tumour formation and metastasis. (A) Schematic representation of Apc-Ras-Sna tumours (green) confined in the midgut (red). Adapted from Campbell et al., 2019. (B) Adult midgut representing Apc-Ras-Sna and Apc-Ras-Sna-TNS clones marked with GFP (green). % GFP coverage and tumour burden were quantified with Image J. (C) The hemolymph was extracted from individual flies and levels of luciferase activity were measured. **** $p < 0.0001$. Mann-Whitney test, T-test.

5.3 Discussion

In this chapter, I demonstrated that the silencing of TNS3 promoted MCF10A cell invasion and proliferation. This was coupled with increased laminin-332 expression in 3D and 2D cultures, filopodia formation and $\alpha 3$ integrin expression in 3D systems. *In vivo*, TNS overexpression reduced tumour formation in both the Apc/Ras and Apc/Ras/Sna backgrounds, while metastasis formation was impaired in the Apc/Ras/Sna background.

Different studies have demonstrated that MCF10A cells can become invasive under certain conditions, such as oncogene overexpression or tumour suppressor gene downregulation. For instance, when the oncogene H-RAS was turned on, it activated different signalling pathways including PI3K and ERK, which are known to encourage cell growth. In addition, MCF10A exhibited invasive behaviour, showing high invasion when plated on matrigel-based 3D cultures (Dow et al., 2008). A published study found that silencing TNS3 in MCF10A promoted cell migration, through a TNS3/TNS4 switch. Indeed, downregulation of TNS4 lowers EGF-induced migration. They also found that EGF stimulation raises the level of TNS4 and lowers TNS3 expression, which speeds up cell migration. Therefore, they propose a reciprocal relationship between TNS3 and TNS4 that promotes EGF signalling, which in turn drives mammary cell migration (Katz et al., 2007). In our study, we did not assess TNS4 expression levels in MCF10A cells, therefore we cannot rule out the possibility that cell invasion induced by TNS3 is also regulated by TNS4. Another study examined the impact of TNS3 overexpression in HEK 293 cells (non-transformed human embryonic kidney cells) on cellular migration and invasion. TNS3 overexpression diminished the cell migration rate towards the ECM and invasion of the BM compared to wild type cells (Martuszevska et al., 2009). However, another study found that TNS3 KD limits cell growth and migration in mesenchymal stem cells (Park et al., 2022). This suggests that TNS3 role in preventing cell migration might be specific for epithelial cells.

Our *in vivo* data showed that TNS overexpression opposed tumour formation and metastasis in a colorectal cancer model in *Drosophila*. TNS levels were assessed in colorectal cancer versus normal mammary tissues using online datasets (TNMplot.com). RNA-seq results showed that TNS3 and TNS4 expression increased significantly in tumours compared to normal tissues, while the expression of TNS1 and TNS2 was reduced (Bartha & Gyórfy, 2021). Consistent with our data, downregulation of tensin in the *Drosophila* wing disc potentiated RasV12-dependent wing disc hyperplasia. These results suggest that tensin in *Drosophila* functions as

a tumor suppressor, by limiting oncogenic Ras signalling (Martínez-Abarca Millán et al., 2023). The detailed molecular mechanism behind this regulation has not been elucidated yet, so further work is needed to determine if tensin restrains Ras-driven oncogenesis and whether this effect is Ras-specific.

Together, data from this chapter indicate that TNS3 in mammalian cells and *Drosophila* tensin act as tumour suppressors, limiting cell growth and proliferation in non-transformed mammary epithelial cells *in vitro* and preventing Apc/Ras driven tumorigenesis *in vivo*.

Chapter 6. General discussion

6.1. Discussion:

In this thesis, I demonstrated that TNS3 expression is upregulated in cancer cells compared to normal mammary epithelial cells, both in the MCF10 series of cell lines and in tissues from a polyoma middle T-drive mouse model of breast cancer. Moreover, I discovered that TNS3 downregulation reduced the invasion of both MCF10DCIS and MCF10CA1 cells. Recent data from our lab demonstrated that the presence of ECM supported breast cancer cell growth, through a pathway which required ECM uptake, followed by lysosomal degradation. In particular, matrigel supported the proliferation of MCF10DCIS and MCF10CA1 cells grown under glutamine starvation (Nazemi et al., 2024), while TNS3 was shown to be required for ECM uptake in breast cancer cells (Shahd Alhadid, Rainero lab, unpublished data). In line with this, I found that TNS3 knockdown reduced the proliferation of MCF10DCIS and MCF10CA1 cells plated on matrigel under glutamine deprivation. Together, this data demonstrated that TNS3 was required for the proliferation and invasion of breast cancer cells.

Mechanistically, my data demonstrate that silencing TNS3 or $\beta 1$ integrin resulted in a significant reduction in laminin-332 expression. Previous reports have shown that filopodia modulate BM deposition (Peuhu et al., 2022). Consistently, my results show that silencing TNS3 and $\beta 1$ integrin significantly reduced the number and length of filopodia, in MCF10DCIS cells. Interestingly, this was accompanied by a significant reduction in the expression of $\alpha 3$ and $\alpha 6$ integrins, suggesting that TNS3 might control laminin-332 expression by modulating $\alpha 3$ and $\alpha 6$ integrin levels. Indeed, $\alpha 3$ and $\alpha 6$ blocking antibodies in MCF10DCIS cells greatly decreased the buildup of laminin-332 and the formation of filopodia. Similar results were obtained in MCF10CA1 cells, where TNS3 knockdown significantly reduced the expression of laminin-332 and $\alpha 3$ integrin, as well as filopodia formation.

Finally, I investigated the function of TNS3 in normal mammary epithelial cells. The findings indicate that after suppressing TNS3, the invasion increased. We measured the expression level of laminin-332 and filopodia formation, revealing a higher level of laminin-332 and $\alpha 3$ integrin expression, as well as increased filopodia formation in TNS3 knockdown MCF10A cells compared to the non-targeting siRNA control. In addition, TNS3 downregulation promoted MCF10A cell proliferation, suggesting that TNS3 has tumour suppressive functions in non-transformed epithelial cells. To investigate the role of TNS in tumour progression *in vivo*, I

tested TNS overexpression in a *Drosophila* colorectal cancer model, which resulted in tumour reduction in both the non-metastatic Apc/Ras background and the metastatic Apc/Ras/Snai background; additionally, TNS overexpression in the Apc/Ras/Snai background significantly reduced metastasis formation.

To summarize, this project results suggest that TNS3 modulated laminin-332 expression via $\alpha3\beta1$ - and $\alpha6\beta1$ -dependent mechanisms. As my results showed, silencing TNS3 decreased integrin protein levels. This could be explained by differences in gene transcription or protein stability. Reports indicate that tensins play a crucial role in stabilizing integrins, as TNS3 and TNS4 have been shown to stabilise $\beta1$ -integrin, which is responsible for mediating cell adhesion, migration, and cellular response (Merour et al., 2022; Muharram et al., 2014). In particular, TNS4 was shown to promote $\beta1$ integrin accumulation by preventing its internalisation and lysosomal degradation (Muharram et al., 2014). In contrast, TNS3 has been shown to promote the internalisation of ligand-bound $\alpha5\beta1$ in ovarian cancer cells overexpressing the small GTPase Rab25 (Rainero et al., 2015). Here, I hypothesize that in breast cancer cells, the presence of TNS3 could stabilize focal adhesions containing $\alpha3\beta1$ and $\alpha6\beta1$, suggesting that TNS3 might stabilise specific integrin heterodimers, while promoting the internalisation of ligand-bound ones. It is important to consider that MCF10 cells do not express Rab25, Furthermore, I believe that adhesion signalling stimulates the formation of filopodia, leading to the accumulation of lamini-332 in the BM and subsequent cell invasion (**figure 6.1**). It has been reported that the formation of filopodia triggers the formation of focal adhesions by connecting $\beta1$ integrin at the filopodia tip to the ECM, thereby initiating the recruitment of focal adhesion proteins (Partridge & Marcantonio, 2006). As a result, focal adhesion formation commences, which contributes to proliferation, invasion, and the formation of filopodia. This could be caused by the activation of cellular signalling pathways, including FAK/Src activation, Junk, and PI3K, which are responsible for the upregulation of invasion and proliferation. Further investigations are required to determine whether TNS3 affects $\alpha3\beta1$ and $\alpha6\beta1$ integrin stability and adhesion signalling in breast cancer cells, and how this process impinges on filopodia formation.

On the other hand, in normal mammary epithelial cells, TNS3 acts as a tumour suppressor in the non-tumorigenic breast epithelial cells MCF10A. In this context, TNS3 might destabilize $\alpha3\beta1$, and therefore prevent filopodia formation and laminin-332 expression. Loss of TNS3

will therefore stabilise focal adhesions, leading to the activation of downstream signalling pathways that are responsible for invasion, proliferation, and migration (**figure 6.1**).

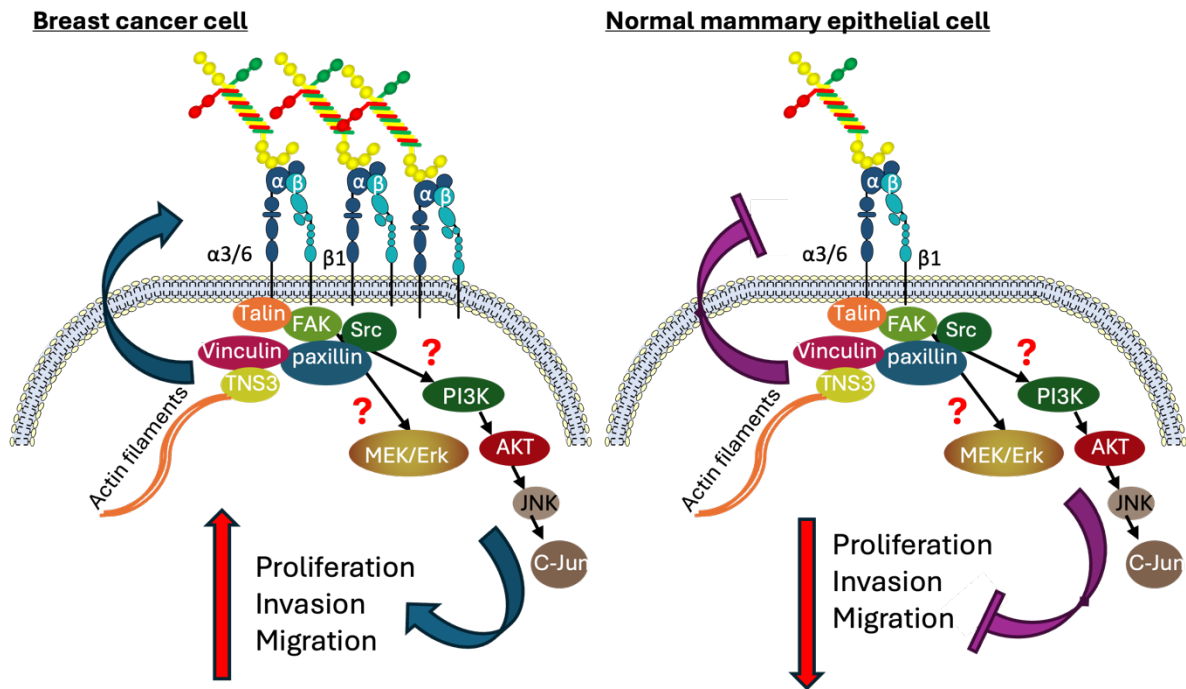


Figure 6.1: working model. In breast cancer cells, laminin-332 interacts with $\alpha3\beta1$ and $\alpha6\beta1$ integrins. Activated integrins initiate the formation of focal adhesion by recruiting focal adhesion proteins like TNS3. This, in turn, can trigger intracellular signaling cascades, including PI3K and MERK/Erk. This led to an increase in proliferation, invasion, and migration. In mammary epithelial cells, laminin-332 binds to $\alpha3\beta1$ and $\alpha6\beta1$ integrins. Activated integrins initiate the formation of focal adhesion by recruiting focal adhesion proteins like TNS3. This may therefore reduce intracellular signaling cascades, such as PI3K and MERK/Erk. This led to a decrease in proliferation, invasion, and migration.

The BM plays a dual role in cancer, being both tumour suppressor in early stages of tumorigenesis and tumour promoter at later stages. This observation might explain the differential role of TNS3 in normal and breast cancer cells. In normal cells, the BM contributes to structural integrity by providing a well-organized, balanced composition that helps maintain cell tissue homogeneity and boundaries (Jayadev & Sherwood, 2017; Meghan A Morrissey et al., 2013). This helps to control cell migration and proliferation. On the other hand, cancers lose this feature due to disruption of the BM, alteration in its composition and compromised stability. Furthermore, once homeostasis is lost, cancer cells detach and move (Jean A Engbring & Hynda K Kleinman, 2003; Pozzi et al., 2017).

One of the primary causes of cancer cell invasion is the high level of matrix mechanical plasticity. As a result, matrix densification is a well-documented aspect of matrix mechanical plasticity that promotes invasion (Chang & Chaudhuri, 2019). During cancer progression,

abnormal BM component deposition favours epithelial-mesenchymal transitions, which promote cancer cell growth and invasion. It has been shown that this occurs through the activation of the FAK/Src axis, which in turn activates PI3K and ERK, both of which are crucial for inducing a cell response such as cell survival, migration and invasion (Fatherree et al., 2022). An *in vivo* study found that in MMP-deficient animals, invadopodia break the BM five times more than wild-type animals (Chang & Chaudhuri, 2019). They used time-lapse imaging to investigate *C. elegans* anchor cell (AC) invasion. They observed that invasion occurred in the absence of MMP. Furthermore, it has been suggested that this occurred through adaptive mechanisms, including an increase in the Arp2/3 complex, which enhances F-actin formation and thus promotes protrusions. This process was powered by ATP, which is produced by the mitochondria located in the protrusions (Kelley et al., 2019). Another possible reason for breaking the BM is proliferation. Proliferation has been shown to increase the size of the tumour, putting more pressure on the BM and thereby weakening it (Chang & Chaudhuri, 2019). This suggests a possible causal connection between proliferation and invasion. Another factor that could influence the change in the composition of BM is its stiffness (Khalilgharibi & Mao, 2021). Studies have reported an increase in the stiffness of the BM with higher collagen levels (Jayadev & Sherwood, 2017; Meghan A Morrissey et al., 2013). One of the primary causes of stiffer BMs is the overproduction of collagen IV and laminin, which contributes to invasive behaviour (Koorman et al., 2022). Furthermore, studies have demonstrated that TGF- β signalling increases collagen synthesis during cancer progression, thereby contributing to the stiffness of BMs. Another factor to consider is ageing; as people get older, their collagen deposition increases (Jayadev & Sherwood, 2017; Meghan A Morrissey et al., 2013).

We believe that the *Drosophila* cancer model we used most accurately represents cancer initiation, as TNS overexpression occurs in stem cells concurrently with APC loss and Ras/Snai activation. As a result, this model does not allow for measuring the effect of TNS overexpression in advanced stages of cancer. Future work should modulate TNS expression levels in established tumours, to determine whether TNS switch from being anti-tumorigenic during cancer initiation to being pro-tumorigenic at later stages

6.2 Conclusion and future direction:

This project demonstrates a dual role of TNS3 in regulating breast cancer progression. It demonstrates how TNS3 links the ECM to initiate cellular physiological processes, such as invasion, proliferation, and filopodia formation. Furthermore, depending on the cell type, TNS3 can act as both a tumour suppressor or promoter. We need further research to elucidate the various roles of TNS3, as there are several questions that remain unanswered.

It would be interesting to determine:

- If TNS3 also affects cancer cell migration, performing wound healing and random cell migration assays.
- It would be important to determine what the molecular mechanisms through which TNS3 affect filopodia extension are, including how $\alpha3\beta1$ and $\alpha6\beta1$ control this process.
- It would also be interesting to elucidate how TNS3 downregulation impinges on focal adhesion signalling, by performing western blot analysis to measure the phosphorylation levels of FAK, MAPK and AKT.
- The protein levels involved in the formation of filopodia can be assessed using a western blot.
- Assess the protein level of different ECM proteins such as collagen and fibronectin.
- To assess the role of TNS3 in mice that has 4 different TNS, this would help to strengthen the ongoing investigation.

Addressing these questions will advance our understanding of the role of TNS3 in breast cancer. Further research into the role of TNS3 and its role in controlling ECM dynamics in breast cancer progression is critical to uncovering novel regulators of tumour progression that will aid in the development of new therapeutic strategies to improve patient outcomes.

References:

- Albasri, A., Aleskandarany, M., Benhasouna, A., Powe, D. G., Ellis, I. O., Ilyas, M., & Green, A. R. (2011). CTEN (C-terminal tensin-like), a novel oncogene overexpressed in invasive breast carcinoma of poor prognosis. *Breast Cancer Research and Treatment*, *126*(1), 47–54. <https://doi.org/10.1007/s10549-010-0890-3>
- Allen, B. G., Bhatia, S. K., Buatti, J. M., Brandt, K. E., Lindholm, K. E., Button, A. M., Szweda, L. I., Smith, B. J., Spitz, D. R., & Fath, M. A. (2013). Ketogenic diets enhance oxidative stress and radio-chemo-therapy responses in lung cancer xenografts. *Clinical Cancer Research*, *19*(14), 3905–3913. <https://doi.org/10.1158/1078-0432.CCR-12-0287>
- Allen, M. D., Thomas, G. J., Clark, S., Dawoud, M. M., Vallath, S., Payne, S. J., Gomm, J. J., Dreger, S. A., Dickinson, S., Edwards, D. R., Pennington, C. J., Sestak, I., Cuzick, J., Marshall, J. F., Hart, I. R., & Jones, J. L. (2014). Altered microenvironment promotes progression of preinvasive breast cancer: Myoepithelial expression of avb6 integrin in DCIS identifies high-risk patients and predicts recurrence. *Clinical Cancer Research*, *20*(2), 344–357. <https://doi.org/10.1158/1078-0432.CCR-13-1504>
- Amereh, M., Edwards, R., Akbari, M., & Nadler, B. (2021). In-silico modeling of tumor spheroid formation and growth. *Micromachines*, *12*(7). <https://doi.org/10.3390/mi12070749>
- Anderson, N. M., & Simon, M. C. (2020). The tumor microenvironment. In *Current Biology* (Vol. 30, Issue 16, pp. R921–R925). Cell Press. <https://doi.org/10.1016/j.cub.2020.06.081>
- Atherton, P., Konstantinou, R., Neo, S. P., Wang, E., Balloi, E., Ptushkina, M., Bennett, H., Clark, K., Gunaratne, J., Critchley, D., Barsukov, I., Manser, E., & Ballestrem, C. (2022). Tensin3 interaction with talin drives the formation of fibronectin-associated fibrillar adhesions. *Journal of Cell Biology*, *221*(10). <https://doi.org/10.1083/jcb.202107022>
- Atoum, M. F., Alzoughool, F., & Al-Hourani, H. (2020). Linkage Between Obesity Leptin and Breast Cancer. In *Breast Cancer: Basic and Clinical Research* (Vol. 14). SAGE Publications Ltd. <https://doi.org/10.1177/1178223419898458>
- Attalla, S., Taifour, T., Bui, T., & Muller, W. (2021). Insights from transgenic mouse models of PyMT-induced breast cancer: recapitulating human breast cancer progression *in vivo*. In *Oncogene* (Vol. 40, Issue 3, pp. 475–491). Springer Nature. <https://doi.org/10.1038/s41388-020-01560-0>
- Bajanca, F., Luz, M., Raymond, K., Martins, G. G., Sonnenberg, A., Tajbakhsh, S., Buckingham, M., & Thorsteinsdóttir, S. (2006). Integrin $\alpha 6 \beta 1$ -laminin interactions regulate early myotome formation in the mouse embryo. *Development*, *133*(9), 1635–1644. <https://doi.org/10.1242/dev.02336>
- Banerjee, S., Lo, W. C., Majumder, P., Roy, D., Ghorai, M., Shaikh, N. K., Kant, N., Shekhawat, M. S., Gadekar, V. S., Ghosh, S., Bursal, E., Alrumaihi, F., Dubey, N. K., Kumar, S., Iqbal, D., Alturaiki, W., Upadhye, V. J., Jha, N. K., Dey, A., & Gundamaraju, R. (2022). Multiple roles for basement membrane proteins in cancer progression and EMT. *European Journal of Cell Biology*, *101*(2). <https://doi.org/10.1016/j.ejcb.2022.151220>

Bartha, Á., & Györffy, B. (2021). TnmpLOT.Com: A web tool for the comparison of gene expression in normal, tumor and metastatic tissues. *International Journal of Molecular Sciences*, 22(5), 1–12. <https://doi.org/10.3390/ijms22052622>

Bauer, S., Kerr, B. J., & Patterson, P. H. (2007). The neurotrophic cytokine family in development, plasticity, disease and injury. *Nature Reviews Neuroscience*, 8(3), 221–232. <https://doi.org/10.1038/nrn2054>

Beedle, M., Jaganathan, A., Albajar-Sigalés, A., Max Yavitt, F., Bera, K., Granero-Moya, I., Zalvidea, D., Kechagia, Z., Wiche, G., Ivaska, J., Anseth, K. S., Shenoy, V. B., & Roca-Cusachs, P. (2023). Fibrillar adhesion dynamics govern the timescales of nuclear mechano-response via the vimentin cytoskeleton. *BioRxiv*.

Benitez Fuentes, J. D., Morgan, E., De Luna Aguilar, A., Mafra, A., Shah, R., Giusti, F., Vignat, J., Znaor, A., Musetti, C., Yip, C. H., Van Eycken, L., Jedy-Agba, E., Piñeros, M., & Soerjomataram, I. (2024). Global Stage Distribution of Breast Cancer at Diagnosis: A Systematic Review and Meta-Analysis. *JAMA Oncology*, 10(1), 71–78. <https://doi.org/10.1001/jamaoncol.2023.4837>

Bessette, D. C., Tilch, E., Seidens, T., Quinn, M. C. J., Wiegmanns, A. P., Shi, W., Cocciardi, S., McCart-Reed, A., Saunus, J. M., Simpson, P. T., Grimmond, S. M., Lakhani, S. R., Khanna, K. K., Waddell, N., Al-Ejeh, F., & Chenevix-Trench, G. (2015). Using the MCF10A/MCF10CA1a breast cancer progression cell line model to investigate the effect of active, mutant forms of EGFR in breast cancer development and treatment using gefitinib. *PLoS ONE*, 10(5). <https://doi.org/10.1371/journal.pone.0125232>

Bhowmick, N. A., Neilson, E. G., & Moses, H. L. (2004). Stromal fibroblasts in cancer initiation and progression. *Nature*, 432(7015), 332–337. <https://doi.org/10.1038/nature03096>

Boutin, A. T., Liao, W. T., Wang, M., Hwang, S. S., Karpinets, T. V., Cheung, H., Chu, G. C., Jiang, S., Hu, J., Chang, K., Vilar, E., Song, X., Zhang, J., Kopetz, S., Futreal, A., Wang, Y. A., Kwong, L. N., & DePinho, R. A. (2017). Oncogenic Kras drives invasion and maintains metastases in colorectal cancer. *Genes and Development*, 31(4), 370–382. <https://doi.org/10.1101/gad.293449.116>

Brock, E. J., Ji, K., Shah, S., Mattingly, R. R., & Sloane, B. F. (2019). *In Vitro* Models for Studying Invasive Transitions of Ductal Carcinoma *In Situ*. In *Journal of Mammary Gland Biology and Neoplasia* (Vol. 24, Issue 1). Springer New York LLC. <https://doi.org/10.1007/s10911-018-9405-3>

Byron, A., Humphries, J. D., Askari, J. A., Craig, S. E., Mould, A. P., & Humphries, M. J. (2009). Anti-integrin monoclonal antibodies. *Journal of Cell Science*, 122(22), 4009–4011. <https://doi.org/10.1242/jcs.056770>

Campbell, K., Rossi, F., Adams, J., Pitsidianaki, I., Barriga, F. M., Garcia-Gerique, L., Batlle, E., Casanova, J., & Casali, A. (2019). Collective cell migration and metastases induced by an epithelial-to-mesenchymal transition in *Drosophila* intestinal tumors. *Nature Communications*, 10(1). <https://doi.org/10.1038/s41467-019-10269-y>

Carmona, G., Perera, U., Gillett, C., Naba, A., Law, A. L., Sharma, V. P., Wang, J., Wyckoff, J., Balsamo, M., Mosis, F., De Piano, M., Monypenny, J., Woodman, N., McConnell, R. E., Mouneimne, G., Van Hemelrijck, M., Cao, Y., Condeelis, J., Hynes, R. O., ... Krause, M. (2016). Lamellipodin promotes invasive 3D cancer cell migration via regulated interactions with Ena/VASP and SCAR/WAVE. *Oncogene*, 35(39), 5155–5169. <https://doi.org/10.1038/onc.2016.47>

Carpenter, P. M., Dao, A. V., Arain, Z. S., Chang, M. K., Nguyen, H. P., Arain, S., Wang-Rodriguez, J., Kwon, S. Y., & Wilczynski, S. P. (2009). Motility induction in breast carcinoma by mammary epithelial laminin 332 (laminin 5). *Molecular Cancer Research*, 7(4), 462–475. <https://doi.org/10.1158/1541-7786.MCR-08-0148>

Caswell, P. T., & Zech, T. (2018). Actin-Based Cell Protrusion in a 3D Matrix. In *Trends in Cell Biology* (Vol. 28, Issue 10, pp. 823–834). Elsevier Ltd. <https://doi.org/10.1016/j.tcb.2018.06.003>

Cha, I. J., Lee, J. H., Cho, K. S., & Lee, S. B. (2017). Drosophila tensin plays an essential role in cell migration and planar polarity formation during oogenesis by mediating integrin-dependent extracellular signals to actin organization. *Biochemical and Biophysical Research Communications*, 484(3), 702–709. <https://doi.org/10.1016/j.bbrc.2017.01.183>

Chávez-Paredes, S., Montoya-García, A., & Schnoor, M. (2019). Cellular and pathophysiological consequences of Arp2/3 complex inhibition: role of inhibitory proteins and pharmacological compounds. In *Cellular and Molecular Life Sciences* (Vol. 76, Issue 17, pp. 3349–3361). Birkhauser Verlag AG. <https://doi.org/10.1007/s00018-019-03128-y>

Chang, J., & Chaudhuri, O. (2019). Beyond proteases: Basement membrane mechanics and cancer invasion. In *Journal of Cell Biology* (Vol. 218, Issue 8, pp. 2456–2469). Rockefeller University Press. <https://doi.org/10.1083/JCB.201903066>

Chang, J., Saraswathibhatla, A., Song, Z., Varma, S., Sanchez, C., Alyafei, N. H. K., Indana, D., Slyman, R., Srivastava, S., Liu, K., Bassik, M. C., Marinkovich, M. P., Hodgson, L., Shenoy, V., West, R. B., & Chaudhuri, O. (2024). Cell volume expansion and local contractility drive collective invasion of the basement membrane in breast cancer. *Nature Materials*, 23(5), 711–722. <https://doi.org/10.1038/s41563-023-01716-9>

Chang, J., Saraswathibhatla, A., Song, Z., Varma, S., Sanchez, C., Srivastava, S., Liu, K., Bassik, M. C., Marinkovich, M. P., Hodgson, L., Shenoy, V., West, R. B., & Chaudhuri, O. (2022). Collective invasion of the basement membrane in breast cancer driven by forces from cell volume expansion and local contractility. *BioRxiv*. <https://doi.org/10.1101/2022.07.28.501930>

Chen, H., Duncan, I. C., Bozorghami, H., & Lo, S. H. (2002). Tensin1 and a previously undocumented family member, tensin2, positively regulate cell migration. *Proceedings of the National Academy of Sciences of the United States of America*, 99(2), 733–738. <https://doi.org/10.1073/pnas.022518699>

Chen, M. B., Lamar, J. M., Li, R., Hynes, R. O., & Kamm, R. D. (2016). Elucidation of the roles of tumor integrin $\beta 1$ in the extravasation stage of the metastasis cascade. *Cancer Research*, 76(9), 2513–2524. <https://doi.org/10.1158/0008-5472.CAN-15-1325>

- Chiang, M. K., Liao, Y. C., Kuwabara, Y., & Lo, S. H. (2005). Inactivation of tensin3 in mice results in growth retardation and postnatal lethality. *Developmental Biology*, 279(2), 368–377. <https://doi.org/10.1016/j.ydbio.2004.12.027>
- Choi, S., Bhagwat, A. M., Al Mismar, R., Goswami, N., Ben Hamidane, H., Sun, L., & Graumann, J. (2018). Proteomic profiling of human cancer pseudopodia for the identification of anti-metastatic drug candidates. *Scientific Reports*, 8(1). <https://doi.org/10.1038/s41598-018-24256-8>
- Chua, I. L. S., Kim, H. W., & Lee, J. H. (2016). Signaling of extracellular matrices for tissue regeneration and therapeutics. *Tissue Engineering and Regenerative Medicine*, 13(1), 1–12. <https://doi.org/10.1007/s13770-016-9075-0>
- Clark, K., Howe, J. D., Pullar, C. E., Green, J. A., Artym, V. V., Yamada, K. M., & Critchley, D. R. (2010). Tensin 2 modulates cell contractility in 3D collagen gels through the RhoGAP DLC1. *Journal of Cellular Biochemistry*, 109(4), 808–817. <https://doi.org/10.1002/jcb.22460>
- Cooper, J., & Giancotti, F. G. (2019). Integrin Signaling in Cancer: Mechanotransduction, Stemness, Epithelial Plasticity, and Therapeutic Resistance. In *Cancer Cell* (Vol. 35, Issue 3, pp. 347–367). Cell Press. <https://doi.org/10.1016/j.ccell.2019.01.007>
- Cowell, C. F., Weigelt, B., Sakr, R. A., Ng, C. K. Y., Hicks, J., King, T. A., & Reis-Filho, J. S. (2013). Progression from ductal carcinoma *in situ* to invasive breast cancer: Revisited. *Molecular Oncology*, 7(5), 859–869. <https://doi.org/10.1016/j.molonc.2013.07.005>
- Cox, T. R., & Erler, J. T. (2011). Remodeling and homeostasis of the extracellular matrix: Implications for fibrotic diseases and cancer. *DMM Disease Models and Mechanisms*, 4(2), 165–178. <https://doi.org/10.1242/dmm.004077>
- Cui, Y., Liao, Y. C., & Lo, S. H. (2004). Epidermal growth factor modulates tyrosine phosphorylation of a novel tensin family member, tensin3. *Molecular Cancer Research*, 2(4), 225–232.
- Dai, Y., Zhang, X., Ou, Y., Zou, L., Zhang, D., Yang, Q., Qin, Y., Du, X., Li, W., Yuan, Z., Xiao, Z., & Wen, Q. (2023). Anoikis resistance—protagonists of breast cancer cells survive and metastasize after ECM detachment. In *Cell Communication and Signaling* (Vol. 21, Issue 1). BioMed Central Ltd. <https://doi.org/10.1186/s12964-023-01183-4>
- Dashti, H. M., Al-Zaid, N. S., Mathew, T. C., Al-Mousawi, M., Talib, H., Asfar, S. K., & Behbahani, A. I. (2006). Long term effects of ketogenic diet in obese subjects with high cholesterol level. *Molecular and Cellular Biochemistry*, 286(1–2), 1–9. <https://doi.org/10.1007/s11010-005-9001-x>
- Dass, S. A., Tan, K. L., Rajan, R. S., Mokhtar, N. F., Adzmi, E. R. M., Rahman, W. F. W. A., Din, T. A. D. A. A. T., & Balakrishnan, V. (2021). Triple negative breast cancer: A review of present and future diagnostic modalities. In *Medicina (Lithuania)* (Vol. 57, Issue 1, pp. 1–18). MDPI AG. <https://doi.org/10.3390/medicina57010062>

Dawson, P. J., Wolman, S. R., Tait, L., Heppner, G. H., Millert, F. R., Haley V A IHospital, J. A., Cancer Program, B., & Ann, B. (1996). *MCF1 OAT: A Model for the Evolution of Cancer from Proliferative Breast Disease* (Vol. 148, Issue 1).

Dehart, G. W., Healy, K. E., & Jones, J. C. R. (2003). *The role of 31 integrin in determining the supramolecular organization of laminin-5 in the extracellular matrix of keratinocytes*. [https://doi.org/10.1016/S0014-4827\(02\)00028-0](https://doi.org/10.1016/S0014-4827(02)00028-0)

Dehesh, T., Fadaghi, S., Seyedi, M., Abolhadi, E., Ilaghi, M., Shams, P., Ajam, F., Mosleh-Shirazi, M. A., & Dehesh, P. (2023). The relation between obesity and breast cancer risk in women by considering menstruation status and geographical variations: a systematic review and meta-analysis. *BMC Women's Health*, 23(1). <https://doi.org/10.1186/s12905-023-02543-5>

Denoyer, D., Kusuma, N., Burrows, A., Ling, X., Jupp, L., Anderson, R. L., & Pouliot, N. (2014). Bone-derived soluble factors and laminin-511 cooperate to promote migration, invasion and survival of bone-metastatic breast tumor cells. *Growth Factors*, 32(2), 63–73. <https://doi.org/10.3109/08977194.2014.894037>

Desgrosellier, J. S., & Cheresch, D. A. (2010). Integrins in cancer: Biological implications and therapeutic opportunities. In *Nature Reviews Cancer* (Vol. 10, Issue 1, pp. 9–22). <https://doi.org/10.1038/nrc2748>

Djomehri, S. I., Burman, B., Gonzalez, M. E., Takayama, S., & Kleer, C. G. (2019). A reproducible scaffold-free 3D organoid model to study neoplastic progression in breast cancer. *Journal of Cell Communication and Signaling*, 13(1), 129–143. <https://doi.org/10.1007/s12079-018-0498-7>

Dow, L. E., Elsum, I. A., King, C. L., Kinross, K. M., Richardson, H. E., & Humbert, P. O. (2008). Loss of human Scribble cooperates with H-Ras to promote cell invasion through deregulation of MAPK signalling. *Oncogene*, 27(46), 5988–6001. <https://doi.org/10.1038/onc.2008.219>

Dowis, K., & Banga, S. (2021). The potential health benefits of the ketogenic diet: A narrative review. In *Nutrients* (Vol. 13, Issue 5). MDPI AG. <https://doi.org/10.3390/nu13051654>

Eroles, P., Bosch, A., Alejandro Pérez-Fidalgo, J., & Lluch, A. (2012). Molecular biology in breast cancer: Intrinsic subtypes and signaling pathways. In *Cancer Treatment Reviews* (Vol. 38, Issue 6, pp. 698–707). <https://doi.org/10.1016/j.ctrv.2011.11.005>

Faraldo, M. M., Romagnoli, M., Wallon, L., Dubus, P., Deugnier, M. A., & Fre, S. (2024). Alpha-6 integrin deletion delays the formation of Brca1/p53-deficient basal-like breast tumors by restricting luminal progenitor cell expansion. *Breast Cancer Research*, 26(1). <https://doi.org/10.1186/s13058-024-01851-4>

Fatherree, J. P., Guarin, J. R., McGinn, R. A., Naber, S. P., & Oudin, M. J. (2021). Chemotherapy-induced collagen IV drives cancer cell invasion through activation of Src/FAK signaling. *BioRxiv*. <https://doi.org/10.1101/2021.04.01.438074>

Fatherree, J. P., Guarin, J. R., McGinn, R. A., Naber, S. P., & Oudin, M. J. (2022). Chemotherapy-Induced Collagen IV Drives Cancer Cell Motility through Activation of Src

and Focal Adhesion Kinase. *Cancer Research*, 82(10), 2031–2044. <https://doi.org/10.1158/0008-5472.CAN-21-1823>

Fred R., Miller, S., J. Santner, Larry Tait, P., & J. Dawson. (2000). MCF10DCIS.com Xenograft Model of Human Comedo Ductal Carcinoma *In Situ*. *Journal of the National Cancer Institute*, 92(14), 1185a–11186. <https://academic.oup.com/jnci/article/92/14/1185a/2905877>
Friedl, P., & Alexander, S. (2011). Cancer invasion and the microenvironment: Plasticity and reciprocity. In *Cell* (Vol. 147, Issue 5, pp. 992–1009). Elsevier B.V. <https://doi.org/10.1016/j.cell.2011.11.016>

Georgiadou, M., Lilja, J., Jacquemet, G., Guzmán, C., Rafeeva, M., Alibert, C., Yan, Y., Sahgal, P., Lerche, M., Manneville, J. B., Mäkelä, T. P., & Ivaska, J. (2017). AMPK negatively regulates tensin-dependent integrin activity. *Journal of Cell Biology*, 216(4), 1107–1121. <https://doi.org/10.1083/jcb.201609066>

Ghannam, S. F., Rutland, C. S., Allegrucci, C., Mongan, N. P., & Rakha, E. (2022). Defining invasion in breast cancer: The role of basement membrane. In *Journal of Clinical Pathology* (Vol. 76, Issue 1, pp. 11–18). BMJ Publishing Group. <https://doi.org/10.1136/jcp-2022-208584>

Givant-Horwitz, V., Davidson, B., & Reich, R. (2005). Laminin-induced signaling in tumor cells. In *Cancer Letters* (Vol. 223, Issue 1, pp. 1–10). Elsevier Ireland Ltd. <https://doi.org/10.1016/j.canlet.2004.08.030>

Goh, J. J. H., Goh, C. J. H., Lim, Q. W., Zhang, S., Koh, C. G., & Chiam, K. H. (2022). Transcriptomics indicate nuclear division and cell adhesion not recapitulated in MCF7 and MCF10A compared to luminal A breast tumours. *Scientific Reports*, 12(1). <https://doi.org/10.1038/s41598-022-24511-z>

Gomes, V., & Salgueiro, S. P. (2022). From small to large-scale: a review of recombinant spider silk and collagen bioproduction. In *Discover Materials* (Vol. 2, Issue 1). Discover. <https://doi.org/10.1007/s43939-022-00024-4>

Gonzales, M., Haan, K., Baker, S. E., Fitchmun, M., Todorov, I., Weitzman, S., & Jones, J. C. R. (1999). A cell signal pathway involving laminin-5, $\alpha 3\beta 1$ integrin, and mitogen-activated protein kinase can regulate epithelial cell proliferation. *Molecular Biology of the Cell*, 10(2), 259–270. <https://doi.org/10.1091/mbc.10.2.259>

Grzesiak, J. J., Cao, H. S. T., Burton, D. W., Kaushal, S., Vargas, F., Clopton, P., Snyder, C. S., Deftos, L. J., Hoffman, R. M., & Bouvet, M. (2011). Knockdown of the $\beta 1$ integrin subunit reduces primary tumor growth and inhibits pancreatic cancer metastasis. *International Journal of Cancer*, 129(12), 2905–2915. <https://doi.org/10.1002/ijc.25942>

Guess, C. M., & Quaranta, V. (2009). Defining the role of laminin-332 in carcinoma. In *Matrix Biology* (Vol. 28, Issue 8, pp. 445–455). <https://doi.org/10.1016/j.matbio.2009.07.008>

Halder, S. K., Sapkota, A., & Milner, R. (2022). The impact of genetic manipulation of laminin and integrins at the blood–brain barrier. In *Fluids and Barriers of the CNS* (Vol. 19, Issue 1). BioMed Central Ltd. <https://doi.org/10.1186/s12987-022-00346-8>

Hamill, K. J., Kligys, K., Hopkinson, S. B., & Jones, J. C. R. (2009). Laminin deposition in the extracellular matrix: A complex picture emerges. *Journal of Cell Science*, 122(24), 4409–4417. <https://doi.org/10.1242/jcs.041095>

Hanahan, D., & Weinberg, R. A. (2000). The Hallmarks of Cancer. In *Cell* (Vol. 100). [https://doi.org/10.1016/s0092-8674\(00\)81683-9](https://doi.org/10.1016/s0092-8674(00)81683-9)

Hayward, M. K., Allen, M. D., Gomm, J. J., Goulding, I., Thompson, C. L., Knight, M. M., Marshall, J. F., & Jones, J. L. (2022). Mechanostimulation of breast myoepithelial cells induces functional changes associated with DCIS progression to invasion. *Npj Breast Cancer*, 8(1). <https://doi.org/10.1038/s41523-022-00464-4>

Hernández Borrero, L. J., & El-Deiry, W. S. (2021). Tumor suppressor p53: Biology, signaling pathways, and therapeutic targeting. In *Biochimica et Biophysica Acta - Reviews on Cancer* (Vol. 1876, Issue 1). Elsevier B.V. <https://doi.org/10.1016/j.bbcan.2021.188556>

Hogan, C. (2012). Impact of interactions between normal and transformed epithelial cells and the relevance to cancer. In *Cellular and Molecular Life Sciences* (Vol. 69, Issue 2, pp. 203–213). <https://doi.org/10.1007/s00018-011-0806-3>

Hu, T., Zhou, R., Zhao, Y., & Wu, G. (2016). Integrin $\alpha 6$ /Akt/Erk signaling is essential for human breast cancer resistance to radiotherapy. *Scientific Reports*, 6. <https://doi.org/10.1038/srep33376>

Huang, H., Li, L., Wu, C., Schibli, D., Colwill, K., Ma, S., Li, C., Roy, P., Ho, K., Songyang, Z., Pawson, T., Gao, Y., & Li, S. S. C. (2008). Defining the specificity space of the human Src homology 2 domain. *Molecular and Cellular Proteomics*, 7(4), 768–784. <https://doi.org/10.1074/mcp.M700312-MCP200>

Huang, Q., Wang, J., Ning, H., Liu, W., & Han, X. (2024). Integrin $\beta 1$ in breast cancer: mechanisms of progression and therapy. *Breast Cancer*. <https://doi.org/10.1007/s12282-024-01635-w>

Hwang, P. Y., Mathur, J., Cao, Y., Almeida, J., Ye, J., Morikis, V., Cornish, D., Clarke, M., Stewart, S. A., Pathak, A., & Longmore, G. D. (2023). A Cdh3- β -catenin-laminin signaling axis in a subset of breast tumor leader cells control leader cell polarization and directional collective migration. *Developmental Cell*, 58(1), 34–50.e9. <https://doi.org/10.1016/j.devcel.2022.12.005>

Hynes, R. O. (2009). Extracellular matrix: not just pretty fibrils Richard. *Science*, 326(5957), 1216–1219. <https://doi.org/10.1126/science.1176009>.

Iikuni, N., Kwan Lam, Q., Lu, L., Matarese, G., & Cava, A. (2008). Leptin and Inflammation. *Current Immunology Reviews*, 4(2), 70–79. <https://doi.org/10.2174/157339508784325046>

Jacquemet, G., Paatero, I., Carisey, A. F., Padzik, A., Orange, J. S., Hamidi, H., & Ivaska, J. (2017). FiloQuant reveals increased filopodia density during breast cancer progression. *Journal of Cell Biology*, 216(10), 3387–3403. <https://doi.org/10.1083/jcb.201704045>

Jayadev, R., & Sherwood, D. R. (2017). Current Biology Basement membranes. In *Current Biology* (Vol. 27, R207-R211). <https://doi.org/10.1016/j.cub.2017.02.006>

Jean A Engbring, & Hynda K Kleinman. (2003). The basement membrane matrix in malignancy. *The Journal of Pathology*, 200(4):465-70. <https://doi.org/10.1002/path.1396>.

Jia, Z., Barbier, L., Stuart, H., Amraei, M., Pelech, S., Dennis, J. W., Metalnikov, P., O'Donnell, P., & Nabi, I. R. (2005). Tumor cell pseudopodial protrusions: Localized signaling domains coordinating cytoskeleton remodeling, cell adhesion, glycolysis, RNA translocation, and protein translation. *Journal of Biological Chemistry*, 280(34), 30564–30573. <https://doi.org/10.1074/jbc.M501754200>

Kalluri, R., & Weinberg, R. A. (2009). The basics of epithelial-mesenchymal transition. In *Journal of Clinical Investigation* (Vol. 119, Issue 6, pp. 1420–1428). <https://doi.org/10.1172/JCI39104>

Katz, M., Amit, I., Citri, A., Shay, T., Carvalho, S., Lavi, S., Milanezi, F., Lyass, L., Amariglio, N., Jacob-Hirsch, J., Ben-Chetrit, N., Tarcic, G., Lindzen, M., Avraham, R., Liao, Y. C., Trusk, P., Lyass, A., Rechavi, G., Spector, N. L., ... Yarden, Y. (2007). A reciprocal tensin-3-cten switch mediates EGF-driven mammary cell migration. *Nature Cell Biology*, 9(8), 961–969. <https://doi.org/10.1038/ncb1622>

Keller, C. R., Ruud, K. F., Martinez, S. R., & Li, W. (2022). Identification of the Collagen Types Essential for Mammalian Breast Acinar Structures. *Gels*, 8(12). <https://doi.org/10.3390/gels8120837>

Kelley, L. C., Chi, Q., Cáceres, R., Hastie, E., Schindler, A. J., Jiang, Y., Matus, D. Q., Plastino, J., & Sherwood, D. R. (2019). Adaptive F-Actin Polymerization and Localized ATP Production Drive Basement Membrane Invasion in the Absence of MMPs. *Developmental Cell*, 48(3), 313-328.e8. <https://doi.org/10.1016/j.devcel.2018.12.018>

Khalilgharibi, N., & Mao, Y. (2021). To form and function: On the role of basement membrane mechanics in tissue development, homeostasis and disease. In *Open Biology* (Vol. 11, Issue 2). Royal Society Publishing. <https://doi.org/10.1098/rsob.200360>

Kikkawa, Y., Hozumi, K., Katagiri, F., Nomizu, M., Kleinman, H. K., & Koblinski, J. E. (2013). Laminin-111-derived peptides and cancer. In *Cell Adhesion and Migration* (Vol. 7, Issue 1, pp. 150–159). Taylor and Francis Inc. <https://doi.org/10.4161/cam.22827>

Kim, B. G., Gao, M. Q., Choi, Y. P., Kang, S., Park, H. R., Kang, K. S., & Cho, N. H. (2012). Invasive breast cancer induces laminin-332 upregulation and integrin β 4 neoexpression in myofibroblasts to confer an anoikis-resistant phenotype during tissue remodeling. *Breast Cancer Research*, 14(3). <https://doi.org/10.1186/bcr3203>

Koorman, T., Jansen, K. A., Khalil, A., Haughton, P. D., Visser, D., Rätze, M. A. K., Haakma, W. E., Sakalauskaite, G., van Diest, P. J., de Rooij, J., & Derksen, P. W. B. (2022). Spatial collagen stiffening promotes collective breast cancer cell invasion by reinforcing extracellular

matrix alignment. *Oncogene*, 41(17), 2458–2469. <https://doi.org/10.1038/s41388-022-02258-1>

Kren, A., Baeriswyl, V., Lehenbre, F., Wunderlin, C., Strittmatter, K., Antoniadis, H., Fässler, R., Cavallaro, U., & Christofori, G. (2007). Increased tumor cell dissemination and cellular senescence in the absence of β 1-integrin function. *EMBO Journal*, 26(12), 2832–2842. <https://doi.org/10.1038/sj.emboj.7601738>

Kular, J. K., Basu, S., & Sharma, R. I. (2014). The extracellular matrix: Structure, composition, age-related differences, tools for analysis and applications for tissue engineering. In *Journal of Tissue Engineering* (Vol. 5). SAGE Publications Ltd. <https://doi.org/10.1177/2041731414557112>

Kyykallio, H., Oikari, S., Álvez, M. B., Dodd, C. J. G., Capra, J., & Rilla, K. (2020). The density and length of filopodia associate with the activity of hyaluronan synthesis in tumor cells. *Cancers*, 12(7), 1–14. <https://doi.org/10.3390/cancers12071908>

Lee, H., Kim, W.-J., Kang, H.-G., Jang, J.-H., Choi, I. J., Chun, K.-H., Kim, S.-J., Lee, H. ; Kim, W.-J. ; Kang, H.-G. ; Jang, J.-H. ; Choi, I. J. ; Chun, K.-H. ; & Kim, S.-J. (2021). Upregulation of LAMB1 via ERK/c-Jun Axis Promotes Gastric Cancer Growth and Motility. *International Journal of Molecular Sciences Article*. <https://doi.org/10.3390/ijms2202>

Lee, S. B., Cho, K. S., Kim, E., & Chung, J. (2003). blistery encodes Drosophila tensin protein and interacts with integrin and the JNK signaling pathway during wing development. In *Development* (Vol. 130, Issue 17, pp. 4001–4010). <https://doi.org/10.1242/dev.00595>

Legerstee, K., & Houtsmuller, A. (2021). A layered view on focal adhesions. *Biology*, 10(11). <https://doi.org/10.3390/biology10111189>

Liao, Y. C., & Lo, S. H. (2021). Tensins - emerging insights into their domain functions, biological roles and disease relevance. *Journal of Cell Science*, 134(4), 1–12. <https://doi.org/10.1242/jcs.254029>

Lin, G., & Scott, J. G. (2012). Context, tissue plasticity, and cancer: Are tumor stem cells also regulated by the microenvironment? *Cancer Cell*, 100(2), 130–134. <https://doi.org/10.1016/j.ccr.2004.12.013>.

Lindgren, M., Jansson, M., Tavelin, B., Dirix, L., Vermeulen, P., & Nyström, H. (2021). Type IV collagen as a potential biomarker of metastatic breast cancer. *Clinical and Experimental Metastasis*, 38(2), 175–185. <https://doi.org/10.1007/s10585-021-10082-2>

Lo, S. H. (2017). Tensins. *Current Biology*, 27(9), R331–R332. <https://doi.org/10.1016/j.cub.2017.02.041>

Lu, P., Weaver, V. M., & Werb, Z. (2012). The extracellular matrix: A dynamic niche in cancer progression. *Journal of Cell Biology*, 196(4), 395–406. <https://doi.org/10.1083/jcb.201102147>

Lu, X., Zhou, B., Cao, M., Shao, Q., Pan, Y., & Zhao, T. (2021). CTEN Inhibits Tumor Angiogenesis and Growth by Targeting VEGFA Through Down-Regulation of β -Catenin in

Breast Cancer. *Technology in Cancer Research and Treatment*, 20. <https://doi.org/10.1177/15330338211045506>

Łukasiewicz, S., Czezelewski, M., Forma, A., Baj, J., Sitarz, R., & Stanisławek, A. (2021). Breast cancer epidemiology, risk factors, classification, prognostic markers, and current treatment strategies. In *Cancers* (Vol. 13, Issue 17). MDPI. <https://doi.org/10.3390/cancers13174287>

Lyons, T. R., O'Brien, J., Borges, V. F., Conklin, M. W., Keely, P. J., Eliceiri, K. W., Marusyk, A., Tan, A. C., & Schedin, P. (2011). Postpartum mammary gland involution drives progression of ductal carcinoma in situ through collagen and COX-2. *Nature Medicine*, 17(9), 1109–1116. <https://doi.org/10.1038/nm.2416>

Machesky, L. M. (2008). Lamellipodia and filopodia in metastasis and invasion. In *FEBS Letters* (Vol. 582, Issue 14, pp. 2102–2111). <https://doi.org/10.1016/j.febslet.2008.03.039>

Martínez-Abarca Millán, A., Soler Beatty, J., Valencia Expósito, A., & Martín-Bermudo, M. D. (2023). Drosophila as Model System to Study Ras-Mediated Oncogenesis: The Case of the Tensin Family of Proteins. *Genes*, 14(7). <https://doi.org/10.3390/genes14071502>

Martorell, Ò., Merlos-Suárez, A., Campbell, K., Barriga, F. M., Christov, C. P., Miguel-Aliaga, I., Batlle, E., Casanova, J., & Casali, A. (2014). Conserved mechanisms of tumorigenesis in the Drosophila adult midgut. *PLoS ONE*, 9(2). <https://doi.org/10.1371/journal.pone.0088413>

Martuszevska, D., Ljungberg, B., Johansson, M., Landberg, G., Oslakovic, C., Dahlbäck, B., & Hafizi, S. (2009). Tensin3 Is a Negative Regulator of Cell Migration and All Four Tensin Family Members Are Downregulated in Human Kidney Cancer. *PLoS ONE*, 4(2). <https://doi.org/10.1371/journal.pone.0004350>

Matro JM, Li T, Cristofanilli M, Hughes ME, Ottesen RA, Weeks JC, Wong YN. (2015). Inflammatory Breast Cancer Management in the National Comprehensive Cancer Network: The Disease, Recurrence Pattern, and Outcome. *Clinical Breast Cancer, Volume 15*(Issue 1, 15(1):1-7). <https://doi.org/10.1016/j.clbc.2014.05.005>.

Meghan A Morrissey, Elliott J Hagedorn, & David R Sherwood. (2013). Cell invasion through basement membrane. *Landes Bioscience, Volume 1;2(3):e26169*. <https://doi.org/10.4161/worm.26169>

Mendonça, F. F., Sobral, D. V., Durante, A. C. R., Miranda, A. C. C., Mejia, J., de Paula Faria, D., Marques, F. L. N., de Barboza, M. F., Fuscaldi, L. L., & Malavolta, L. (2024). Assessment of bioactive peptides derived from laminin-111 as prospective breast cancer-targeting agents. *Amino Acids*, 56(1). <https://doi.org/10.1007/s00726-023-03379-x>

Mercogliano, M. F., Bruni, S., Elizalde, P. V., & Schillaci, R. (2020). Tumor Necrosis Factor α Blockade: An Opportunity to Tackle Breast Cancer. In *Frontiers in Oncology* (Vol. 10). Frontiers Media S.A. <https://doi.org/10.3389/fonc.2020.00584>

Merour, E., Hmidan, H., Marie, C., Helou, P. H., Lu, H., Potel, A., Hure, J. B., Clavairoly, A., Shih, Y. P., Goudarzi, S., Dussaud, S., Ravassard, P., Hafizi, S., Lo, S. H., Hassan, B. A., &

- Parras, C. (2022). Transient regulation of focal adhesion via Tensin3 is required for nascent oligodendrocyte differentiation. *ELife*, *11*. <https://doi.org/10.7554/eLife.80273>
- Miihkinen, M., Grönloh, M. L. B., Popović, A., Vihinen, H., Jokitalo, E., Goult, B. T., Ivaska, J., & Jacquemet, G. (2021). Myosin-X and talin modulate integrin activity at filopodia tips. *Cell Reports*, *36*(11). <https://doi.org/10.1016/j.celrep.2021.109716>
- Min Hu, Guillermo Peluffo, Rebecca Gelman, Stuart Schnitt, & Kornelia Polyak. (2009). Role of COX-2 in epithelial–stromal cell interactions and progression of ductal carcinoma in situ of the breast. *PNAS*, *106*(9):3372-7. <https://doi.org/10.1073/pnas.0813306106>.
- Mirzoyan, Z., Sollazzo, M., Allocca, M., Valenza, A. M., Grifoni, D., & Bellosta, P. (2019). *Drosophila melanogaster*: A model organism to study cancer. *Frontiers in Genetics*, *10*(March), 1–16. <https://doi.org/10.3389/fgene.2019.00051>
- Miskin, R. P., Warren, J. S. A., Ndoye, A., Wu, L., Lamar, J. M., & Dipersio, C. M. (2021). Integrin $\alpha 3 \beta 1$ promotes invasive and metastatic properties of breast cancer cells through induction of the brn-2 transcription factor. *Cancers*, *13*(3), 1–17. <https://doi.org/10.3390/cancers13030480>
- Mitchell, K., Svenson, K. B., Longmate, W. M., Gkirtzimanaki, K., Sadej, R., Wang, X., Zhao, J., Eliopoulos, A. G., Berditchevski, F., & DiPersio, C. M. (2010). Suppression of integrin $\alpha 3 \beta 1$ in breast cancer cells reduces cyclooxygenase-2 gene expression and inhibits tumorigenesis, invasion, and cross-talk to endothelial cells. *Cancer Research*, *70*(15), 6359–6367. <https://doi.org/10.1158/0008-5472.CAN-09-4283>
- Mouneimne, G., & Brugge, J. S. (2007). Tensins: A New Switch in Cell Migration. In *Developmental Cell* (Vol. 13, Issue 3, pp. 317–319). <https://doi.org/10.1016/j.devcel.2007.08.010>
- Muharram, G., Sahgal, P., Korpela, T., DeFranceschi, N., Kaukonen, R., Clark, K., Tulasne, D., Carpen, O., & Ivaska, J. (2014). Tensin-4-dependent MET stabilization is essential for survival and proliferation in carcinoma cells. *Developmental Cell*, *29*(4), 421–436. <https://doi.org/10.1016/j.devcel.2014.03.024>
- Murphy, K. N., & Brinkworth, A. J. (2021). Manipulation of focal adhesion signaling by pathogenic microbes. *International Journal of Molecular Sciences*, *22*(3), 1–48. <https://doi.org/10.3390/ijms22031358>
- Naba, A., Clauser, K. R., Hoersch, S., Liu, H., Carr, S. A., & Hynes, R. O. (2012). The matrisome: In silico definition and *in vivo* characterization by proteomics of normal and tumor extracellular matrices. *Molecular and Cellular Proteomics*, *11*(4), 1–18. <https://doi.org/10.1074/mcp.M111.014647>
- Nazemi, M., Yanes, B., Martinez, M. L., Walker, H. J., Pham, K., Collins, M. O., Bard, F., & Rainero, E. (2024). The extracellular matrix supports breast cancer cell growth under amino acid starvation by promoting tyrosine catabolism. *PLoS Biology*, *22*(1). <https://doi.org/10.1371/journal.pbio.3002406>

- Nisticò, P., Modugno, F. Di, Spada, S., & Bissell, M. J. (2014). β 1 and β 4 integrins: from breast development to clinical practice. *Breast Cancer Res.* <http://breast-cancer-research.com/content/16/5/459>
- Nizioł, M., Zińczuk, J., Zaręba, K., Guzińska-Ustymowicz, K., & Pryczynicz, A. (2021). Increased tensin 4 expression is related to the histological type of gastric cancer. *World Journal of Clinical Oncology*, 12(12), 1202–1214. <https://doi.org/10.5306/wjco.v12.i12.1202>
- Nolan, J., Mahdi, A. F., Dunne, C. P., & Kiely, P. A. (2020). Collagen and fibronectin promote an aggressive cancer phenotype in breast cancer cells but drive autonomous gene expression patterns. *Gene*, 761. <https://doi.org/10.1016/j.gene.2020.145024>
- Nurmik, M., Ullmann, P., Rodriguez, F., Haan, S., & Letellier, E. (2020). In search of definitions: Cancer-associated fibroblasts and their markers. In *International Journal of Cancer* (Vol. 146, Issue 4, pp. 895–905). Wiley-Liss Inc. <https://doi.org/10.1002/ijc.32193>
- Onursal, C., Dick, E., Angelidis, I., Schiller, H. B., & Staab-Weijnitz, C. A. (2021). Collagen Biosynthesis, Processing, and Maturation in Lung Ageing. In *Frontiers in Medicine* (Vol. 8). Frontiers Media S.A. <https://doi.org/10.3389/fmed.2021.593874>
- Orsaria, P., Grasso, A., Ippolito, E., Pantano, F., Sammarra, M., Altomare, C., Cagli, B., Costa, F., Perrone, G., Soponar, G., Caggiati, L., Vanni, G., Buonomo, O. C., & Altomare, V. (2021). Clinical outcomes among major breast cancer subtypes after neoadjuvant chemotherapy: Impact on breast cancer recurrence and survival. *Anticancer Research*, 41(5), 2697–2709. <https://doi.org/10.21873/ANTICANRES.15051>
- Oskarsson, T. (2013). Extracellular matrix components in breast cancer progression and metastasis. *Breast*, 22(S2), S66–S72. <https://doi.org/10.1016/j.breast.2013.07.012>
- Pan, B., Guo, J., Liao, Q., & Zhao, Y. (2018). β 1 and β 3 integrins in breast, prostate and pancreatic cancer: A novel implication (Review). *Oncology Letters*, 15(4), 5412–5416. <https://doi.org/10.3892/ol.2018.8076>
- Pang, X., He, X., Qiu, Z., Zhang, H., Xie, R., Liu, Z., Gu, Y., Zhao, N., Xiang, Q., & Cui, Y. (2023). Targeting integrin pathways: mechanisms and advances in therapy. In *Signal Transduction and Targeted Therapy* (Vol. 8, Issue 1). Springer Nature. <https://doi.org/10.1038/s41392-022-01259-6>
- Park, G. C., Kim, H. S., Park, H. Y., Seo, Y., Kim, J. M., Shin, S. C., Kwon, H. K., Sung, E. S., Lee, J. C., & Lee, B. J. (2020). Tensin-3 regulates integrin-mediated proliferation and differentiation of tonsil-derived mesenchymal stem cells. *Cells*, 9(1). <https://doi.org/10.3390/cells9010089>
- Park, G. C., Kim, J. M., Shin, S. C., Cheon, Y. Il, Sung, E. S., Lee, M., Lee, J. C., & Lee, B. J. (2022). Tensin Regulates Fundamental Biological Processes by Interacting with Integrins of Tonsil-Derived Mesenchymal Stem Cells. *Cells*, 11(15). <https://doi.org/10.3390/cells11152333>

- Partridge, M. A., & Marcantonio, E. E. (2006). Initiation of Attachment and Generation of Mature Focal Adhesions by Integrin-containing Filopodia in Cell Spreading. *Molecular Biology of the Cell*, 17, 4237–4248. <https://doi.org/10.1091/mbc.E06>
- Peuhu, E., Jacquemet, G., Scheele, C. L. G. J., Isomursu, A., Laisne, M. C., Koskinen, L. M., Paatero, I., Thol, K., Georgiadou, M., Guzmán, C., Koskinen, S., Laiho, A., Elo, L. L., Boström, P., Hartiala, P., van Rheenen, J., & Ivaska, J. (2022). MYO10-filopodia support basement membranes at pre-invasive tumor boundaries. *Developmental Cell*, 57(20), 2350–2364.e7. <https://doi.org/10.1016/j.devcel.2022.09.016>
- Poff, A. M., Ari, C., Seyfried, T. N., & D’Agostino, D. P. (2013). The Ketogenic Diet and Hyperbaric Oxygen Therapy Prolong Survival in Mice with Systemic Metastatic Cancer. *PLoS ONE*, 8(6). <https://doi.org/10.1371/journal.pone.0065522>
- Pozzi, A., Yurchenco, P. D., & Iozzo, R. V. (2017). The nature and biology of basement membranes. In *Matrix Biology* (Vols. 57–58, pp. 1–11). Elsevier B.V. <https://doi.org/10.1016/j.matbio.2016.12.009>
- Qian, X., Li, G., Vass, W. C., Papageorge, A., Walker, R. C., Asnaghi, L., Steinbach, P. J., Tosato, G., Hunter, K., & Lowy, D. R. (2009). The Tensin-3 Protein, Including its SH2 Domain, Is Phosphorylated by Src and Contributes to Tumorigenesis and Metastasis. *Cancer Cell*, 16(3), 246–258. <https://doi.org/10.1016/j.ccr.2009.07.031>
- Rainero, E. (2018). Extracellular matrix internalization links nutrient signalling to invasive migration. *International Journal of Experimental Pathology*, 99(1), 4–9. <https://doi.org/10.1111/iep.12265>
- Rainero, E., Howe, J. D., Caswell, P. T., Jamieson, N. B., Anderson, K., Critchley, D. R., Machesky, L., & Norman, J. C. (2015). Ligand-Occupied Integrin Internalization Links Nutrient Signaling to Invasive Migration. *Cell Reports*, 10(3), 398–413. <https://doi.org/10.1016/j.celrep.2014.12.037>
- Ramovs, V., Secades, P., Song, J. Y., Thijssen, B., Kreft, M., & Sonnenberg, A. (2019). Absence of integrin $\alpha3\beta1$ promotes the progression of HER2-driven breast cancer in vivo. *Breast Cancer Research*, 21(1). <https://doi.org/10.1186/s13058-019-1146-8>
- Ramovs, V., te Molder, L., & Sonnenberg, A. (2017). The opposing roles of laminin-binding integrins in cancer. In *Matrix Biology* (Vols. 57–58, pp. 213–243). Elsevier B.V. <https://doi.org/10.1016/j.matbio.2016.08.007>
- Rousselle, P., & Scoazec, J. Y. (2020). Laminin 332 in cancer: When the extracellular matrix turns signals from cell anchorage to cell movement. In *Seminars in Cancer Biology* (Vol. 62, pp. 149–165). Academic Press. <https://doi.org/10.1016/j.semcancer.2019.09.026>
- Santner, S. J., Dawson, P. J., Tait, L., Soule, H. D., Eliason, J., Mohamed, A. N., Wolman, S. R., Heppner, G. H., & Miller, F. R. (2001). Malignant MCF10CA1 cell lines derived from premalignant human breast epithelial MCF10AT cells. In *Breast Cancer Research and Treatment* (Vol. 65, (2):101-10). <http://dio.org/0.1023/a:1006461422273>

Sarantelli, E., Mourkakis, A., Zacharia, L. C., Stylianou, A., & Gkretsi, V. (2023). Fascin-1 in Cancer Cell Metastasis: Old Target-New Insights. In *International Journal of Molecular Sciences* (Vol. 24, Issue 14). Multidisciplinary Digital Publishing Institute (MDPI). <https://doi.org/10.3390/ijms241411253>

Saraswathibhatla, A., Indana, D., & Chaudhuri, O. (2023). Cell-extracellular matrix mechanotransduction in 3D HHS Public Access. *Nat Rev Mol Cell Biol*, 24(7), 495–516. <https://doi.org/10.1016/j.cell.2014.05.046>

Scherz-Shouval, R., Santagata, S., Mendillo, M. L., Sholl, L. M., Ben-Aharon, I., Beck, A. H., Dias-Santagata, D., Koeva, M., Stemmer, S. M., Whitesell, L., & Lindquist, S. (2014). The reprogramming of tumor stroma by HSF1 is a potent enabler of malignancy. *Cell*, 158(3), 564–578. <https://doi.org/10.1016/j.cell.2014.05.045>

Shih, Y. P., Sun, P., Wang, A., & Lo, S. H. (2015). Tensin1 positively regulates RhoA activity through its interaction with DLC1. *Biochimica et Biophysica Acta - Molecular Cell Research*, 1853(12), 3258–3265. <https://doi.org/10.1016/j.bbamcr.2015.09.028>

Shinchi, Y., Hieda, M., Nishioka, Y., Matsumoto, A., Yokoyama, Y., Kimura, H., Matsuura, S., & Matsuura, N. (2015). SUV420H2 suppresses breast cancer cell invasion through down regulation of the SH2 domain-containing focal adhesion protein tensin-3. *Experimental Cell Research*, 334(1), 90–99. <https://doi.org/10.1016/j.yexcr.2015.03.010>

Silverstein, M. J., & Lagios, M. D. (2015). Treatment selection for patients with ductal carcinoma in situ (DCIS) of the breast using the University of Southern California/Van Nuys (USC/VNPI) Prognostic Index. *Breast Journal*, 21(2), 127–132. <https://doi.org/10.1111/tbj.12368>

Singer, C. F., Gschwantler-Kaulich, D., Fink-Retter, A., Haas, C., Hudelist, G., Czerwenka, K., & Kubista, E. (2008). Differential gene expression profile in breast cancer-derived stromal fibroblasts. *Breast Cancer Research and Treatment*, 110(2), 273–281. <https://doi.org/10.1007/s10549-007-9725-2>

So JY, Lee HJ, Kramata P, Minden A.& Suh, N. (2014). Differential Expression of Key Signaling Proteins in MCF10 Cell Lines, a Human Breast Cancer Progression Model. *Mol Cell Pharmacol*, Vol. 4, Issue 1, pp 31-40. <https://doi.org/PMC3928091>

Soguel, L., Durocher, F., Tchernof, A., & Diorio, C. (2017). Adiposity, breast density, and breast cancer risk: Epidemiological and biological considerations. In *European Journal of Cancer Prevention* (Vol. 26, Issue 6, pp. 511–520). Lippincott Williams and Wilkins. <https://doi.org/10.1097/CEJ.0000000000000310>

Song, Y.(2024). Dysfunctional adipocytes promote tumor progression through YAP/TAZ-dependent cancer-associated adipocyte transformation. *Nature Communications*, 15(1). <https://doi.org/10.1038/s41467-024-48179-3>

Soule HD, M. (1990). Isolation and characterization of a spontaneously immortalized human breast epithelial cell line, MCF-10. *Cancer Res.* 5;50(18):6075-86. PMID: 1975513.

Speer, J., Barcellona, M., Jing, L., Liu, B., Lu, M., Kelly, M., Buchowski, J., Zebala, L., Luhmann, S., Gupta, M., & Setton, L. (2021). Integrin-mediated interactions with a laminin-presenting substrate modulate biosynthesis and phenotypic expression for cells of the human nucleus pulposus. *European Cells and Materials*, 41, 793–810. <https://doi.org/10.22203/eCM.v041a50>

Chandrasekaran S, Guo NH, Rodrigues RG, Kaiser J, Roberts DD. (1998). Pro-adhesive and Chemotactic Activities of Thrombospondin-1 for Breast Carcinoma Cells Are Mediated by $\alpha 3\beta 1$ Integrin and Regulated by Insulin-like Growth Factor-1 and CD98. *J Biol Chem*. Vol. 16, Issue 274,11408-16. <https://doi.org/10.1074/jbc.274.16.11408>

Sun, B. (2021). The mechanics of fibrillar collagen extracellular matrix. In *Cell Reports Physical Science* (Vol. 2, Issue 8). Cell Press. <https://doi.org/10.1016/j.xcrp.2021.100515>

Sun, L., Guo, S., Xie, Y., & Yao, Y. (2023). The characteristics and the multiple functions of integrin $\beta 1$ in human cancers. In *Journal of Translational Medicine* (Vol. 21, Issue 1). BioMed Central Ltd. <https://doi.org/10.1186/s12967-023-04696-1>

Tamkun, J. W., & Hynes, R. O. (1983). Plasma fibronectin is synthesized and secreted by hepatocytes. *Journal of Biological Chemistry*, 258(7), 4641–4647. [https://doi.org/10.1016/s0021-9258\(18\)32672-3](https://doi.org/10.1016/s0021-9258(18)32672-3)

Torgler CN, Narasimha M, Knox AL, Zervas CG, Vernon MC & Brown, N H. (2004). Tensin Stabilizes Integrin Adhesive Contacts in Drosophila. In *Developmental Cell* (Vol. 6, 357-69). [https://doi.org/10.1016/s1534-5807\(04\)00055-3](https://doi.org/10.1016/s1534-5807(04)00055-3)

Troughton, L. D., O’Loughlin, D. A., Zech, T., & Hamill, K. J. (2022). Laminin N-terminus $\alpha 31$ is upregulated in invasive ductal breast cancer and changes the mode of tumour invasion. *PLoS ONE*, 17(3 March). <https://doi.org/10.1371/journal.pone.0264430>

Tsuruta, D., Kobayashi, H., Imanishi, H., Sugawara, K., Ishii, M., & Jones, J. C. R. (2008). *Laminin-332-Integrin Interaction: A Target For Cancer Therapy?*. *Curr Med Chem*. Vol 15(20):1968-75. <https://doi.org/10.2174/092986708785132834>

Tyan, S. W., Hsu, C. H., Peng, K. L., Chen, C. C., Kuo, W. H., Lee, E. Y. H. P., Shew, J. Y., Chang, K. J., Juan, L. J., & Lee, W. H. (2012). Breast cancer cells induce stromal fibroblasts to secrete ADAMTS1 for cancer invasion through an epigenetic change. *PLoS ONE*, 7(4). <https://doi.org/10.1371/journal.pone.0035128>

Uchio-Yamada, K., Monobe, Y., Akagi, K. I., Yamamoto, Y., Ogura, A., & Manabe, N. (2016). Tensin2-deficient mice on FVB/N background develop severe glomerular disease. *Journal of Veterinary Medical Science*, 78(5), 811–818. <https://doi.org/10.1292/jvms.15-0442>

Underwood, R. A., Carter, W. G., Usui, M. L., & Olerud, J. E. (2009). Ultrastructural localization of integrin subunits $\beta 4$ and $\alpha 3$ within the migrating epithelial tongue of in vivo human wounds. *Journal of Histochemistry and Cytochemistry*, 57(2), 123–142. <https://doi.org/10.1369/jhc.2008.952176>

Veß, A., Blache, U., Leitner, L., Kurz, A. R. M., Ehrenpfordt, A., Sixt, M., & Posern, G. (2017). A dual phenotype of MDA-MB-468 cancer cells reveals mutual regulation of tensin3 and

adhesion plasticity. *Journal of Cell Science*, 130(13), 2172–2184. <https://doi.org/10.1242/jcs.200899>

Walker, C., Mojares, E., & Del Río Hernández, A. (2018). Role of extracellular matrix in development and cancer progression. In *International Journal of Molecular Sciences* (Vol. 19, Issue 10). MDPI AG. <https://doi.org/10.3390/ijms19103028>

Weaver, VM., Lelièvre, S., Lakins, JN., Chrenek, M. A., Jones, J. C. R., Giancotti, F., Werb, Z., & Bissell, M. J. (2002). $\beta 4$ integrin-dependent formation of polarized three-dimensional architecture confers resistance to apoptosis in normal and malignant mammary epithelium. *Cancer Cell*, 2 (3):205-16. [https://doi.org/10.1016/s1535-6108\(02\)00125-3](https://doi.org/10.1016/s1535-6108(02)00125-3)

Westman, E. C., Yancy, W. S., Mavropoulos, J. C., Marquart, M., & McDuffie, J. R. (2008). The effect of a low-carbohydrate, ketogenic diet versus a low-glycemic index diet on glycemic control in type 2 diabetes mellitus. *Nutrition and Metabolism*, 5(1). <https://doi.org/10.1186/1743-7075-5-36>

Xu, M. Y., Porte, J., Knox, A. J., Weinreb, P. H., Maher, T. M., Violette, S. M., McAnulty, R. J., Sheppard, D., & Jenkins, G. (2009). Lysophosphatidic acid induces $\alpha\beta 36$ integrin-mediated TGF- β activation via the LPA2 receptor and the small G protein G α_q . *American Journal of Pathology*, 174(4), 1264–1279. <https://doi.org/10.2353/ajpath.2009.080160>

Yam, J. W. P., Ko, F. C. F., Chan, C. Y., Jin, D. Y., & Ng, I. O. L. (2006). Interaction of deleted in liver cancer 1 with Tensin2 in caveolae and implications in tumor suppression. *Cancer Research*, 66(17), 8367–8372. <https://doi.org/10.1158/0008-5472.CAN-05-2850>

Yang, G. Y., Xu, K. Sen, Pan, Z. Q., Zhang, Z. Y., Mi, Y. T., Wang, J. S., Chen, R., & Niu, J. (2008). Integrin $\alpha 6 \beta 6$ mediates the potential for colon cancer cells to colonize in and metastasize to the liver. *Cancer Science*, 99(5), 879–887. <https://doi.org/10.1111/j.1349-7006.2008.00762.x>

Yin, C., Ma, B., Zhang, X., Lan, L., Ren, G., Xu, J., & Wang, J. (2022). Overexpression of Laminin 5 $\gamma 2$ Chain Correlates with Tumor Cell Proliferation, Invasion, and Poor Prognosis in Laryngeal Squamous Cell Carcinoma. *Journal of Oncology*, 2022. <https://doi.org/10.1155/2022/7248064>

Zhang, H., Berg, J. S., Wang, Y., Lång, P., Sousa, A. D., Bhaskar, A., Cheney, R. E., & Strömblad, S. (2004). Myosin-X provides a motor-based link between integrins and the cytoskeleton. *Nature Cell Biology*, 6(6), 523–531. <https://doi.org/10.1038/ncb1136>

Zhao, C., Wu, M., Zeng, N., Xiong, M., Hu, W., Lv, W., Yi, Y., Zhang, Q., & Wu, Y. (2020). Cancer-associated adipocytes: Emerging supporters in breast cancer. In *Journal of Experimental and Clinical Cancer Research* (Vol. 39, Issue 1). BioMed Central Ltd. <https://doi.org/10.1186/s13046-020-01666-z>

Zheng, J., & Hao, H. (2023). The importance of cancer-associated fibroblasts in targeted therapies and drug resistance in breast cancer. In *Frontiers in Oncology* (Vol. 13). Frontiers Media SA. <https://doi.org/10.3389/fonc.2023.1333839>

Zhou, B., Zong, S., Zhong, W., Tian, Y., Wang, L., Zhang, Q., Zhang, R., Li, L., Wang, W., Zhao, J., Chen, X., Feng, Y., Zhai, B., Sun, T., & Liu, Y. (2020). Interaction between laminin-5 γ 2 and integrin β 1 promotes the tumor budding of colorectal cancer via the activation of Yes-associated proteins. *Oncogene*, 39(7), 1527–1542. <https://doi.org/10.1038/s41388-019-1082-1>

Zhu, J., Xiong, G., Trinkle, C., & Xu, R. (2014). Integrated extracellular matrix signaling in mammary gland development and breast cancer progression. *Histology and Histopathology*, 29(9), 1083–1092. <https://doi.org/10.14670/HH-29.1083>